แกซิฟิเคชั่นและรีฟอร์มมิ่งโดยพร้อมกันของชีวมวลบนนิกเกิล/โดโลไมต์ในฟลูอิดไดซ์เบด

นายอนวรรตน์ เกตุคง

วิทยานิพนธ์นี้เป็นส่วนหนึ่งของการศึกษาตามหลักสูตรปริญญาวิทยาศาสตรดุษฎีบัณฑิต
สาขาวิชาเคมีเทคนิค ภาควิชาเคมีเทคนิค
คณะวิทยาศาสตร์ จุฬาลงกรณ์มหาวิทยาลัย
ปีการศึกษา 2551

SIMULTANEOUS GASIFICATION AND REFORMING OF BIOMASS ON Ni/DOLOMITE IN FLUIDIZED BED

Mr. Anawat Ketcong

A Dissertation Submitted in Partial Fulfillment of the Requirements
for the Degree of Doctor of Philosophy Program in Chemical Technology
Department of Chemical Technology
Faculty of Science
Chulalongkorn University
Academic Year 2008

Thesis Title SIMULTANEOUS GASIFICATION AND REFORMING OF BIOMASS ON Ni/DOLOMITE IN FLUIDIZED BED
By Mr. Anawat Ketcong
Field of study Chemical Technology
Thesis Principal Advisor Associate Professor Tharapong Vitidsant, Ph.D.
Thesis Co-advisor Professor Kaoru Fujimoto, Ph.D.

Accepted by the Faculty of Science, Chulalongkorn University in Partial Fulfillment of the Requirements for the Doctoral Degree

S. Hannongbua ....Dean of the Faculty of Science
(Professor Supot Hannongbua, Ph.D)

THESIS COMMITTEE

........................Chairman
(Professor Pattarapan Prasassarakich, Ph.D.)

T. Vitidsant .... Thesis Advisor
(Associate Professor Tharapong Vitidsant, Ph.D.)

Kaoru Fujimoto .... Thesis Co-advisor
(Professor Kaoru Fujimoto, Ph.D.)

........................Member
(Assistant Professor Prapan Kuchonthara, Ph.D.)

Chawalit N.srivichai ....Member
(Chawalit Ngamcharussrivichai, Ph.D.)

.... External Member
(Viboon Sricharoenchaikul, Ph.D.)

.... External Member
(Suchada Butnark, Ph.D.)

อนวรรตน์ เกตุคง : แกซิฟิเคชันและรีฟอร์มิงพร้อมกันของชีวมวลบนนิกเกิล/โดโลไมต์ในฟลูอิไดซ์เบด. (SIMULTANEOUS GASIFICATION AND REFORMING OF BIOMASS ON Ni/DOLOMITE IN FLUIDIZED BED) อ. ที่ปรึกษาวิทยานิพนธ์หลัก: รศ.ดร. ธราพงษ์ วิทิตศานต์, อ.ที่ปรึกษาวิทยานิพนธ์ร่วม: Prof. Kaoru Fujimoto, Ph.D., 133 หน้า

ไพโรไลซิสของชีวมวลตามด้วยแกซิฟิเซชั่นด้วยไอน้ำเพื่อผลิตแก๊สสังเคราะห์ถูกศึกษาโดยใช้โปรแกรมควบคุมอุณหภูมิการเกิดปฏิกิริยา(TPR) ทาร์ถูกผลิตออกมาที่อุณหภูมิ 200-400 องศาเซลเซียส และที่อุณหภูมิ 400 องศาเซลเซียส ทาร์ถูกผลิตออกมาเล็กน้อย ปฏิกิริยาแกซิฟิเคชั่นของชาร์ที่ได้จากไพโรไลซิสของชีวมวลถูกศึกษาโดยใช้โปรแกรมควบคุมที่อุณหภูมิสูง จากการทดลองพบว่า แก๊สผลิตภัณฑ์ (ไฮโดรเจน, คาร์บอนมอนอกไซด์, คาร์บอนไดออกไซด์ และ มีเทนปริมาณน้อยๆ) เริ่มถูกปล่อยออกมาที่อุณหภูมิ 600 องศาเซลเซียส การแกซิฟายมากสุดที่อุณหภูมิ 830 องศาเซลเซียส จนกระทั่งที่อุณหภูมิ 850 องศาเซลเซียส ชาร์ถูกแกซิฟายจนหมด ร้อยละการเปลี่ยนแปลงคาร์บอนในเบดนิ่งมีค่าร้อยละ 62-77 โดยหลักคาร์บอนอ้างอิง ระหว่างชีวมวล 4 ชนิด (เศษไม้สน, ไม้ไผ่, กะลามะพร้าว และ ซังข้าวโพด) พบว่า ซังข้าวโพดสามารถไพโรไลซ์ได้ดีที่สุดและได้ปริทาณชาร์น้อยที่สุด (ร้อยละ 21.7) เศษไม้สนไพโรไลซ์ได้ยากที่สุดและได้ปริมาณชาร์มากที่สุด(ร้อยละ 28.2 โดยน้ำหนัก)

แกซิฟิเคชั่นและการรีฟอร์มมิ่งไอน้ำโดยพร้อมกันของชีวมวลบนโดโลไมต์ที่มีปริมาณนิกเกิลสูงในฟลูอิดไดซ์เบดถูกศึกษาผลิตภัณฑ์แก๊สในเครื่องปฏิกรณ์ 1 เครื่อง ตัวแปรที่ทำการศึกษา เช่น อุณหภูมิ, อัตราการป้อนไอน้ำ, อัตราการป้อนชีวมวล, อัตราการไหลของแก๊สสำหรับการเกิดฟลูอิดไดเซชั่นม อัตราการป้อนออกซิเจน, ชนิดของตัวเร่งปฏิกิริยา ถูกทำการศึกษาเพื่อผลิตแก๊สผลิตภัณฑ์ปริมาณสูงรวมถึงการกำจัดทาร์ พบว่าที่อุณหภูมิ 780 °C, อัตราการป้อนไอน้ำ 222 มิลลิโมลต่อชั่วโมง แก๊สสำหรับฟลูอิดไดเซชั่น 450 มิลลิลิตรต่อนาที เหมาะสมสำหรับการแกซิฟิเคชั่นและรีฟอร์มมิ่ง นอกจากนี้ ตัวเร่งปฏิกิริยา นิกเกิล/โดโลไมต์ และ นิกเกิล/โดโลไมต์ที่เติมทังสเตน ถูกทำการศึกษา พบว่า นิกเกิล/โดโลไมต์ที่เติมทังสเตนมีประสิทธิภาพสูงในการผลิตแก๊สผลิตภัณฑ์ ชีวมวลชนิดต่างๆ (เศษไม้สน, ไม้ไผ่, กะลามะพร้าว, ซังข้าวโพด และ กะลาปาล์ม) ถูกเลือกเพื่อศึกษาความแตกต่างของแกซิฟิเคชั่นและรีฟอร์มมิ่งของชีวมวลแต่ละชนิด

ภาควิชา: ....เคมีเทคนิค.............ลายมือชื่อนิสิต: ....อนวรรตน์ เกตุคง..................
สาขาวิชา:............เคมีเทคนิค............ลายมือชื่ออ.ที่ปรึกษาวิทยานิพนธ์หลัก: ....
ปีการศึกษา:............2551..................ลายมือชื่ออ.ที่ปรึกษาวิทยานิพนธ์ร่วม: Kaoru Fujimoto

4873868323 : MAJOR CHEMICAL TECHNOLOGY
KEYWORD : BIOMASS / PYROLYSIS / GASIFICATION / REFORMING / FIXED BED / FLUIDIZED BED /Ni/DOLOMITE

ANAWAT KETCONG : SIMULTANEOUS GASIFICATION AND REFORMING OF BIOMASS ON Ni/DOLOMITE IN FLUIDIZED BED. THESIS PRINCIPLE ADVISOR: ASSOC. PROF. THARAPONG VITIDSANT, Ph.D, THESIS COADVISOR: PROF. KAORU FUJIMOTO, Ph.D., 133 pp.

Pyrolysis of biomasses accompanied by its successive steam gasification to synthesis gas was studied by a Temperature Programmed Reaction (TPR) method. Tars were produced at 200-400 °C and little tars were produced above 400 °C. Reactions of char, which was formed during pyrolysis of biomass, were subjected to the reactions with steam by Temperature Programmed Reaction (TPR) method. Gas formations started at around 600 °C and reached the maximum level about 830 °C irrespective of the low material and finished at 850 °C. The main gaseous products of the char gasification were H_2, CO, CO_2 and lesser amount of CH_4. The carbon conversion in the fixed bed was around 62-77% in carbon basis. Among the four types (pine wood chip, bamboo, coconut and corncob), corncob was the most suitable biomass to be pyrolyzed. On the other hand, pine wood chip was more difficult to be pyrolized. The amount of char obtained in the pyrolysis was the largest for pine wood chip (28.2 wt%) and the smallest for corncob (21.7wt%) in dry basis.

Simultaneous gasification and steam reforming of the biomass on Ni/dolomite catalyst in fluidized bed reactor were studied in the gaseous production in the one stage reactor. The parameters such as temperature, steam flow rate, biomass feed rate, gas flow rate for fluidization, oxygen flow rate and catalyst types were studied to produce the high gaseous products including tar elimination. The temperature at 780 °C, steam flow rate of 222 mmol/h, gas flow rate for fluidization 450 ml/min and oxygen input 50 ml/min were found to be the suitable conditions. The Ni/Dolomite and the developed Ni/Dolomite were also studied about their performance. It can be confirm that Ni/Dolomite and the newly developed Ni-WO_3/Dolomite show high performance in biomass gasification. The various types of biomass (pine wood chip, coconut shell, bamboo, corncob and palm shell) were selected to study the difference of gas production in gasification and reforming.

Department:......Chemical Technology.....Student's signature:...Anawat Ketcong...

Field of study:..Chemical Technology..Thesis Principle Advisor's signature:...T. Vitidsant...

Academic year:.........2008..............Co-advisor's signature:...Kaoru Fujimoto...

ACKNOWLEDGMENTS

Firstly, I would like to grateful my advisor, Assoc. Prof. Dr. Tharapong Vitidsant, and my co-advisor, Prof. Dr.Kaoru Fujimoto at The University of Kitakyushu in Japan, for the biggest chance in my life, kindly advice, acknowlegde and great support. . My Ph.D. would not have successive without both persons.

I would like to sincerely appeciate Prof. Dr. Pattarapan Prasassarakich for the thesis defense chairman

I also would mostly like to thankful Dr. Chawalit Ngamcharussrivichai for his help and advice when I was in Japan and also is my committee, Assist. Prof. Dr. Prapan Kuchonthara, Dr. Viboon Sricharoenchaikul, Dr. Suchada Butnark for serving member of committee.

The kindness of Prof. Dr. Xiaohong Li and Prof. Dr. Kenji Asami at The University of Kitakyushu are also appreciated.

The kindness of Assoc.Prof. Dr. Somkiat Ngamprasertsit and Assoc. Prof. Dr. Kejvalee Pruksathorn is also appreciated.

The three types of the performance Ni/Dolomite were gotten from Dr. Kazuhiro Sato at Takuma company. I would like to thankful him for help and acknowledgement.

All members in Laboratory of Prof. Dr. Kaoru Fujimoto, Hiroshima Takada, Yoko Murakami, Masaki Kobayashi and his family, Tani Haruki and Yoko Yamakuchi for the good relationship and good memory.

The kindness and love from my parents and my family, I am so appreciate. They helped and supported me always.

I would like to thank Dr. Jumluck Srinakrueng who adviced and supported me to work thesis project in Japan.

The help of Miss Touchakarn Boonyaprasit, Mr. Pitak Choomongkol and Mr. Pitt Pruksathorn for food sending and register when I was in Japan is also thanked.

Finally, I have to thankful officers, my friends and seniors at Department of Chemical Technology for their help, encourage and good friendship.

CONTENTS

PAGE

PAGE

LIST OF TABLES

TABLE **PAGE**

LIST OF FIGURES

FIGURE PAGE

FIGURE PAGE

FIGURE PAGE

CHAPTER 1

Introduction

Biomass is the product of photosynthesis and is thought to be one of the most promising renewable energy resources. Gasification of biomass with steam has been known to produce gases (H_2, CO, CO_2 and CH_4), light and heavy hydrocarbon (tar) and char. The complete gasification of biomass, which produces synthesis gas is a promising process for its utilization, where syngas can be converted to methanol, DME, hydrocarbons or hydrogen. Biomass gasification with steam is operated at high temperature (～1000 °C) to gasify all of biomass (including tar) or at lower temperature (～800 °C) while co-producing tar and hydrocarbons.

Chaudhari *et al.* [1] have studied the optimum conditions for producing gases from biomass-derived char to show that a steam flow rate of 2.5 g/h/g of the biomass derived char (BDC) and 650-700 °C are suitable for the production of synthesis gas having lower ratio (1.33) of H_2/CO. Biomass gasification with the fluidized bed by varying catalysts was studied and also was investigated with regard to the suitable parameters such as temperatures, steam/biomass ratio and biomass species to produced the higher yield of synthesis gas and tar removal. Asadullah *et al.* [2-8], Rapagna *et al*. [9] and Franco *et al.* [10] studied the biomass gasification in a fluidized bed reactor to find the suitable conditions. Asadullah *et al.* [2-8] developed two types of reactor which were single bed and duel bed reactors the different biomass types such as cedar wood, jute stick, baggase and rice straw. Single bed reactor was effective in the cedar gasification and not suitable for rice straw since the catalyst deactivated quickly because of the high ash content and fixed carbon. However, cedar wood, jute stick, baggase using the duel fluidized bed reactor with $Rh/CeO_2/SiO_2$ are effective at low temperature. Rapagna *et al.* [9] investigated the two stages gasification process, which composed of a fluidized bed gasifier and a secondary catalytic fixed bed reactor. Two types of nickel catalysts or calcined dolomite are tested after the fluidized bed gasifier, showing that fresh nickel catalysts are active for the reforming of methane and tars, where hydrogen is higher than 60% by volume. Franco *et al.* [10] have claimed that the temperature of 830 °C and steam to biomass ratio of 0.6-0.7 (w/w) could produce the higher gaseous products and reduce heavier hydrocarbons by 3-5%.

Recently, Ni-supported dolomite (Ni/Dolomite) catalyst [11-13] was studied for catalytic performance in the tar gasification to claim that it is an effective catalyst for fixed bed gasification of tar. The Ni/Dolomite catalyst showed excellent activity for the gasification of tar and its model compounds (toluene and naphthalene) and resistance against coking.

Tar elimination, which is heavy hydrocarbon, was investigated with catalyst. Srinakruang *et al.* [11-12] have claimed that Ni/Dolomite is the performance and effective catalyst for tar gasification. The characteristics of this catalyst were described elsewhere [11-13]. The structures of NiO, $NiMgO_2$ and CaO forms depended on the calcination temperature and reduction temperature to form reduced nickel ($Ni^{(0)}$). Furthermore, the support catalysts were also investigated such as dolomite, Al_2O_3 and SiO_2, which it found that Ni based on dolomite catalyst shows excellent catalytic activity and anti-coking character in steam gasification of toluene and naphthalene.

According to the literature reviews [2-8, 10, 14, 15-16], the apparatus in fluidized bed gasification process were developed to reduce tar and char. Most of the experimental set ups in the literature review were two stages, which one is the biomass gasification as the primary reactor and then gaseous products were flowed into the catalytic gasification as the secondary reactor. Nowadays, there were the applications to manage the gasification in the single reaction, which include pyrogasification, the catalytic tar and char gasification. Asadullah *et al.* [2-8] have modified the gasifier as the single-bed and duel bed and claimed that the rapid deactivation was found probably in the single bed because of high ash content (22.6%) and fixed carbon (28.4%) in the rice straw biomass. The duel-bed reactor inhibited the catalyst deactivation drastically.

In this research work, the experiment is divided into two parts. The first part is the basic studies of biomass pyrolysis and biomass pyrolysis followed by catalytic gasification with fixed bed. The characteristics of gas products are studied by Temperature Program Reaction (TPR) method. Also, char from biomass pyrolysis process is investigated the characteristics of steam gasification with and without catalyst by Temperature Program Reaction (TPR) method at higher temperature. The various types of biomass [solf wood and hard wood] are selected to study the decompositions of biomass pyrolysis and the characteristics of gas products.

The second part is of the biomass gasification with fluidized bed in the one stage reactor. The new efficiency apparatus of biomass catalytic steam reforming and gasification are set up and studied the gas products at the various parameters. The amounts of gases, tar and char at various parameters are presented in this book. Furthermore, the catalytic tar gasification was also studied with various types of Ni/Dolomite catalyst.

CHAPTER 2

Theory and Literature Reviews

Renewable energy is of growing importance in satisfying environmental concerns over fossil fuel usage and its contribution to the greenhouse effect. Wood and other forms of biomass are some of the main renewable energy resources available and provide the only source of renewable liquid, gaseous and solid fuels. Wood and biomass can be used in a various way to provide energy:

- by direct combustion to provide heat for use in heating, for steam production and hence electricity generation;
- by gasification to provide gaseous fuels which are subjected to combustion, or to an engine or turbine for electricity generation;
- by fast pyrolysis to provide a liquid fuel that can substitute for fuel oil in any static heating or electricity generation application. The liquid can also be used to produce a range of specialities and commodity chemicals.

2.1. Pyrolysis

Biomass is a mixture of hemicellulose, cellulose, lignin and minor amounts of other organics which each pyrolyse or degrade at different rates and by different mechanisms and pathways. Lignin decomposes over a wider temperature range compared to cellulose and hemicellulose which rapidly degrade over narrower temperature ranges, hence the apparent thermal stability of lignin during pyrolysis. The decomposition rate and extent of each components depends on the process parameters including reactor (pyrolysis) temperature, biomass heating rate and pressure. The degree of secondary reaction (and hence the product yields) of the gas/vapor products depends on the time-temperature history to which they are subjected before collection, which includes the influence of the reactor configuration.

Although some research has been carried out on the individual components of biomass, most applied and larger scale work has focused on whole biomass as the cost of pre-separation is considered too high. In addition, the separation and recovery of pure forms of lignin and hemicellulose are difficult due to structural changes in processing, although pure cellulose is relatively easy to produce.

Fast pyrolysis is a high temperature process in which biomass is rapidly heated in the absence of oxygen. As a result it decomposes to generate mostly vapors and aerosols and some charcoal. Liquid production requires very low vapor residence time to minimize secondary reactions of typically 1 s, although acceptable yields can be obtained at residence times of up to 5 s if the vapor temperature is kept below 400 ºC. After cooling and condensation, a dark brown mobile liquid is formed which has a heating value about half of that of conventional fuel oil. While it is related to the traditional pyrolysis processes for making charcoal, fast pyrolysis is an advanced process, which is carefully controlled to give high yields of liquid. Research has shown that maximum liquid yields are obtained with high heating rates, at reaction temperatures around 500 ºC and with short vapor residence times to minimize secondary reactions. A compilation of published data is shown in Figure 2.1 for typical products from fast pyrolysis of wood [17]. Fast pyrolysis processes have been developed for production of food flavours (to replace traditional slow pyrolysis processes which had much lower yields), speciality chemicals and fuels. These utilise very short vapor residence times of between 30 and 1500 ms and reactor temperatures around 500 ºC. Both residence time and temperature control is important to ``freeze" the intermediates of most chemical interest in conjunction with moderate gas/vapor phase temperatures of 400-500 ºC before recovery of the product to maximize organic liquid yields.

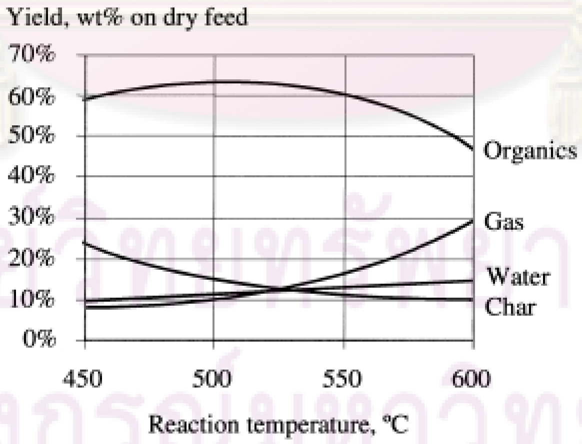

Figure 2.1 Typical yields of organic liquid, reaction water, gas and char from fast pyrolysis of wood, wt% on dry feed basis [17-23].

The essential features of a fast pyrolysis process are:

- very high heating and heat transfer rates, which usually requires a finely ground biomass feed;
- carefully controlled pyrolysis reaction temperature of around 500 ºC in the vapour phase, with short vapour residence times of typically less than 2 s;
- rapid cooling of the pyrolysis vapours to give the bio-oil product.

The main product, bio-oil, is a miscible mixture of polar organics (about 75-80 wt%) and water (about 20-25 wt%). It is obtained in yields of up to 80 wt% in total (wet basis) on dry feed, together with by product char and gas which are, or can be, used within the process so there are no waste streams. Liquids for use as fuels can be produced with longer vapour residence times (up to around 5 s) and over a wider temperature range although yields might be affected in two ways: secondary volatiles decomposition at temperatures above 500 ^{o}C and condensation reactions at gas/vapour product temperatures below 400 ºC. Most woods give maximum liquid yields of up to 80 wt% dry feed basis at 500-520 ºC with vapour residence times not more than 1 s. Very short residence times result in incomplete depolymerisation of the lignin due to random bond cleavage and inter-reaction of the lignin macromolecule resulting in a less homogenous liquid product, while longer residence times can cause secondary cracking of the primary products, reducing yield and adversely affecting bio-oil properties. Evidence from SEC (selective exclusion chromatography) analysis of the liquids would suggest that the reactor configuration and the dominant mode of heat transfer strongly influence the average molecular weight of the products [24-26].

It is important to remember that pyrolysis always gives three products (gas, liquid and solid) of which the liquid is a homogenous hydrophilic (oleophobic) mixture of polar organics and water from both the pyrolysis reaction and the original water in the feedstock. A sound understanding of the inherent processes will allow any of these products to be maximized and it is the engineer's challenge to optimize the process by maximizing product quantity and quality while paying proper attention to minimize costs and minimize environmental concerns.

There are two important requirements for heat transfer in a pyrolysis reactor:

1. to the reactor heat transfer medium (solid reactor wall in ablative reactors, gas and solid in fluid and transport bed reactors, gas in entrained flow reactors);
2. from the heat transfer medium to the pyrolysing biomass.

Two main ways of heating biomass particles in a fast pyrolysis system can be considered: gas+solid heat transfer as in an entrained flow reactor where heat is transferred from the hot gas to the pyrolysing biomass particle by primarily convection and solid + solid heat [27] and Aston [15-16]. Fluid bed pyrolysis utilises the inherently good solids mixing to transfer approximately 90% of the heat to the biomass by solid + solid heat transfer with a probable small contribution from gas-solid convective heat transfer of up to 10%. Circulating fluid bed [28] and transport reactors also rely on both gas + solid convective heat transfer from the fluidizing gas and solid + solid heat transfer from the hot fluidizing solid although the latter may be less significant than fluid beds due to the lower solids bulk density. Some radiation effects occur in all reactors. The important feature of ablative heat transfer is that the contact of the biomass and the hot solid abrades the product char of the particle exposing fresh biomass for reaction. This removes particle size limitations in certain ablative reactors (e.g. the NREL vortex reactor), but at the expense of producing microcarbon, which is difficult to remove from the vapor phase and reports to the liquid product. Attrition of the char from the pyrolysing particle can also occur in both fluid and circulating fluidized beds, due to contact of the biomass with in-bed solids where solids mixing occurs. In fluid bed reactors, however, attrition of the product char is relatively low and it has been observed that the char particles have the original particle shape, but are slightly reduced in size by char layer shrinkage and attrition.

Char removal is an essential requirement for large particles (>2 mm) to avoid slow pyrolysis reactions. The low thermal conductivity of biomass gives low heating rates through larger particles, which leads to increased char formation. Hot char is known to be catalytically active. It cracks organic vapors to secondary char, water and gas both during primary vapor formation and in the reactor gas environment. Therefore, its rapid removal from the hot reactor environment and minimal contact with the pyrolysis vapor products is essential.

Since the thermal conductivity of biomass is very poor (0.1 W/mK along the grain, ca 0.05 W/mK cross grain), reliance on gas+solid heat transfer means that biomass particles have to be very small to fulfil the requirements of rapid heating to achieve high liquid yields. Claimed temperature increases of 10,000 ^{o}C/s may be achieved at the thin reaction layer but the low thermal conductivity of wood will prevent such temperature gradients throughout the whole particle. As particle size increases, liquid yields reduce as secondary reactions within the particle become increasingly significant .

A consistent method of expressing product yields is required to remove ambiguities in the comparison of product yields. It is recommended that the water in the feed should be discounted in the final pyrolysis products with only the water of pyrolysis being quoted and the product yields expressed on a dry feed basis. As a rule of thumb, the water of pyrolysis is typically 12 wt% of dry feed.

It is necessary to distinguish between temperature of reaction and reactor temperature. The latter is much higher due to the need for a temperature gradient to effect heat transfer. For fast pyrolysis the lower limit on wood decomposition is approximately 435 ^{o}C for obtaining acceptable liquid yields of at least 50% with low reaction times. The effect of temperature is well understood in terms of total product yield with a maximum at typically 500-520 ^{o}C for most forms of woody biomass. Other crops may have maxima at different temperatures. The effect of temperature is less well understood in terms of product fuel quality.

The effect of vapour residence time on organic liquid yield is relatively well understood although the interaction of temperature and residence time is less understood. Studies by, for example, Diebold [27] has attempted to interlink both primary liquids formation and secondary cracking, but one essential component, which is neglected the variation of water yield with temperature and residence time. There is extensive literature on the mechanisms and pathways of fast pyrolysis, which has been reviewed [15-16]. It is believed that at temperatures below 400 ^{o}C, secondary condensation reactions occur and the average molecular weight of the liquid product decreases. Boroson et al. [29] have demonstrated that the average molecular weight decreases with the degree of secondary reaction, i.e. increasing residence time and temperature.

For chemicals, it is considered necessary to ``freeze'' the process at the appropriate time-temperature point in the envelope to maximise yield. In one case this has led to a commercial reactor design where vapour residence times down to 30 ms are claimed. Fuels have less specific process requirements and most work has focused on maximising liquid yield rather than product quality. There is no definition of product quality in terms of physical or chemical properties or composition, and this area will need to be addressed as more applications are tested and alternative supplies of bio-fuel-oil become available.

This has long been a major difficulty for researchers. The pyrolysis vapours have similar properties to cigarette smoke and capture by almost all collection devices is very inefficient. The product vapours are not true vapours but rather a mist or fume and are typically present in an inert gas at relatively low concentrations, which increases cooling and condensation problems. They can be characterised as combination of true vapours, micron sized droplets and polar molecules bonded with water vapour molecules. This contributes to the collection problem as the aerosols need to be impinged onto a surface to permit collection, even after cooling to below the dew point temperature. Electrostatic precipitators are effective and are now used by many researchers but can create problems from the polar nature of the product and arcing of the liquids as they flow, causing the electrostatic precipitator to short out. Larger scale processing usually employs some type of quenching or contact with cooled liquid product which is effective. Careful design is needed to avoid blockage from differential condensation of heavy ends. The rate of cooling appears to be important. Slow cooling leads to preferential collection of the lignin derived components, which is a viscous liquid which can lead to blockage of heat exchange equipment and liquid fractionation. Very rapid cooling of the product has been suggested to be effective as occurs typically in a direct contact quench. Transfer lines from the reactor through the cyclone(s) to the liquid collection system should be maintained at >400 ^{o}C to minimize liquid deposition and collection.

Some char is inevitably carried over from cyclones and collects in the liquid. Subsequent separation has proved difficult. Some success has been achieved with hot gas filtration in a ceramic cloth bag house filter [27] and also candle filters for short run durations. Liquid filtration has also proved difficult as the liquid can have a gel-like consistency, apparently due to some interaction of the lignin derived fraction with the char. This aspect of char reduction and/or removal will be increasingly important as more demanding applications are introduced which require lower char tolerances in terms of particle size and total quantity. Possible solutions include changing process conditions to reduce the nature of the pyrolytic lignin, increasing the degree of depolymerisation of the lignin-derived fraction of the liquid, changing the feedstock to one with a lower lignin content, or adding chemicals to the liquid for example to improve handling properties or reduce char-lignin interactions.

2.2 Gasification

It is customary to report the content of moisture, volatile matter, fixed carbon and ash as proximate analysis. Table 2.1 gives the proximate analysis of 13 biomasses reported by Raveendran et al [30]. Upon heating the biomass was dried up to 120 ^{o}C and was devolatalized the volatile matter up to 350 ^{o}C. Char was gasified above 350 ^{o}C. Therefore, it is customary to classify the entire gasifier process as drying, devolatiliation and gasification. Depending upon the nature of environment inert or reactive prevailing during gasification the process is called pyrolysis for inert environment and gasification for reactive environment. Pyrolysis is the devolatilization of volatile matter in inert medium to produce pyrolytic liquids, solid char and gaseous fuel. The liquid product may also be upgraded to refined fuels. The solid char may be used as a fuel. The gaseous fuel is high in hydrocarbons with high calorific value. Since the bulk density and calorific values of pyrolytic liquid and solid char are very high they have high-energy density compared to original mass [18-23]. When the environment is reactive (air) complete gasification of biomass takes place yielding gaseous fuel and ash.

Table 2.1 Proximate analysis of biomasses [30]

No.	Biomass	VM (daf) (%)	Ash (db) (%)	Fixed carbon (100 -VM)(%)
1	Bagasse	84.2	2.9	15.8
2	Coconut coir	82.8	0.9	17.2
3	Coconut shell	80.2	0.7	19.8
4	Coir pith	73.3	7.1	26.7
5	Corn cob	85.4	2.8	14.6
6	Corn stalks	80.1	6.8	19.9
7	Cotton gin waste	88.0	5.4	12.0
8	Groundnut shell	83.0	5.9	17.0
9	Millet husk	80.7	18.1	19.3
10	Rice husk	81.6	23.5	18.4
11	Rice straw	80.2	19.8	19.8
12	Subabul wood	85.6	0.9	14.4
13	Wheat straw	83.9	11.2	16.1

2.2.1. Variables

The variable affecting the rate of gasification are to be identified and quantified. The variables are given below:

No.	Variable	Characteristics	
1	Size	Big	Small
2	Shape	Powdery	Lump
3	Structure	Porous	Non-porous
4	Environment	Inert	Reactive
5	Flow of medium	Static	Continuous
6	Heating rate	Slow	Fast
7	Temperature	< 500 ^{o}C	> 500 ^{o}C
8	Ash	Catalytic	Non-catalytic

Since pyrolysis and gasification of biomass are thermochemical processes, the temperature and rates of heating have pronounced effects on the weight loss of biomass. Thermogravimetric analysis (TGA) measures and records the weight loss of sample biomass as the temperature is raised at desired uniform rate. In addition the effect of environment such as inert and reacting atmosphere with and without flowing can be studied. For determining the characteristics of pyrolysis and also kinetic parameters, TGA is used extensively. Kinetic parameters are calculated using the net weight loss with simplifying assumptions, which do not necessarily correspond to the complex chemical reaction in the thermal degradation of biomass. However, TGA data provide useful comparisons of reaction parameters such as temperature and heating rates.

2.2.1.1. Size

Smaller the biomass size better would be the heat transfer. The temperature would be uniform resulting in reaction taking place throughout the particle. Whenever reaction controls the gasification, the rate of reaction will be maximum and increase exponentially with temperature. However, there is a limitation on the size above which heat transfer would be controlling. Maa [31] has shown that the pyrolysis of cellulose material is reaction controlled for size less than 0.2 cm, for sizes 0.2–6 cm both heat transfer and reaction control, whilst above 6 cm heat transfer controls.

2.2.1.2. Shape

Bio-residues are generally powder in nature. At present they are pelletized before gasification so as to reduce the volume of gasifier. Pelletization consumes power thus reducing the available energy. Lumps on the other hand can be gasified conveniently. However, lumps beyond 6 cm size are not suitable. In order to have uniform rate of gasification yielding uniform composition of producer gas, the lumps are cut into small chips having size less than 2.5 cm. Chipping is also an energy consuming operation.

2.2.1.3. Structure

If the biomass is highly porous, the surface area for reaction is very high and the diffusion of the reactant/product would be easy. Uniform temperature could be achieved throughout biomass resulting in continuous reaction at all portions of biomass yielding uniform composition of product gases. When the biomass is less porous, the temperature varies from the maximum at the exterior to the minimum at the interior. The reaction takes place only at the exterior surface. This surface shrinks with reaction. Because of the non-uniformity in temperature, drying, pyrolysis and gasification take place simultaneously yielding non-uniform composition of gases. GrØnli et al [32] have studied thermogravimetric analysis and devolatilization kinetics of hard woods such as alder, beech, birch, oak, and soft woods such as Douglas fir, pine A, pine B, redwood and spruce. They have observed that in the case of soft woods, the decomposition starts at lower temperature, the maximum temperature of weight loss for hemicellulose is higher and hemicellulose & cellulose zones are wider.

2.2.1.4. Environment

Generally, it is observed that reactive environment (air/oxygen) results in complete gasification of biomass while inert environment (nitrogen/argon) aids devolatilization (pyrolysis) yielding more char. Pyrolysis of biomass has attracted the attention of many investigators [33-34] as it yields solid, liquid and gaseous fuel from biomass.

Commercial gasifiers employ air at substoichiometric quantity to generate producer gas. Depending upon the type of contact between biomass and air, the gasifier is called down draft, updraft or cross flow gasifier. Each type has its own advantages and disadvantages in generating quality producer gas. Thus, the understanding on the effect of environment on gasification has come to the natural end. Hence, the present gasifiers produce gases with low calorific values due to dilution by nitrogen.

2.2.1.5. Flow of medium

Williams and Besler [33-34] have observed that the secondary degradation of char to gases can be prevented in pyrolysis of biomass by sweeping away the devolatilized gases by inert gases such as nitrogen. This yields more char equal to fixed carbon content in the biomass. Therefore, many investigators have carried out the pyrolysis studies with flowing nitrogen. Safi et al [35] have carried out studies on global degradation kinetics of pine needles in air. An air flow rate of 50 ml/min was maintained. The char obtained at different heating rates were less than the available fixed carbon, due to the presence of reactive medium such as air. If the medium were static, then there is a possibility of secondary degradation of char taking place. This may result in complete gasification of biomass. However, no attempt is reported so far on the effect of static inert or static reactive medium on the gasification of biomass.

2.2.1.6. Heating rates

Bridgwater [18-23] reported the influence of pyrolysis reaction parameters such as temperature and heating rates to determine the yield and composition of the derived products. In fast pyrolysis with high heating rates of up to 1000 ^{o}C/min at temperature below 650 ^{o}C and with rapid quenching the liquid, intermediate products of pyrolysis condenses without further breaking down higher molecular weight species into gaseous products. Formation of char is minimized by high heating rates. Gaseous products form at high heating rates to high maximum temperature. If the desired end product is the liquid hydrocarbon or bio-oil, fast pyrolysis is preferred. Fluidized bed, cyclonic, entrained flow, vortex and ablative reactors are recommended for fast pyrolysis.

Slow pyrolysis requires low heating rates and low maximum temperature. Maximum yield of char via secondary coking and repolymerization reaction is observed at slow heating rates coupled with a low final maximum temperature (less than 500 ^{o}C) and with long gas and solid residence times. Therefore, slow pyrolysis has been used for the production of char. Fixed bed reactor, multiple hearths and rotary kiln are used for slow pyrolysis. Even though the rate of purging of gaseous products to prevent the secondary reaction influences the pyrolysis, no attempt has been made so far to evaluate its effect. William and Besler [33-34] have carried out a detailed study on the influence of temperature and heating rate on slow pyrolysis of biomass in a static batch reactor at heating rates of 5, 20,40 and 80 K/min to a final temperature of 300, 420, 600 and 720 ^{o}C with nitrogen as purging gas. Slow pyrolysis has yielded aqueous, oil, gas and char. The gaseous, liquid and solid products of pyrolysis are analyzed for composition, yield and calorific value.

The observations made are as follows:

- A decrease in the yield of char and a corresponding increase in the yield of oil and gas resulted with increase in temperature for each heating rate.
- At 420 ^{o}C and above, the aqueous yield remained virtually constant at about 37 wt%.
- Very high char yield has been obtained at 300 ^{o}C as char has retained partially pyrolysed material such as hydrocarbons of high molecular weight.
- The high molecular weight hydrocarbon within char volatilizes and degrades thermally as the temperature was increased.
- The oil yield increases steadily from 300 to 720 ^{o}C at all heating rates.
- The oils are highly oxygenated.
- An increase in carbon and hydrogen and a decrease in sulfur and oxygen contents of the oil with heating rates were observed.
- The gas yield also increases with temperature at all heating rates.
- The char yield decreases with temperature and with heating rates.
- The calorific values of oils and char were essentially independent of heating rates and were found to be an average 23 and 32 MJ/kg, respectively.
- The yields of CO, CO_2, H_2 CH_4 and C_2H_6 increased with heating rates.
- Total calorific values were 13.6, 15.7, and 15.8 MJ/m3 at heating rates of 5, 20, 40 and 80 K/min, respectively.
- The calorific values of gases were fairly independent of heating rates above 5 K/min.
- Water and oil were evolved throughout the higher temperature.

The advantage of gasification is that using the syngas is more efficient than direct combustion of the original fuel; more of the energy contained in the fuel is extracted. Syngas may be burned directly in internal combustion engines, used to produce methanol and hydrogen, or converted via the Fischer-Tropsch process into synthetic fuel. Gasification can also begin with materials that are not otherwise useful fuels, such as biomass or organic waste. In addition, the high-temperature combustion refines out corrosive ash elements such as chloride and potassium, allowing clean gas production from otherwise problematic fuels. Gasification of fossil fuels is currently widely used on industrial scales to generate electricity. However, almost any type of organic material can be used as the raw material for gasification, such as wood, biomass, or even plastic waste. Thus, gasification may be an important technology for renewable energy. In particular biomass gasification is carbon neutral.Gasification relies on chemical processes at elevated temperatures >700°C, which distinguishes it from biological processes such as anaerobic digestion that produce biogas. In a gasifier, the carbonaceous material undergoes several different processes:

1.The pyrolysis (or devolatilization) process occurs as the carbonaceous particle heats up. Volatiles are released and char is produced, resulting in up to 70% weight loss for coal. The process is dependent on the properties of the carbonaceous material and determines the structure and composition of the char, which will then undergo gasification reactions.

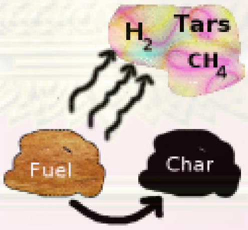

2. The combustion process occurs as the volatile products and some of the char reacts with oxygen to form carbon dioxide and carbon monoxide, which provides heat for the subsequent gasification reactions. Letting **C** represent a carbon-containing organic compound, the basic reaction here is $C + \frac{1}{2}O_2 \rightarrow CO$.

3. The gasification process occurs as the char reacts with carbon dioxide and steam to produce carbon monoxide and hydrogen, via the reaction. $(C + \frac{1}{2} H_2O \rightarrow CO_2 + H_2)$

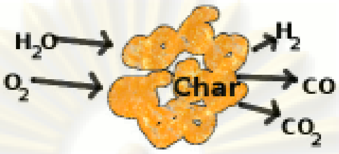

4. In addition, the reversible gas phase water gas shift reaction reaches equilibrium very fast at the temperatures in a gasifier. This balances the concentrations of carbon monoxide, steam, carbon dioxide and hydrogen. $(CO + H_2O \rightarrow CO_2 + H_2)$

In essence, a limited amount of oxygen or air is introduced into the reactor to allow some of the organic material to be "burned" to produce carbon monoxide and energy, which drives a second reaction that converts further organic material to hydrogen and additional carbon dioxide.

2.3. Biomass Pyrolysis and Gasification

Biomass is a renewable energy source because the energy it contains comes from the sun. Through the process of photosynthesis, chlorophyll in plants captures the sun's energy by converting carbon dioxide from the air and water from the ground into carbohydrates, complex compounds composed of carbon, hydrogen, and oxygen as shown in Figure 2.2. When these carbohydrates are burned, they turn back into carbon dioxide and water and release the sun's energy they contain. In this way, biomass functions as a sort of natural battery for storing solar energy. As long as biomass is produced sustainably—with only as much used as is grown—the battery will last indefinitely.

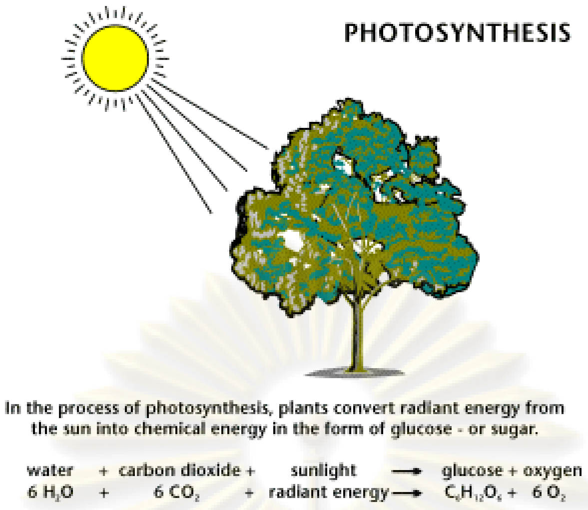

Figure 2.2 The process of photosynthesis in biomass production [36].

Gasification is a process that converts carbonaceous materials, such as coal, petroleum, or biomass, into carbon monoxide and hydrogen by reacting the raw material at high temperatures with a controlled amount of oxygen. The resulting gas mixture is called synthesis gas or syngas and is itself a fuel. Gasification is a very efficient method for extracting energy from many different types of organic materials, and also has applications as a clean waste disposal technique. The gasification of biomass is a developing energy technology among various systems for the energetic utilisation of biomass, which has the following main advantages compared to conventional combustion technologies.

1. The combined heat and power generation via biomass gasification techniques connected to gas-fired engines or gas turbines can achieve significantly higher electrical efficiencies between 22 % and 37 % compared to biomass combustion technologies with steam generation and steam turbine (15 % to 18 %). If the produced gas is used in fuel cells for power generation, an even higher overall electrical efficiency can be attained in the range between 25 % and 50 %, even in small scale biomass gasification plants and under partial load operation.
2. Due to the improved electrical efficiency of the energy conversion via gasification, the potential reduction in CO_2 is greater than with combustion. The formation of NO_x compounds can also be largely prevented and the removal of pollutants is easier for various substances. The NO_x advantage, however, may be partly lost if the gas is subsequently used in gas-fired engines

or gas turbines. Significantly lower emissions of NO_x, CO and hydrocarbons can be expected when the produced gas is used in fuel cells instead of using it in gas-fired engines or gas turbines.

3. Pyrolysis of biomass generates three different energy products in different quantities: coke, oils and gases. Flash pyrolysis gives high oil yields, but because of the technical efforts needed to process pyrolytic oils this energy generating system does not seem to be very promising at the present stage of development. However, pyrolysis as a first stage in a two-stage gasification plant for straw and other agricultural feedstocks posing technical difficulties in gasification does deserve consideration.

In most biomass gasification processes, air is used as gasifying agent with the result, that a low calorific value gas (3-5 MJ/m^3) is generated, which can be used after cleaning in gas-fired engines or gas turbines. For gas turbines connected to a steam turbine, medium calorific value gas (12-15 MJ/m^3) is more favourable than low calorific gas. Steam injection into the gas turbine combustion chamber (Cheng process) requires at least medium calorific value gas. The production of methanol or hydrogen via biomass gasification or the use of producer gas in low-temperature fuel cells also require either gasifiers operating with highly-enriched oxygen and steam or indirectly heated (allothermic) gasifiers must be used with steam as a gasification medium to generate the necessary medium calorific value raw gas with high hydrogen content.

Gasification of wood and wood-type residues and waste in fixed bed or fluidised bed gasifiers with subsequent burning of the gas for heat production is state of the art. The wood gasifiers employed primarily in the Scandinavian countries are used almost entirely for heat generation. Significantly greater technical problems are posed by gasification of straw and other solid agricultural feedstocks, which mostly have higher concentrations of nitrogen, sulphur, chlorine and alkalines. The gasification of herbaceous biomass is still at an early stage of research and development. Intensified development efforts on gasification technologies for herbaceous biomass feedstocks are desirable as the potential supply of this group of fuels is comparatively large.

Thorough gas cleaning and perfect adaptation of the gas from biomass gasification to the specific requirements of the gas utilisation systems are the prerequisites for gas use in gas-fired engines, gas turbines and fuel cells. Tar compounds can be removed effectively by increasing the gas temperature or by catalytic tar cracking with dolomite or nickel. However, even for wood gasifiers there is still no economically viable solution of the tar problem. None of the gasifier types currently on the market have been successfully tested in connection to gas-fired engines in long term operation under practical conditions in combined heat and power stations.

Gani A et al [37] studied on (1) analysis of the main compositions for several types of biomass, which includes Indonesian agricultural biomass of palm oil fiber and bagasse, (2) fundamental pyrolysis and combustion characteristics for the biomass samples selected by a thermo-gravimetric (TG) analysis, (3) the pyrolysis and combustion characteristics for the simulated biomass, which consists of mixture of cellulose with lignin chemicals, to discuss the effect of the cellulose and lignin content in the biomass on the pyrolysis and combustion characteristics, and (4) elucidation of the reason for difference of the reactivity for the actual biomass samples from that for the simulated biomass samples by means of observation of morphological change before and after the reaction.

As a representative result of the pyrolysis tests, Figures 2.4a and 2.4b show profiles of fraction of the mass decrease of combustibles for several types of biomass such as hinoki sawdust, rice husk, palm oil fiber, corn stalk, rice straw, larch bark and bagasse, comparing with the cellulose and lignin chemicals. The vertical axis represents fraction of mass decrease of combustibles. The cellulose and lignin chemicals are also tested as references since the biomass mainly consists of these compounds as shown in Figure 2.3. From both the figures, the pyrolysis starts at about 473 K for all of the samples. The combustibles in the biomass react at the two stages during pyrolysis. At the first stage, the mass rapidly decreases due to cellulose volatilization. After that, the slow mass decrease occurs at the second stage due to lignin decomposition. Focusing on pattern of the profile of mass decrease, trend of the mass decrease for bark differs from that for the others. The cellulose chemical decomposes at high decomposition rate within narrow temperature range. While, decomposition rate of the lignin chemical becomes slower than that of the cellulose chemical. Comparing these results for the actual biomass samples with those for the cellulose and lignin chemicals, the profile for bark relatively comes near to that for the lignin. This is because the bark contains the highest lignin content as shown in Figure 2.3. On the contrary, the profile for rice husks approaches to that for the cellulose. These results suggest that the volatilization behavior of biomass depends on its own component such as the cellulose and lignin content. Generally, the lignin is harder to decompose than the cellulose since part of lignin consists of benzene rings [37].

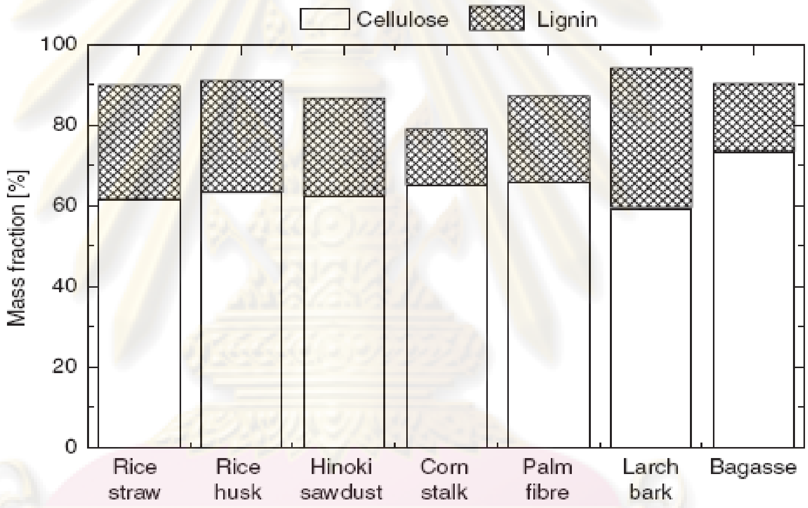

Figure 2.3 Cellulose and lignin contents in several types of biomass [37].

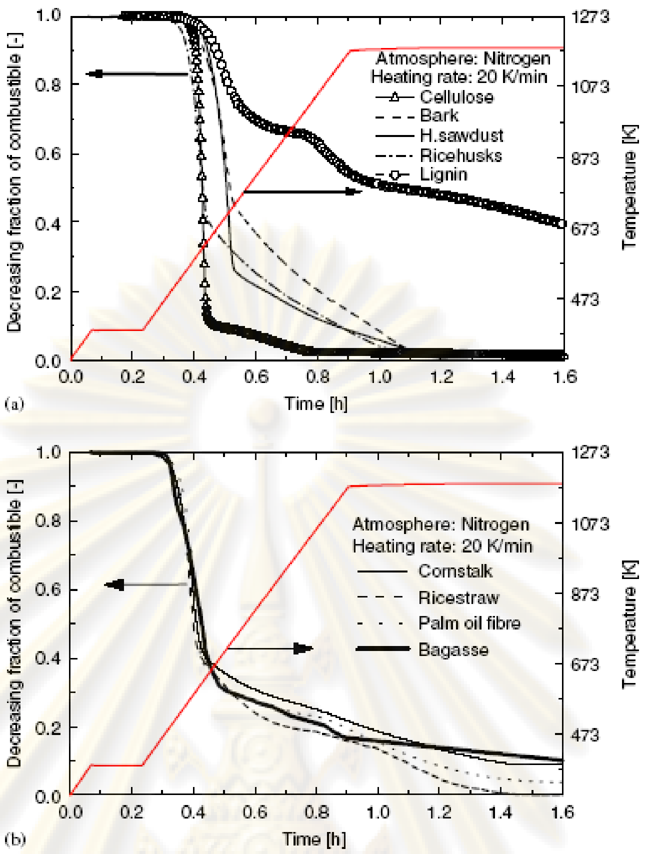

Figure 2.4 Residual fraction of combustibles for several types of biomass, cellulose and lignin during pyrolysis [37].

Changes of fraction of mass decrease of combustibles during combustion for several types of biomass, lignin and cellulose are shown in Figures 2.5a and 2.5b. Trend of the mass decrease for combustion differs from that for pyrolysis obtained before. The results show that the reaction rate for all of the samples during combustion becomes faster than that during pyrolysis. Comparing the result for bark with that for the lignin chemical, as an example, the reaction rate for bark becomes much higher than that for the lignin even if the lignin content in the bark is the highest of all of the biomass samples. These results suggest that cellulose content in the biomass may enhance the ignition characteristics and decomposition of lignin since the cellulose compounds have the structure of branching chain of polysaccharides and no aromatic compounds, which are easily volatilized. Consequently, the biomass will burn at the flowing steps. First, the cellulose components in the biomass are volatilized, so that the porosity in the char particles of biomass increases and that oxygen easily diffuses into the char particles. Next, the lignin components in the biomass can also react with oxygen diffused even if the reactivity of lignin itself is low. In other words, this discussion suggests that the char morphology will be one of the important indices to evaluate the biomass reactivity during combustion.

The results above-mentioned show the reaction characteristics for the actual biomass samples. Additionally, the results suggest that the cellulose and lignin content in the biomass affects the reactivity qualitatively. In order to quantitatively elucidate effect of the cellulose and lignin content on the pyrolysis and combustion characteristics for the biomass, the simulated biomasses are made by means of mixing the cellulose with lignin chemicals in various concentration ratios. In this experiment, the cellulose compositions of the simulated biomasses are varied from 0% to 100%, and the other component is lignin. Figures 2.6a and 2.6b shows profiles of mass decrease fraction of combustibles for several simulated biomasses with different cellulose and lignin contents during pyrolysis and combustion at heating rate 20 K/min, respectively. The results for pyrolysis show that the over all reaction rate decreases with an increase of the lignin content. Profiles of the mass decrease seem to cellulose and lignin contents during pyrolysis and combustion at heating rate 20 K/min, respectively. The results for pyrolysis show that the over all reaction rate decreases with an increase of the lignin content. Profiles of the mass decrease seem to rise up proportionally to the lignin content in the simulated biomass. While, for combustion, the similar tendency to the results for pyrolysis is obtained especially before about 0.8 h. After that, the mass suddenly decreases due to the lignin combustion. This result means that the lignin in the biomass controls the reaction rate during combustion.

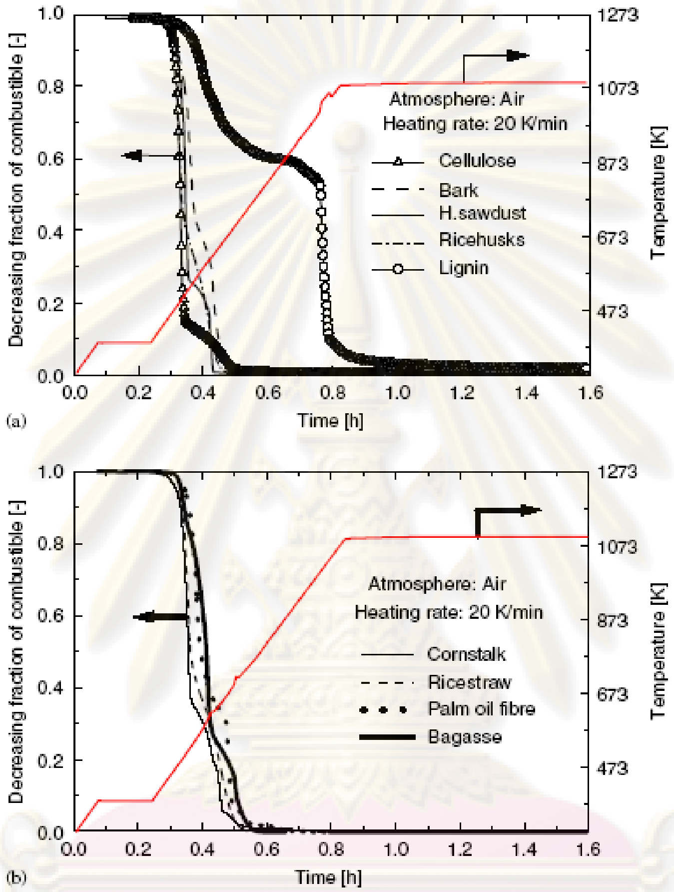

Figure 2.5 Residual fraction of combustibles for several types of biomass, cellulose and lignin during combustion [37].

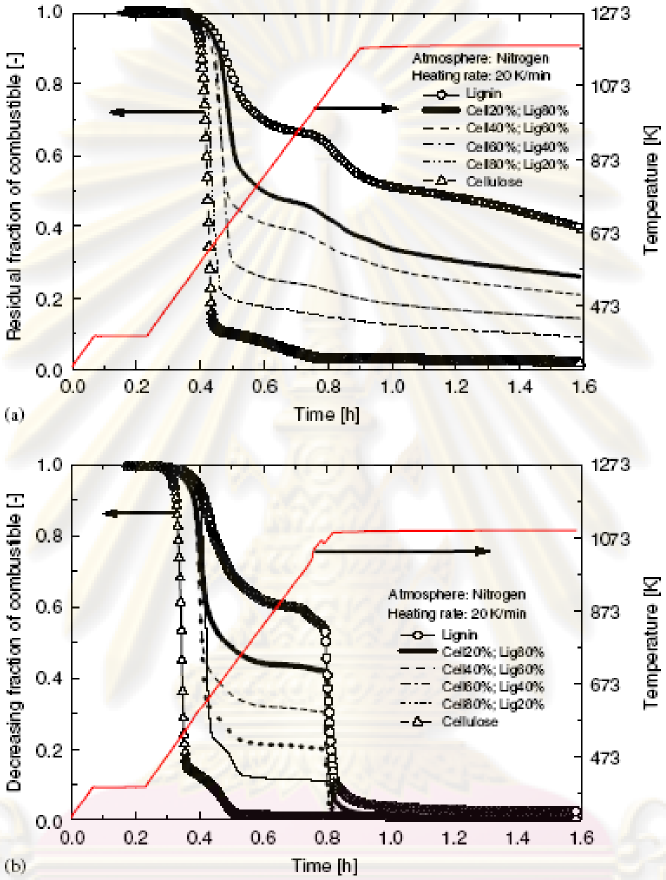

Figure 2.6 Residual fraction of combustibles of cellulose, lignin and their mixture [37].

Morphological change of the simulated and actual biomass samples before and after pyrolysis and combustion are observed by a scanning electron microscope (SEM). Figures 2.7a – 2.7c show the surface morphology of the raw material of Hinoki sawdust and the cellulose and lignin chemicals, respectively. It can be observed from this figure that Hinoki sawdust has fibrous and porous structure. The cellulose chemical also has the similar structure, as shown in Figure 2.7b. While, morphology of the lignin chemical is observed to be lumpy solid, as shown in Figure 2.7c. From these observation results, hinoki sawdust and cellulose chemical can easily decompose and burn, comparing with the lignin chemical. Figures 2.8a and 2.8b, as an example, shows the morphological structure after 1 h pyrolysis for Hinoki sawdust and the simulated biomass of 60% cellulose and 40% lignin, respectively. From Figure 2.8a, the morphology of the actual biomass is still to be fibrous and porous, even if the pyrolysis proceeds. Under this condition, oxygen can diffuse easily inside the particle during combustion. While the simulated biomass shown in Figure 2.8b, it can be observed that the cellulose and lignin chemicals seem to react individually. In other words, the lignin chemical does not react much, so that the shape of the lignin remains lumpy solid. This is one of the reasons why the combustion reactivity for the simulated biomass differs from that for the actual biomass samples. The combustion reactivity of the biomass deeply relates to the char morphology formed.

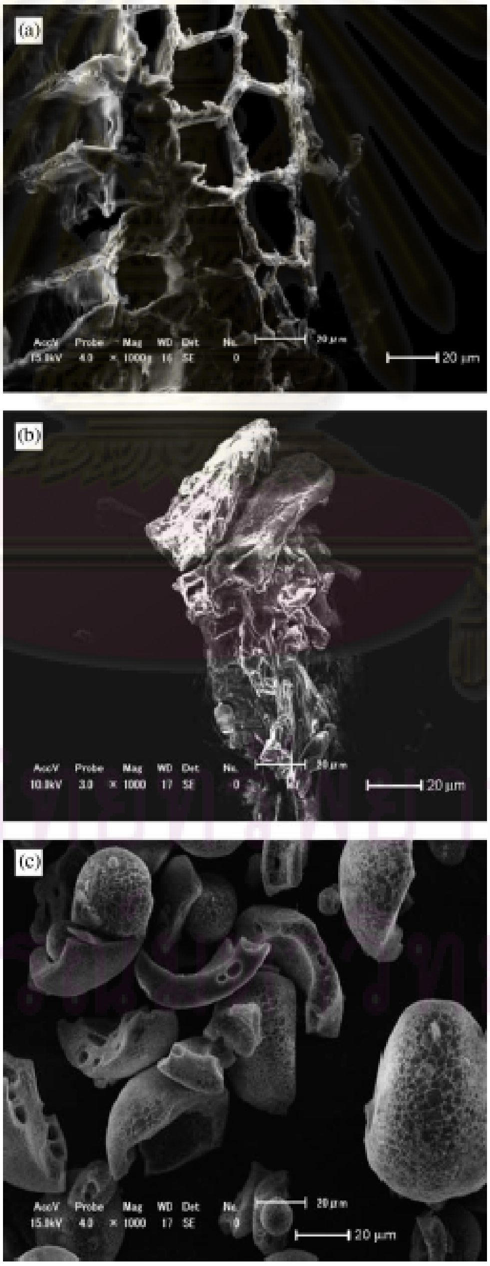

Figure 2.7 Morphology of (a) Hinoki sawdust, (b) cellulose, and (c) lignin chemicals before reaction [37].

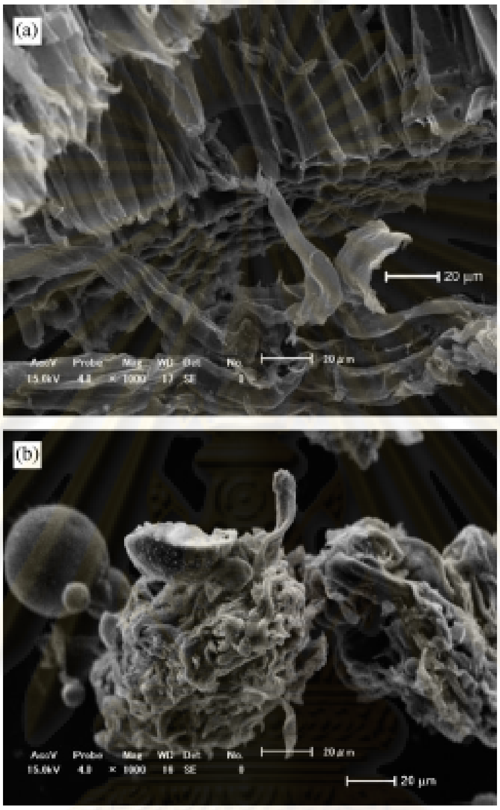

Figure 2.8 Morphology of (a) Hinoki sawdust and (b) the simulated biomass (60% cellulose; 40% lignin) after 1 h pyrolysis [37].

2.4. Definition and Composition of Tar [38]

Biomass fuels and residues can be converted to energy via thermal, biological and physical processes. Each process area is described with the greatest emphasis on the technologies that are attracting the most attention in the research, demonstration and commercial arenas. Thermo-chemical conversion covers different processes combustion, gasification and pyrolysis with interleaved boundaries. Biomass gasification is gaining attention as a route for biomass energy production, but producer gas from this process usually contains unacceptable levels of tar. Tar can cause operational problems in downstream processes by blocking gas coolers, filter elements and engine suction channels. Most producer gas applications also require removal of at least part of the dust and tar before the gas can be used. Hence, the tar control and convert is a key issue for a successful application of biomass-derived producer gas.

Tar is a complex mixture of condensable hydrocarbons, but a unique definition is lacking. Generally, producer gas from biomass gasifiers contains tar, which forms a serious problem for its use in e.g. engines and turbines. Besides tar also light hydrocarbons and ammonia are nearly completely removed. There are still many questions related to tar and the problems they may cause. Tar, itself is a complex mixture of condensable hydrocarbons, which still requires to be satisfactorily defined. It is also necessary to understand its composition and formation in order to design systems for its optimum removal or conversion and for minimizing its formation in the gasifier and interactions downstream to the end use device. As the formula (1) shows, the product gas formed from biomass gasification contains the major components CO, H_2, CO_2, CH_4, H_2O, and N_2 , in addition to organic (tars) and inorganic (H_2S, HCl, NH_3,alkalimetals) impurities and particulates.The organic impurities range from low molecular weight hydrocarbons to high molecular weight polynuclear aromatic hydrocarbons. The lower molecular weight hydrocarbons can be used as fueling as turbine or engine applications, but are undesirable products in fuel cell applications and methanol synthesis. The higher molecular weight hydrocarbons are collectively known as “tar”. These tars tend to be refractory and are difficult to remove by thermal, catalytic or physical processes. And also tar can condense or polymerize into more complex structures in exit pipes, heat exchangers or on particulate filters, leading to choking and attrition, which can result in decrease of total efficiency and a increase in the cost of the process. So the aspect of tar cracking or removaling as clean-up is one of the most important technical uncertainties in implementation of gasification technologies and is discussed below:

$$\begin{aligned}\text{Biomass} + O_2\,(\text{or } H_2O) &\rightarrow CO, CO_2, H_2O, H_2, CH_4 + \text{other hydrocarbons}\\ &\rightarrow \text{tar} + \text{char} + \text{ash} \qquad (1)\\ &\rightarrow HCN + NH_3 + HCl + H_2S + \text{other sulfur gases}\end{aligned}$$

One of the issues associated with biomass gasifier tars is how they are defined. More often than not, tar is given an operational definition by that conducting biomass gasification R&D. An excellent report by Milne et al. [39-40] describes in detail the operational definitions of biomass gasification tars as published. In the literature and provides a comprehensive survey of tar formation and conversion. It is not the intent of this report to provide the definition of “tars” but, for the most part , “tars’’ are considered to be the condensable fraction of the organic gasification products and are largely aromatic hydrocarbons ,including benzene. The diversity in the operational definitions of “tars” usually comes from the variable product gas compositions required for a particular end-use application and how the “tars” are collected and analyzed. Tar sampling protocols are being developed to help standardize the way tars Are collected [41]; however, these methods are not yet widely established. Regardless of how “tar” is defined, tar removal, conversion, or destruction is seen as one of the greatest

Tars are formed during gasification in a series of complex reactions. The formation of tar is highly dependent on the reaction conditions. Due to increased reaction temperature, secondary reactions occur in the gas phase which convert oxygenated tar compounds to light hydrocarbons, aromatics, oxygenates and olefins subsequently forming higher hydrocarbons and larger PAH intertiary processes [39-40]. The tar formations chime proposed by Elliott and and summarized by Milne [39-40] is presented in Figure 2.9, Elliott [42] reviewed the composition of biomass pyrolysis products and gasifier tars from various processes. Figure 2.9 shows the transition as a function of process temperature from primary products to phenolic compounds to aromatic hydrocarbons, and Table1 shows the classes of chemical components in each major regime based on GC/MS analysis of collected “tars”. In a later publication, Baker et al.[43] showed a conceptual relationship between the yield of “tars” and the reaction temperature as shown in Figure 2.10.They cited levels of “tar” for various reactors with updraft gasifiers having 12 wt% of wood and downdraft less than1%. Steam-blown, fluid-bed gasifiers had tar levels of 15% at 600 ^{o}C and 4% at 750 ^{o}C. For oxygen-blown fluid-bed, the levels of “tar” were 4.3% at 750 ^{o}C and1.5% at 810 ^{o}C. The entrained flow gasifier of Battelle Columbus Laboratories, operated at 1000 ^{o}C, had ‘‘tar’’ levels of 1%. Table 2.2 tabulates the variety of reported levels of ‘‘tar’’. For the tar element composition, not enough data were found to establish a relationship with temperature. The carbon, hydrogen and oxygen contents in tar do not seem to vary with temperature, but only a sample of four species with just few points was available as a support for this judgment. The mass percentage of carbon in tar remains approximately at 54.5%, the percentage of hydrogen at 6.5% and the percentage of all organic contaminants with a molecular weight larger than benzene [58].

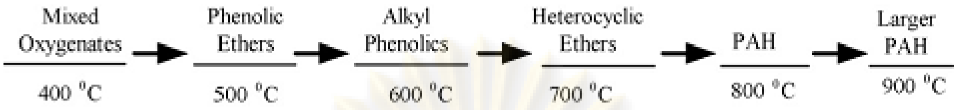

Figure 2.9 Tar maturation scheme proposed by Elliott [42].

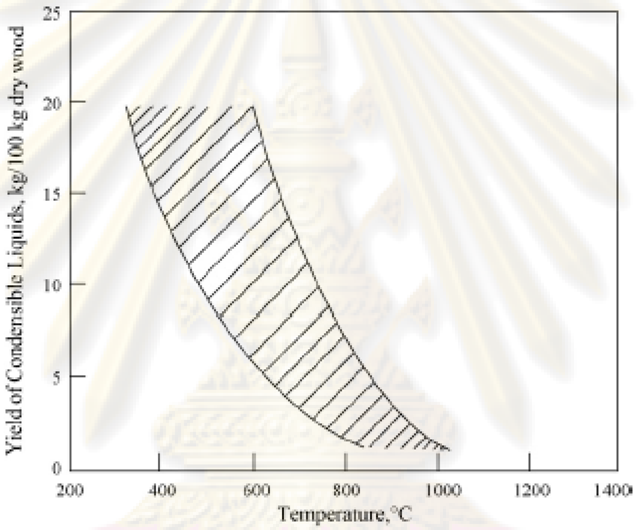

Figure 2.10 ‘‘Tar’’ yield as a function of the maximum temperature exposure [43].

2.4.1. *Tar classes*

Based on the molecular weight of tar compounds, some researchers [45-46] divided tar components into five groups, as shown in Table 1.Tar leads to fouling once the gas becomes (over) saturated with it. This leads to aerosol formation and depositions inside the installation. These fouling phenomena are not of concern as long as all the tar is present in the gas phase. It is therefore believed that the tar problem is fundamentally not concerned with the tar quantity, but is with the properties and the composition of the tar.

Table 2.2 List of tar compounds that are considered for different tar classes [38]

Tar class	Class name	Property	Representative compounds
1	GC-undetectable	Very heavy tars, cannot be detected by GC	Determined by subtracting the GC-detectable tar fraction from the total gravimetric tar
2	Heterocyclic aromatics	Tars containing hetero atoms; highly water soluble compounds	Pyridine, phenol, cresols, quinoline, isoquinoline, dibenzophenol
3	Light aromatic (1 ring)	Usually light hydrocarbons with single ring; do not pose a problem regarding condensability and solubility	Toluene, ethylbenzene, xylenes, styrene
4	Light PAH compounds (2–3 rings)	2 and 3 rings compounds; condense at low temperature even at very low concentration	Indene, naphthalene, methylnaphthalene, biphenyl, acenaphthalene, fluorene, phenanthrene, anthracene
5	Heavy PAH compounds (4–7 rings)	Larger than 3-ring, these components condense at high-temperatures at low concentrations	Fluoranthene, pyrene, chrysene, perylene, coronene

The condensation behaviour of tar is an integral effect of all tar components that are present in the syngas. The components their individual contribution to the total tar vapour pressure is there in decisive. When the tar vapour pressure exceeds the aturation pressure of the tar, the gas becomes (over) saturated according Raoult's Law [47]. Thermodynamically, this state leads to condensation of the saturated vapour. The tar dewpoint is the temperature at which the real total partial pressure of tar equals the saturation pressure of tar. Hence, in condensation related issues, the tar dewpoint is a powerful parameter to evaluate the performance of gas cleaning systems. It is believed that, when the dewpoint of tar is reduced to levels below the lowest expected temperature, fouling related problems by condensation or tar aerosols are solved. To use this approach in design issues, a calculation tool has been developed to predict the tar dewpoint on basis of the concentration of the individual tar components in the syngas. An illustration of the relation between the tar dewpoint and tar concentration is summarized by Bergman [48] and shown in Figure 2.11. Condensation curves are given for the individual tar classes, e.g. the dewpoint curve for class 5 is calculated including only class 5 tars. Furthermore, each tar component is contributes equal to the total concentration on mass basis. The dewpoint calculation excludes tar class 1, as the components are not known. For a CFB gasifier it is believed that tars that belong to class 1 start to condense around 300–350 °C [48]. Even at low class 5 tar concentration of circa 0.1 mg/m^3, the corresponding dewpoint (°C) exceeds the dewpoint valid for high concentration of class 2, 3, and class 4 tar (e.g. 1000 mg/m^3). It can be derived from Figure 2.11 that class 5 tars dominate the dewpoint of tar. Even for very low concentrations of class 5 tars (e.g. <1 mg/m^3) a dewpoint below 100 °C can be obtained. The graph clearly points out that, dependent on the concentration in the syngas, classes 2 and 4 need to be partially removed for a proper tar dewpoint of about 25 °C. The class 3 tar compounds do not condense at concentration as high as 10,000 mg/m^3, and play an unimportant role in this matter.

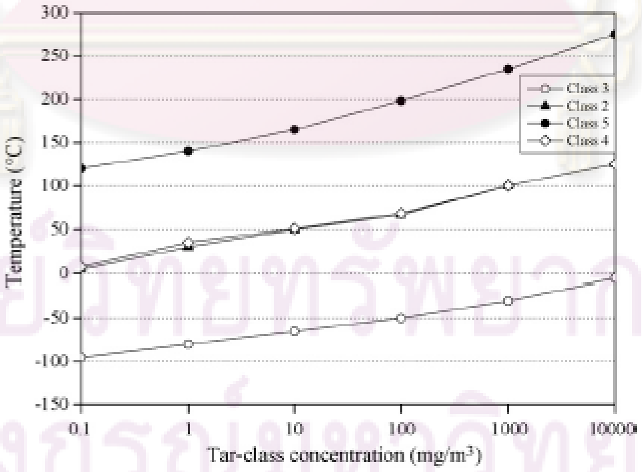

Figure 2.11 The tar dewpoint of the different tar classes in relation to the concentration [38].

2.4.2. Tar heat enthalpy and entropy

Evaluation of the thermodynamic properties of tar is important in the development and analysis of biomass or coal related processes as gasification, liquefaction, pyrolysis. Specifically, the evaluation of the enthalpy and entropy of these compounds is essential for performing first and second law analyses. Until now several studies have been made on the specific heat, enthalpy, and entropy of tar. Eisermann [49] proposed one method for evaluating the specific heat, enthalpy, and entropy of tar. Hyman and Kay [50] proposed one correlation formula for the specific heat of the tar produced in the gasification of coal:

$$C_T = \frac{1}{D}(4.94 \times 10^{-3} T) \tag{1}$$

where C_T is the specific heat (kJ/kg tar K), D the specific gravity at 289 K/289 K and T is the temperature (K).

For the formula, Lowry [28] proposed that using a typical specific gravity value of 1.17, the equation can be rearranged to give:

$$C_T = 4.22 \times 10^{-3} T \tag{2}$$

standard enthalpy of tar.

Tar produced from different resource, the results is different, for example, two widely different coals (a Pittsburgh seam and a Wyodak seam) have been given a heat content value of 130,000 BTU per gallon. Eisermann *et al.* [49] proposed the following equation for the enthalpy and entropy:

$$H = H^o + \int C_T dT, H^o = -\Delta H^o + \eta_C H^o_{CO_2} + \eta_S H^o_{SO_2} + \frac{\eta_H}{2} H^o_{H_2O}, \Delta H^o$$

$$= 30{,}980 kJ/kJtar, S = S^o + \int \frac{C_T}{T} dT, S^o \tag{3}$$

$$= a_1 + a_2 \exp\left(-a_3\left(\frac{H}{C} + N\right)\right) + a_4\left(\frac{O}{C+N}\right) + a_5\left(\frac{N}{C+N}\right) + a_6\left(\frac{S}{C+N}\right)$$

where S^o is the standard entropy (kJ/kmol carbon K), $a_1 = 37.1635$, $a_2 = -31.4767$, $a_3 = 0.564682$, $a_4 = 20.1145$, $a_5 = 54.3111$, and $a_6 = 44.6712$.

Thunman [51] proposed the another formula of heating value of tar. A general assumption for the heating value of tar is that the composition of tar is close to that of wood between 673 and 923 K, so the heating value of tar is between 22 and 26 MJ/kg (combustible substance), and between 973 and 1273 K, the composition is close to that of lumped hydrocarbons, whose heating value is about 40 MJ/kg. However, no further data were found to make a model. So, initially, it was thought that the heating value of tar could be determined from the heating value of its components, but the different substances present in tar and their amount were too difficult to find. Finally, a general correlation of Mason and Gandhi [52] was adopted:

$$HHV = 146.58X_{C,tar} + 568.78X_{H,tar} - 51.53X_{O,tar} \qquad (4)$$

where HHV is the high heating value, is expressed in Btu/lb. As 1 Btu/lb = 2.326 kJ/kg, it becomes in kJ/kg: $HHV = 340.95\ X_{C,tar} + 1322.98\ X_{H,tar} - 119.86\ X_{O,tar.}$

2.4.3. Tar analysis

During the past decades, several institutes have developed methods for the sampling and analysis of tars, on-line and offline. The sampling part of the off-line methods is based on trapping the tar by condensation on cold surfaces or filters, by absorption in a cold organic solvent or by adsorption on a suitable sorbents. The analysis of the tars is most often performed by gas chromatography (GC) or gravimetrically (by weighing the collected tars, after careful evaporation of the solvent and condensed water). The latter method has been used for over a decade in the framework of the worldwide UNDP/World Bank monitoring program. Recently, on-line methods have been developed and improvements of these methods are being further investigated. Among these methods, the European tar protocol is the most popular and accepted by researchers.

In the series of impinger bottles, the first impinger bottle acts as moisture collector, in which water and tar condensed from the process gas by absorption in isopropanol. The heat released by gas cooling and condensation is removed either in an external water bath or by an additional heat exchanger before the condenser. The heat exchanger may be necessary for high moisture producer gases (e.g. from steam gasification) and should be designed to meet the demands of the gasifier. The condenser is a standard impinger bottle or can optionally be equipped with an internal liquid quench system which is especially suitable for producer gases containing higher tar levels. When using a liquid quench, isopropanol is the circulating liquid. After the moisture collector the gas is passed through a series of 4 impingers with solvent and 1 final impinger which is empty. Direct condensation of the liquid effluent without diluting media, e.g. with cold trapping, can result in further reaction of the trapped compounds. Finemeshed frits give better results than coarse-meshed frits; G3 frits should be installed in the impinger train. If G3 frits give a too high a pressure drop (e.g. 0.5 bar), G2 frits should be used. Petersen column is an alternative equipment for the 6 impinger bottles in Figure 2.12, which consists of two washing stages filled with isopropanol. It is jacket cooled. The cooling fluid and cooling temperature can be selected as required. Gas chromatograph is the main analysis apparatus, which is (or should be) fitted with a capillary column, a flame ionization detector and a data processing system. The stationary phase of the capillary column should be bonded poly(5%diphenyl/95%dimethylsiloxane). The recommended dimensions are an internal diameter of 0.25–0.32 mm and a length of 30–60 m. It should be noted that this length is suited to the defining of total GC-tar but for determining individual compounds the length is suited to the defining of total GC-tar but for determining individual compounds the length may be to short. The typical gas chromatograph parameters are: column temperature program: 50 ^{o}C for 5 min. To 325 ^{o}C at 8 ^{o}C/min, stop for 5 min; injector: split, 1:75; injector temperature: 275 ^{o}C; detector temperature: 300 ^{o}C; injection volume: 1–2 ml; carrier gas: hydrogen or helium, column pressure adjusted so that the linear velocity of hydrogen is 30–55 cm/s and helium 20–40 cm/s.

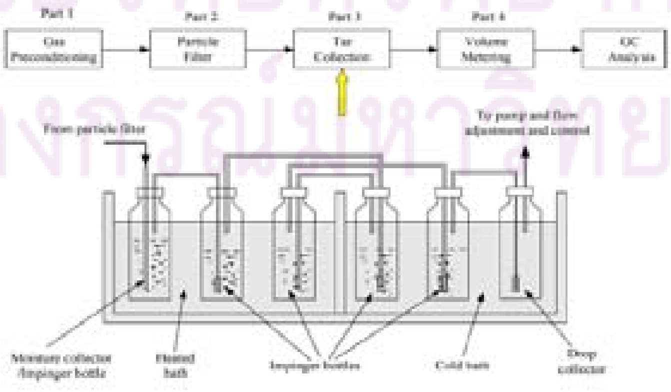

Figure 2.12 Collection of moisture and tar [38].

2.4.4. Tar and char formation behavior **[53]**

Pyrolysis behavior of wood at gasification temperature (800 °C) was investigated focusing on the behaviors of the wood constituent polymers [cellulose, hemicellulose (glucomannan and xylan) and lignin (milled wood lignin)] by T. Hosoya *et al.* [53]. Tar compositions (iso-propanol-soluble and water-soluble tar fractions), which were characterized with GPC, GC–MS, GC-FID (oxime-TMS analysis), capillary electrophoresis and ^{1}H NMR analysis, were quite different between wood polysaccharides and lignin.

Figure 2.13 shows the reactors after pyrolysis in N_2 at 800 °C for 30 s with the temperature profile of the reactor. Both i-PrOH and water-soluble fractions from wood polysaccharide samples (cellulose, glucomannan and xylan) and milled wood lignin (MWL) were recovered form the upper part (>14 cm from the bottom) of the reactor wall with the corresponding wall temperature of less than 400 °C. Secondary char (char after volatilization) formation behavior was different between wood polysaccharide samples and MWL.Wood polysaccharide samples formed secondary char at the reactor wall (10–16 cm from the bottom) and this was very close to the place where tar fractions were recovered. Only very small amount of carbonized products were observed around 2–10 cm from the bottom of the reactor. On the other hand, secondary char from lignin was observed from the bottom to the upper side of the reactor continuously. These differences would derive from the different reactivities of the volatile products toward carbonization as described later.

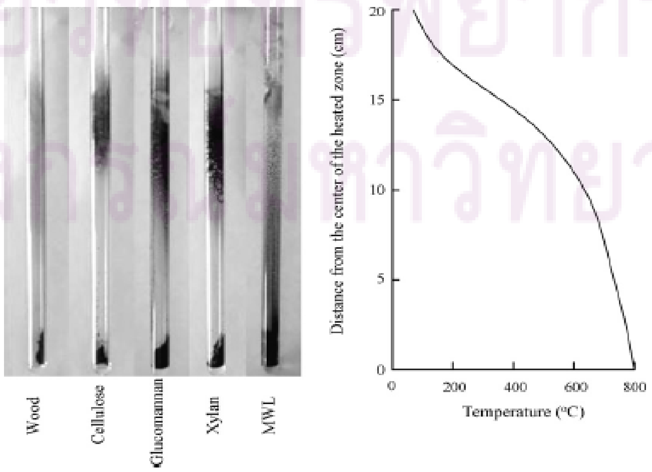

Fig. 2.13 Pyrolysis reactors after pyrolysis of wood and its constituent polymers in N_2 at 800 °C for 30 s with the temperature profile of the furnace [53].

2.4.5. Fractional composition of the pyrolysis products

Table 2.3 summarizes the fractional compositions (oven dry basis) of the pyrolysis products. Cellulose formed small amount (10.0 wt%) of char with large amount (72.0 wt%) of the tar fraction, while MWL (lignin) produced large amount (40.6 wt%) of char with comparatively small amount (38.2 wt%) of the tar fraction. Hemicellulose (glucomannan and xylan) showed the tendency between cellulose and MWL. These results are also supported with the papers [53, 30]. The amount of the product water was positively related with the amount of the char fraction in the wood polysaccharides pyrolysis. MWL produced much less amount of the product water although substantial amount of the char fraction is formed. These differences are understandable with their different chemical structures. Lignin has aromatic rings which are in more dehydrated states than the sugar moiety of wood polysaccharides. It is also noted that wood polysaccharide samples, especially cellulose, formed substantial amounts (5.2–21.6 wt%) of the water-soluble fractions.

Table 2.3 Fractional compositions after pyrolysis of wood and its cell wall constituents (wt%, oven dry basis)

	Gas	Tar			Product water	Char
		Total	i-PrOH-soluble	Water-soluble		
Wood	11.4	41.6	37.1	4.5	9.2	37.7
Cellulose	12.9	72.0	50.4	21.6	5.1	10.0
Glucomannan	13.0	41.3	32.3	9.0	15.3	30.4
Xylan	14.1	54.3	49.1	5.2	11.5	20.1
MWL	12.1	38.2	37.1	1.1	9.2	40.6

2.4.6. i-PrOH-soluble fraction

Figure 2.14 shows the GPC chromatograms (Detector: UV220 nm) of the i-PrOH-soluble fractions. Although the products analyzed in these chromatograms are only those with the adsorbing ability of UV220 nm, the products are observed in wide MW ranges of 100–2000 as polystyrene standard. These results indicate that the i-PrOH-soluble fractions contain certain amount of high MW products, which are difficult to be analyzed with GC. With refractive index (RI) detector, GPC analysis was difficult due to a large peak of the solvent, i-PrOH. The chromatographic pattern obtained from wood is observed as a sum of those from wood polysaccharide samples and MWL.

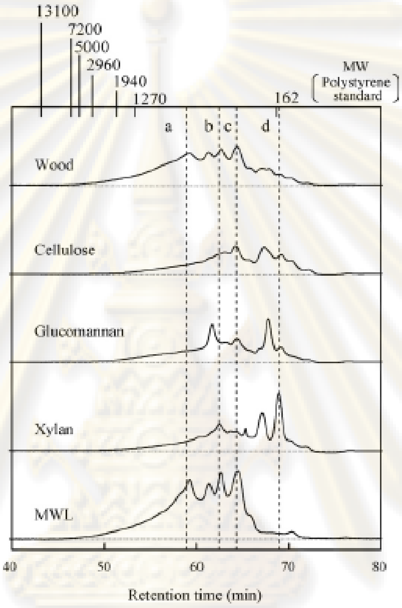

Figure 2.14 GPC chromatograms of i-PrOH-soluble fractions obtained from wood and its constituent polymers. Retention times of 4,40-dihydroxy-3,30-dimethoxy-stilbene (a), coniferylaldehyde (b), vanillin and 5-hydroxymethylfurfural (c) and furfural (d); detector: UV220 nm [53] .

Figure 2.15 shows the total-ion chromatograms of the i-PrOH soluble fractions in their GC–MS analysis. Identification of the products was conducted with the retention times and mass fragmentation patterns compared with those of the authentic compounds. Table 4 summarized the identification results with their major mass fragments. Identification of compounds 6, 7, 11 and 24 was carried out by comparing their mass fragmentation patterns. Wood polysaccharide samples formed the products categorized into C_2–C_3 carbonyls, anhydrosugars, carboxylic acids, furans and C_5–C_6 carbonyls, although their yields were different between wood polysaccharide types. 2-Hydroxymethylenemethylene-tetrahydrofuran-3-one (7) is a specific product inxylan pyrolysis with revision of the chemical structure. Compound

15 with an expected MW of 114 is also observed as a large peak. Although compound 15 has not been identified yet, the crystals were isolated with the same MW and different melting point from compound 7 in the syrup obtained by dry distillation of xylan. Benzene-type aromatic compounds were not detected from wood polysaccharide samples. On the other hand, aromatic monomers with 4-hydroxy-3-methoxyphenyl (guaiacyl) moiety, which is the consistent aromatic ring of Japanese cedar wood lignin, were mainly identified in the i-PrOH-soluble fraction from MWL. Many of these products contain carbonyl and/or $C_\alpha = C_\beta$ groups. Dimeric aromatic compounds were scarcely observed in the chromatograms probably due to their low volatility. It is also noted that demethylation products such as catecol-type compounds, which are expected to be formed through homolytic cleavage of phenyl-methyl ether at this temperature, were scarcely observed in the chromatogram. Table 5 summarizes the yields (oven dry basis) of some major products from wood polysaccharides determined by oxime-TMS analysis (for C_2–C_3 carbonyls, anhydrosugars and furans) and CE (for carboxylic acids). Total yields of these products correspond to 18.7–43.7 wt% of the i-PrOH-soluble fractions.

2.4.7. Reaction mechanism and kinetic

Tar decomposition mainly occurs due to cracking, steam and dry reforming reactions as shown below [53].

Cracking: $pC_nH_x \rightarrow qC_mH_y + rH_2$.

Stream reforming: $C_nH_x + nH_2O \rightarrow (n + x/2)H_2 + nCO$.

Dry reforming: $C_nH_x + nCO_2 \rightarrow (x/2)H_2 + 2nCO$.

Carbon formation: $C_nH_x \rightarrow nC + (x/2)H_2$.

C_nH_x represents tar, and C_mH_y represents hydrocarbon with smaller carbon number than C_nH_x.

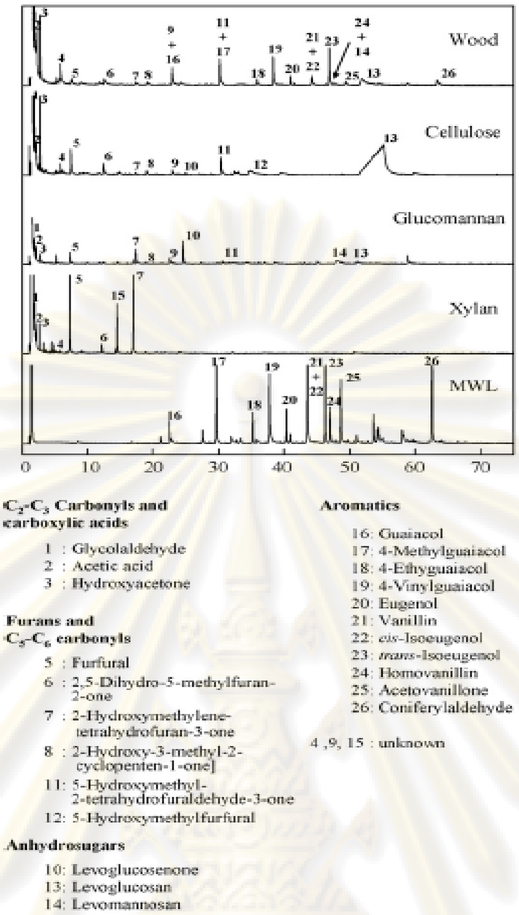

Figure 2.15 Total-ion chromatograms of i-PrOH-soluble tar fractions obtained from wood and its constituent polymers in GC–MS analysis[53].

2.4.8. Decomposition mechanism

After analysis of experimental results, Jess [54] presented the reaction scheme of thermal conversion of tar (aromatic hydrocarbons) in the presence of H_2 and H_2O, and shown in Figure 2.16. From which, it is can conclude that benzene is the key component of thermal decomposition of tar (aromatic hydrocarbons), and a carbonaceous residue (soot) is formed, above all from naphthalene. The soot as well as the organic cracking products (e.g. methane) primarily formed react with H2O in consecutive reaction steps. He also pointed that the thermal conversion of aromatic hydrocarbons in product gases from pyrolysis and gasification of solid fuels, temperatures of ~1200 ^{o}C are necessary at residence times of technical relevance (<10 s). To convert the soot and organic cracking products primarily formed to CO and H_2, even higher temperatures of at least 1400 ^{o}C are required.

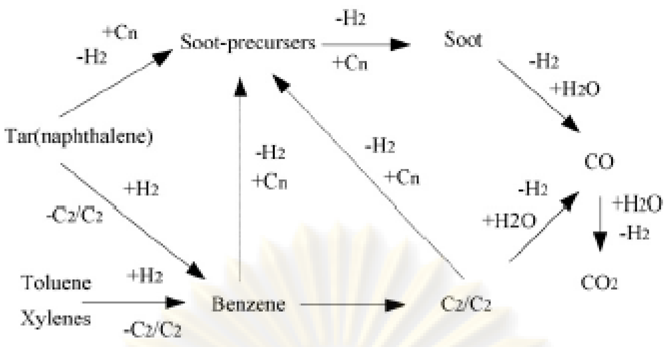

Figure 2.16 Simplified reaction scheme of thermal conversion of aromatic hydrocarbons the presence of hydrogen and steam [38].

Nair *et al.* [55] proposed naphthalene decomposition scheme by Pulsed Corona method, and shown in Figure 2.17, which is proposed according to the product distribution observed during experiments. By products were mainly formed by an oxidation mechanism. Intermediate compounds seen in Figure 2.17 lead to byproduct formation of naphthalene-dione and phthalicanhydride, which was observed by GC/MS analysis, as well. The main path for ring opening is via naphthoxy formation and its decomposition to indenyl via a thermal mechanism, which largely governs the decomposition scheme. After analysis and discussion, he proposed the complete scheme for corona processing in a fuel gas mixture as shown in Figure 2.18.

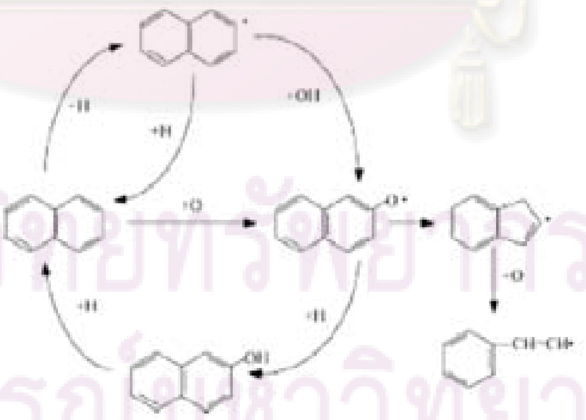

Figure 2.17 Naphthalene decomposition scheme [38].

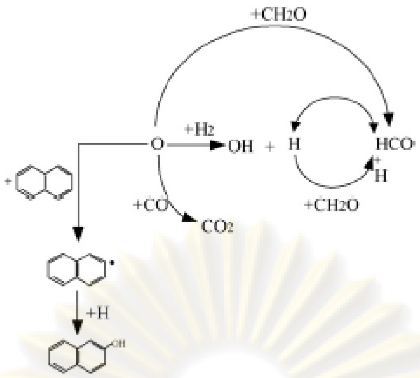

Figure 2.18 Main reaction pathways for reactive radicals in corona processing of fuel gas for naphthalene removal at 200 °C [38] .

Unimolecular and bimolecular decomposition mechanism for tar transformations, and give a example, unimolecular reactions and bimolecular decomposition of vanillin, is shown in Figures. 2.19 and 2.20.

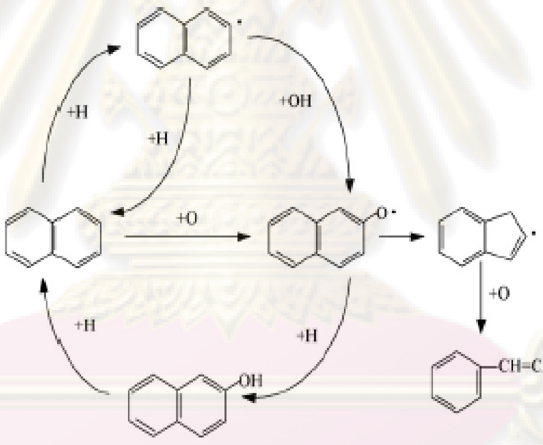

Figure 2.19 Unimolecular reactions of vanillin [38].

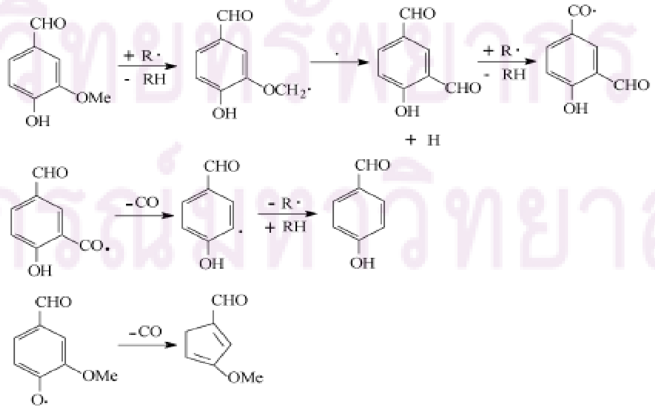

Figure 2.20 Bimolecular decomposition of vanillin [38].

2.5. Reaction Kinetic

2.5.1. Model component

Because of the complexity of tar, several researchers have studied these decomposition reactions using model biomass tar compounds such as phenol, toluene, 1-methyl-naphthalene, naphthalene and so on. The general reaction kinetic equations used are shown in the following:

$$-r_{tar} = k_{app}C_{tar}, k_{app} = \frac{[-\ln(1-X)]}{\tau}, \tau = \frac{W}{v_0}, k_{app}$$

$$= k_{0,app}e^{(-E_{app}/RT)} \qquad (1)$$

Devi *et al.* [56] used naphthalene component as the tar model, the catalytic activity of olivine is investigated via steam reforming. During dry reforming reaction with CO_2, naphthalene conversion of about 80% is observed and both steam and dry reforming reaction of naphthalene forms more than 50% gaseous products over 10 h pretreated olivine. The apparent rate constant and the apparent activation energy for naphthalene decomposition, over 10 h pretreated olivine under syngas mixture, is calculated assuming a first-order reaction with respect to naphthalene. The temperature dependency is calculated according to Arrhenius' Las, apparent activation energy for naphthalene conversion over 10 h pretreated olivine calculated is 187 kJ mol^{-1} with frequency factor of 2.06 x 10^9 m^3 kg^{-1} h^{-1}.

Jess [54] used naphthalene, toluene and benzene as aromatic hydrocarbon. The kinetics of the thermal conversion in the presence of hydrogen and steam were studied. The experiments were performed in a tubular flow reactor at a total pressure of 160 kPa, temperatures of 700–1400 ^{o}C, residence times of 0.3–2 s and different gas-phase concentrations of hydrogen, steam and the aromatics. The mechanisms of primary and consecutive reactions are presented as reaction schemes that are supported by kinetic calculations. The following order of reactivity is obtained: toluene >> naphthalene > benzene. Besides gaseous organic cracking products such as methane and ethane, condensed products and a carbonaceous residue (soot) is formed, principally from naphthalene. Soot formation is strongly inhibited by hydrogen. Steam has only a little influence on the conversion of the aromatics. Under the given reaction conditions, neither the soot primarily formed nor the organic cracking products such as methane are completely converted by steam to carbon monoxide and hydrogen, even at the highest temperature.

Swierczynski *et al.* [57-58] use toluene as model component of tar. A model study in laboratory scale fixed bed reactor of toluene steam-reforming is studied, the toluene conversion obtained with Ni/olivine at 560 ^{o}C is the same as with olivine at 850 ^{o}C. A kinetic model established, taking into consideration a zero order for water and first-order for toluene gives the kinetic parameters (E_a = 196 kJmol^{-1} and A (k') = 3.14 x 10^{13} m^{3} (kg cat h^{-1}) comparable to those reported for steam-reforming of benzene or tars on commercial nickel catalysts

Taralas *et al.* [59] used toluene as model component of tar. Thermal destruction of vaporized toluene in the presence of a [N_2 + H_2O + O_2] in air and [N_2 + H_2 + H_2O] gas mixtures are examined. Experiments were performed in a non-isothermal tubular flow reactor at a total pressure of ca. 101.3 kPa, temperature range of 973–1223 K. In presence of oxygen containing molecules (molar ratios of [H_2O + O_2]/C_7H_8 were varied between 1.78 and 3.52), a first-order reaction rate could express the effects of temperature and residence time. Thermal destruction of toluene in [N_2 + H_2 + H_2O] gas mixture ([H_2 + H_2O]/C_7H_8) 3.52, and ($0.40 < \tau < 0.90$ s) was studied as reference. Activation energies of the thermal destruction of toluene are: 356 ± 5 kJ mol^{-1} in [N_2 + H_2O + O_2] atmosphere, 2.3 x 10^{15} s^{-1} the frequency factor.

The temperature dependence ($1098 < T < 1223$ K) of the rate constant for overall hydrodealkylation reaction

$$C_7H_8(g) + H_2(g) \quad \rightarrow \quad C_6H_6(g) + CH_4(g)$$

- $\Delta H_{r\,(1173\,K)}$ = 101 kJ mol^{-1} was determined. The rate constant was calculated from the toluene conversion at different temperatures and as plotted according to the Arrhenius law, the calculated activation energy E is 250 ± 10 kJ mol^{-1} in [N_2 + H_2 + H_2O] gas mixture and the frequency factor 3.3 x 10^{10} mol$^{-0.5}$ m$^{1.5}$ s^{-1}. A chemical reaction network and a free-radical mechanism have been suggested to explain the products concentration distribution. The free-radical mechanism has been used to interpret the experimental trends at gas residence times ($\tau < 5$ s).

2.6. The Steam Catalytic Gasification Development in Fluidized bed

Rapagna *et al.* [9] investigated catalytic gasification tests with two nickel steam reforming catalysts (one spent and one fresh), as well as with calcined dolomite. The initial average diameter of the biomass particles was 1.1 mm. The aim of experiments was to characterise the influence of operating parameters on the catalytic draft transformation of tar components into CO and H_2, in presence of steam, so as to obtain useful data for the design of industrial units. There is general consensus on the effectiveness of nickel catalysts for tar reforming, but suitable operating conditions, such as temperature and space time, need further assessment.

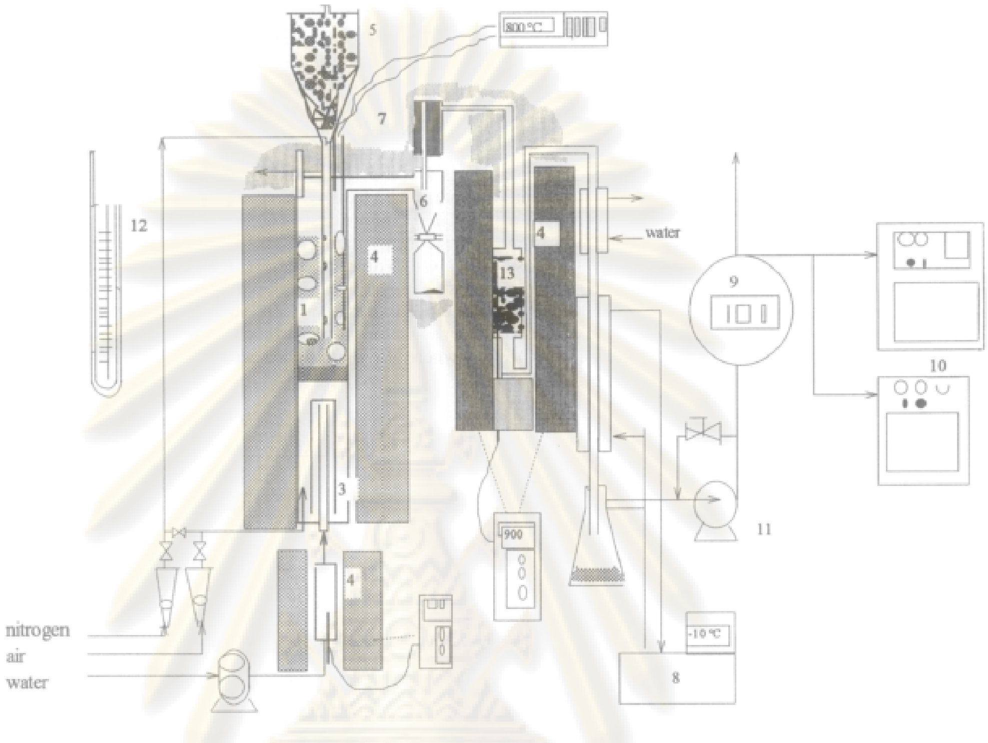

Figure2.21 Bench scale gasification plant. (1) fluidised bed reactor, (2)gas distributor, (3) wind box, (4) electric furnaces, (5) biomass feeder, (6) cyclone, (7) ceramic filter, (8) cooling system, (9) gas flow meter, (10) gas chromatographs, (11) pump, (12) water manometer, (13) catalytic fixed bed reactor [9].

Figure 2.21 provides a schematic representation of the bench scale facility utilised in this study. Its major components are: biomass feeding system, fluidised bed gasifier, catalytic fixed bed, gas cooling system, metering and analysing for the off-gases. The fluidised bed gasifier consists of an austenitic stainless steel cylindrical vessel of internal diameter 62 mm fitted with an alumina porous distributor plate, designed to allow for a good gas distribution at all temperatures. The bed is located in a cylindrical Carbolite Furnace provided with temperature and heating rate control systems. The temperatures in the reactor are measured by means of two thermocouples, one immersed in the bed and the other located under the distributor. The bed inventory is sand particles (d_p = 348 um, ρ_p = 2640 kg/m^3). Water for the generation of steam (the fluidizing gas) is fed to an electrically heated boiler by means of a peristaltic pump at a constant flow rate. The biomass feeding probe (of internal diameter 8 mm and cooled by means of air flowing through a jacket) is designed to deliver the biomass well inside the bubbling bed. The secondary catalytic fixed bed reactor (of internal diameter of 60 mm) is located after a ceramic candle filter and heated by means of a cylindrical electric furnace. The temperature is measured with a thermocouple located inside the reactor which is filled with catalyst: either one of the two nickel catalysts or calcined dolomite. Some further runs with calcined dolomite were performed by placing it directly in the gasifier, in place of the sand particles.

The operating conditions in the gasifier (temperature, biomass/steam ratio and biomass feed rate) were kept constant for all the runs (770 ^{o}C, 1 and 764 kg of biomass per hour per m^{3} of bed, respectively). The influence of the operating conditions in the catalytic converter on the production of gases, especially H,, was investigated over the temperature range of 660-830 ^{o}C, for Gas Hourly Space Velocities (GHSV) in the range 9000-27,700 h^{-1}. About 2 m^{3} of dry gas (at ambient conditions) per kg of daf biomass were obtained by utilising the fresh catalyst at the highest temperature level, with more than 60% by volume being hydrogen. The lowest tar residue was 0.45 g/kg of daf biomass, which increased slightly over the three hours gasification time. Substantial carbon deposition was observed, mainly on the catalyst layers contacting the inlet gas.

Franco *et al.* [10] studied steam gasification in an atmospheric fluidized bed. The experimental work was carried out at atmospheric pressure, on a bench scale fluidised bed gasifier described in Figure 2.22. The gasifier was circular in cross-section with an inside diameter of 70 mm and was 500 mm, total height. The gasifier was placed inside an electrical furnace, which provided the heat for reactions. The biomass was fed under gravity to the top of the gasifier by a continuous feeding system, composed of a screw feeder and a variable speed motor. A flow of nitrogen was used to facilitate biomass feeding and to provide counter flow to the gas flow in the feeding tube from the gasifier. The analysis of the solids collected in the cyclone showed that some fine particles, a mixture of unconverted char and sand, were elutriated out of the gasifier. The gasifying/fluidising medium (steam) was introduced through a gas distributor composed of 12 injectors of 8 mm diameter with four holes of 1.5 mm placed at the bottom end. The steam was produced in a generator and the steam flow rate was controlled with a water pump supplying water to the generator.

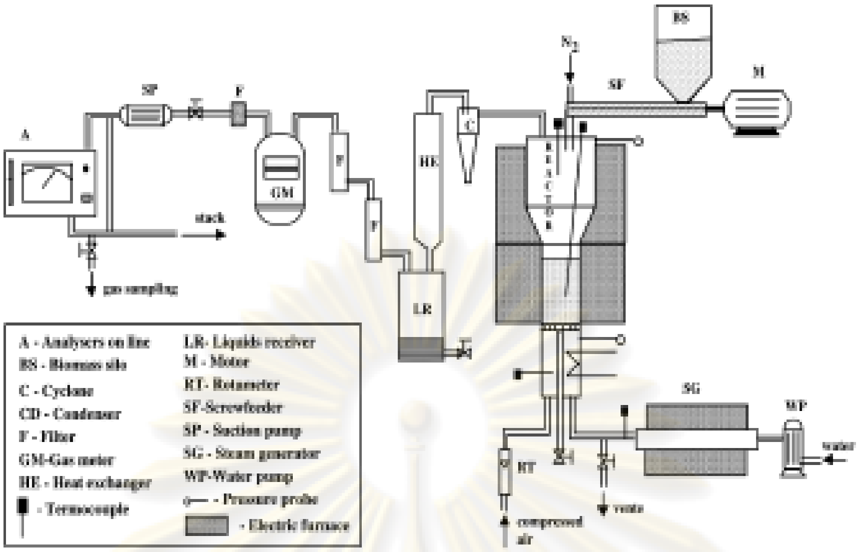

Figure 2.22 Schematic diagram of the installation [10].

Wood wastes of the more common biomass species in Portugal were chosen for this study: pine: Pinus pinaster (softwood), eucalyptus: Eucalyptus globulus and holm-oak (hardwood).

The effects of experimental conditions on the gasification process and on the gas composition were evaluated. Apart from the biomass species, the relevant conditions included some aspects of the fluidised bed gasification process like reaction temperature, fuel/steam ratio, and steam flow rate/fluidisation velocity. The ranges of experimental conditions used in this work were the following: reaction temperature 700–900 ^{o}C; freeboard temperature-750 ^{o}C; flow rate of wood-5.7–11.5 g/min; flow rate of steam- 4.6 g/min; steam/biomass ratio-0.4–0.85; wood moisture content-9.5–12% (wet basis); particle size-1250–2000 mm. The particle size was selected to avoid problems of feeding and to provide minimum variations in the mass flow rate. It is difficult to classify biomass particles within a restricted size range because of irregular shapes. The feed contained some fines and considering the scale-up effect, the size used was what could be equivalent to chips that could be fed to an industrial scale gasifier. It is not likely that biomass feed in an industrial plant would have a high concentration of fines which could always be recycled back to the bed to maximize their conversion. The final gas composition of the gasification process is the result of the combination of a series of complex and competing reactions, given below, occurring to a varying degree.

Oxidation

$$C + O_2 \rightarrow CO_2 \quad (1)$$

$$C + \frac{1}{2}O_2 \rightarrow CO \quad (2)$$

Boudouard

$$C + CO_2 \rightarrow 2CO \quad (3)$$

Water gas

primary : $C + H_2O \rightarrow CO + H_2$ (4)

secondary : $C + 2H_2O \rightarrow CO_2 + 2H_2$ (5)

Methanation

$$C + 2H_2 \rightarrow CH_4 \quad (6)$$

Water–gas shift

$$CO + H_2O \rightarrow CO_2 + H_2 \quad (7)$$

Steam reforming

$$CH_4 + H_2O \rightarrow CO + 3H_2 \quad (8)$$

The operating temperature was found to have a strong influence on the gas composition. The rise in temperature gave rise to a significant increase in H_2 content by 10–20% and a reduction in heavier hydrocarbons by 3–5%, while the CO amount decreased slightly in the range 730 and 850 ^{o}C and then remained constant. The steam/biomass ratio was also observed to be an influential parameter on gasification reactions. A steam/biomass ratio of about 0.6–0.7 w/w was found to produce higher energy and carbon conversion, greater gas yields, and gas composition favouring H_2 formation. The nature of biomass species appeared to have influence on the gasification process to some extent because it resulted in variations in gas composition. The variations in the gas composition were, however, not observed so significant with respect to the nature of biomass and hence one could be replaced by another without any major consequences in the process. This is advantageous, because the availability of biomass wastes is very seasonal. Various gasification reactions may be involved but the water–gas shift reaction appears to be dominant for temperatures up to about 830 ^{o}C for both the holm-oak and eucalyptus. For the temperature 830–900 ^{o}C, though this reaction took place, water–gas reactions and the Boudouard reaction appear to prevail. When pine wastes were gasified, boudouard and water–gas reactions appeared to have an important role, over the whole temperature range, therefore, the importance of water–gas shift reaction was found to take place to an extent less significant and this reaction was probably dominant only over a narrow temperature range. The reason for this has not been elucidated but differences in the mineral matter associated catalytic effects and/or the porous structure of the pine waste, compared to the eucalyptus and oak wastes, may be significant.

Asadullah *et al.* [2-8] studied the catalytic gasification of real biomass (wood powder) with Rh/CeO_2/SiO_2. Figure 2.23 shows a laboratory scale continuous feeding and fluidized bed gasifier of biomass. The gasifier is made of quartz glass with the height of 66 cm. The fluidized bed of 5 cm height and 15 mm i.d. is located just at a middle of the reactor. The biomass feeder consisted of a conical glass vessel with a screw valve at the bottom, allowing continuous feeding of biomass particles by vibrating the vessel with an electric vibrator. An inner tube of 8.5 mm i.d. made of quartz is inserted from the feeder to the catalyst bed. Nitrogen flow of 60 ml/min was usually used for transporting the biomass particles to the catalyst through an inner tube. Air was introduced into the gasification reactor from the bottom portion so as to reach the catalyst bed through a quartz distributor. The flow of air and the gases formed in the fluidized bed kept the catalyst particles fluidized. The process was carried out under atmospheric pressure by adding 3 g of a catalyst which was pretreated under an H_2 stream of 40 ml/min at 773 K for 30 min to the fluidized bed. The product gas was successively passed through a filter and an ice water condenser so as to remove any solid or liquid materials from the product gas steam. The clean sample of the product gas was collected from the sampling port by micro syringe and analyzed by gas chromatography (GC). CO, CO_2, CH_4, H_2, and H_2O were formed as the products. In the non-catalyzed and dolomite-catalyzed reaction, a small amount of C_2 product was formed. The concentration of CO, CO_2, CH_4, and C_2 products was determined by FID-GC equipped with a methanator using a stainless steel column packed with Gasukuropack 54.The concentration of hydrogen was determined by TCD-GC using a stainless steel column packed with a molecular siever 13X used for transporting the biomass particles to the catalyst bed through an inner tube.

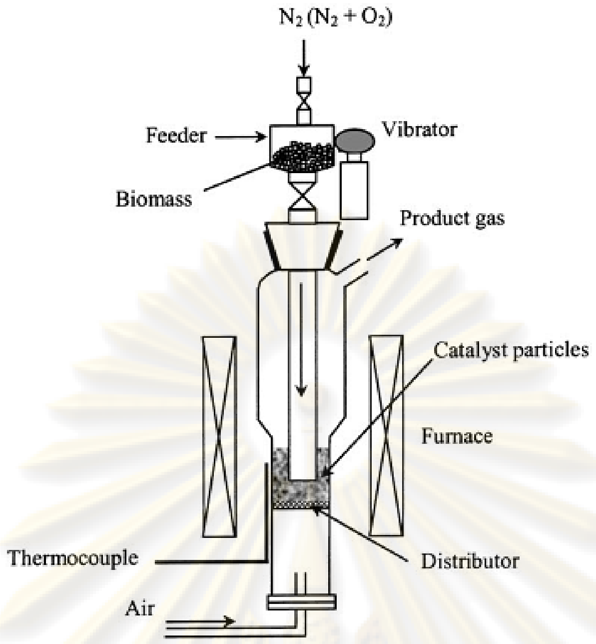

Figure 2.23 Schematic diagram of the reactor system [2-8].

The gasification of biomass (cedar wood) on $Rh/CeO_2/SiO_2$(60) catalyst in a fluidized bed reactor efficiently proceeded to produce syngas between the temperatures of 823 and 973 K. About 98–99% of the carbon in the biomass was converted to the gas product at 873 K. However, on the conventional nickel-based catalyst and on dolomite this value is 73 and 43%, respectively, at the same temperature. The rest of the carbon was related to the tar and char, which caused the deactivation of the conventional catalysts. Since almost all the carbon in the biomass was converted to the gas product on the $Rh/CeO_2/SiO_2$ (60) catalyst, the deactivation related to the tar or char deposition on the catalyst surface was not observed. It is demonstrated that $Rh/CeO_2/SiO_2$ (60) catalyst is applicable to the gasification of real biomass at much lower temperatures than conventional methods.

About 150 mg/min of biomass was the optimum feeding rate on 3 g of the catalyst using the ER of 0.3. The gas composition and also the C-conv were very dependent on the co- and counter-current feeding of biomass and air. In the counter-current feeding, the C-conv and syngas formation was higher than co-current feeding of air and biomass. The catalyst activity was quite stable even in the long reaction period (4 h). The TGA results showed that the combustion activity of carbon materials on the $Rh/CeO_2/SiO_2$(60) catalyst was much higher than on conventional catalysts and that the reaction was highly exothermic, so that the catalyst surface remained clean and self-immunized to maintain the activity during the reaction in the fluidized bed reactor.

In the feeding line of the reactor, the biomass first thermally decomposed to the tar, char, steam, and a small fraction of product gas (Figure 2.24). Then the volatile tar and solid char contacted with the catalyst particles in the lower part of the catalyst bed where oxygen is present and a part of the tar and char may take part in the combustion reaction to form CO_2 and H_2O. Then the catalyst with adsorbed tar and/or char quickly moves up due to the fluidization and begins to be reduced at the upper part, where the tar and char take part in the reforming reaction in the presence of steam on the catalyst surface to form CO and H_2. In the fluidized bed catalyst, if oxygen is used, the characteristic reduction and oxidation cycle of the catalyst exists. And thus an ideal catalyst must convert the tar and char to useful gas in the presence of steam and/or oxygen completely by the reforming and combustion reactions. The combustion reaction is faster than the reforming reaction. Furthermore, the biomass-derived tar is more active than the char. Consequently, the tar usually takes part in the reforming reaction on the reduced surface at the upper part; however, the char is more refractory in nature and takes part in the combustion reaction on the oxidized catalyst at the bottom part.

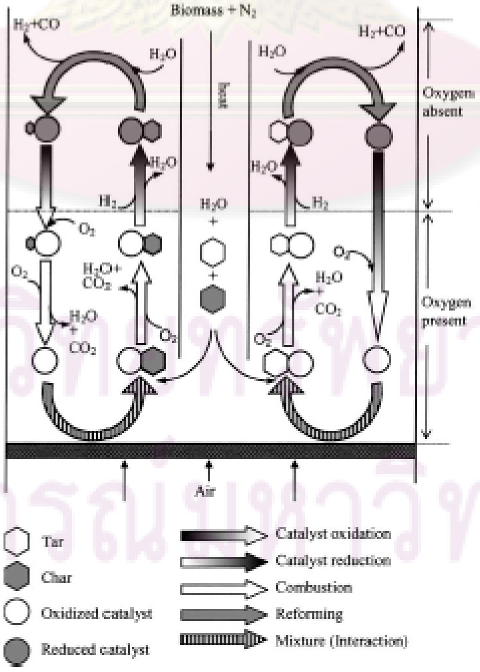

Figure 2.24 Possible mechanism of the catalytic gasification of biomass [2-8].

The sketch diagram of the single and dual bed reactor is shown in Figures 2.25a and 2.25b. The reactor was made of quartz glass. An inner tube was inserted from the top. Cellulose and biomass were supplied from the top of the reactor together with N_2 from the port A. The biomass feeder consisted of a glass vessel with a small pore at the bottom and it was vibrated by the vibrator and the feeding rate was controlled by the vibrating rate. The gasifier was composed of a fluidized bed section at the middle of the reactor. In the gasification of biomass with oxygen, O_2 and N_2 were supplied from the port B. In the pyrogasification, N_2 was supplied from the port B. In the case of steam reforming of biomass, N_2 and steam was supplied from the port B. The microfeeder was used for steam feeding. The product gas was collected and analyzed by gas chromatography (GC).

For the dual bed reactor, and this consisted of two fluidized-bed sections. First section was located at the bottom of the conical part on the outer quartz tube and the other one was at the bottom of the inner tube. The catalyst particles were placed in the fluidized-bed section of inner tube. The biomass was fed from the feeder by vibrating with an electric vibrator and transported through the side tube under nitrogen flowing. In the case of this dual-bed gasifier, oxygen was supplied through a capillary tube which was inserted to the inner tube from the top of the fluidized-bed reactor. At first, biomass was pyrolyzed in the outer tube to form the tar and char mainly. The char accumulated in the conical bed section and the tar reached the catalyst-bed and took part in the reforming reaction. In contrast, all the biomass-derived products in the feeding tube go to the catalyst-bed in the single-bed type.

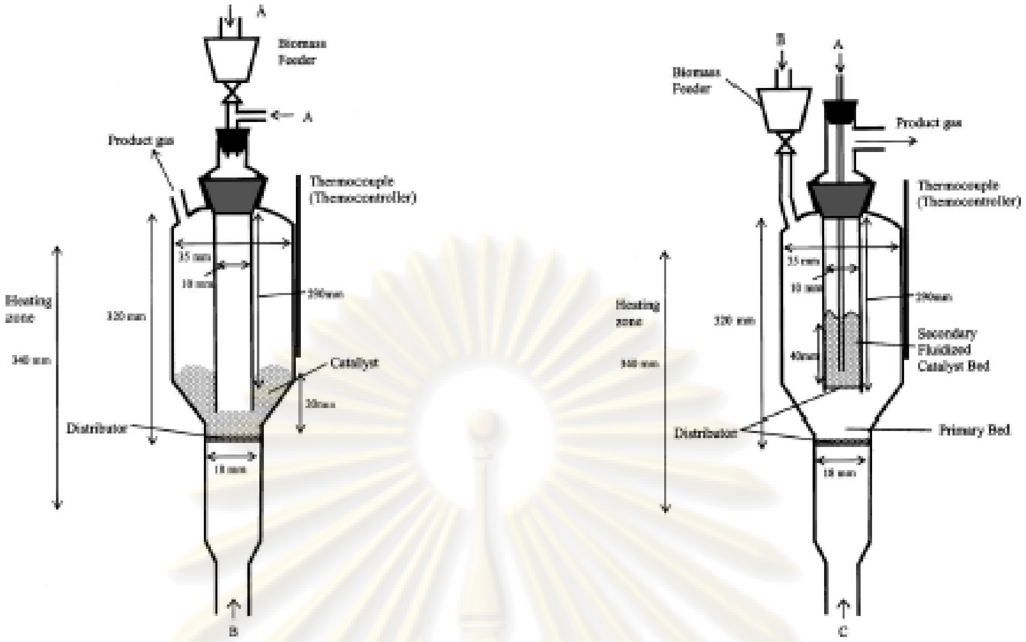

Figure 2.25 Schematic diagram of the single-bed reactor(a) and the dual-bed reactor(b). (a) Gasification with air A: N_2 + biomass, B: $O_2 + N_2$; pyrogasification A: N_2 + biomass, B: N_2; steam reforming A: N_2 + biomass, B: $H_2O + N_2$; solid carbon (char + coke) estimation A: N_2, B: O_2. (b) Activity test of biomass gasification A: O_2, B: N_2 + biomass, C: N_2; coke estimation A: O_2, B:N_2, C: N_2; char estimation A: N_2, B: O_2, C: O_2 [2-8].

From the result of the gasification of cellulose over novel $Rh/CeO_2/SiO_2$ catalysts, it is found that the gasification process consists of the reforming of tar and the combustion of solid carbon. The novel $Rh/CeO_2/SiO_2$ was tested in the gasification with air, pyrogasification, and steam reforming of cedar wood. As a result, $Rh/CeO_2/SiO_2$ gave higher yield of syngas than the conventional steam reforming Ni catalyst. Furthermore, the performance between single and dual bed reactors was compared. Single bed reactor was effective in the gasification of cedar, however, it was not suitable for the gasification of rice straw since a rapid deactivation was observed. Gasification of rice straw, jute stick, baggase using the fluidized dual-bed reactor and $Rh/CeO_2/SiO_2$ was also investigated. Especially, the catalyst stability in the gasification of rice straw clearly was enhanced by using the fluidized dual bed reactor.

In this thesis work, the one stage reactor for steam catalytic biomass gasification was developed and also investigated the suitable conditions such as temperatures, steam flow rates etc. The Ni/Dolomite and the developed Ni/Dolomite doped with WO_3 catalyst were used in this experiment. The completed biomass gasification to form the most of synthesis gas is our target.

2.7. Literature Reviews

The type and quality of the apparatus that is used in laboratory is one of the most important considerations.

Chaudhari *et al.* [1] studied the optimum condition for producing gases from biomass-derived char. It was observed that a steam flow rate of 2.5 g/h/g of biomass derived char (BDC) and 650-700 ^{o}C were suitable for the production of synthesis gas having lower (1.33) ratio of H_2/CO.

Asadullah *et al.* [2-8] investigated the gasifier with two fluidized-bed sections. The first section is a single bed type with the catalyst on the large distributor. The other type is dual-bed type, where the catalyst was placed on the fluidized-bed section of the inner tube. The biomass was fed from feeder by vibrating the vessel with an electric vibrator with nitrogen flow. It was found that dual-bed reactor combined with $Rh/CeO_2/SiO_2$(30) catalyst was more effective than single-bed reactor in term of higher carbon conversion of product gases (H_2,CO and CH_4).

Catalytic biomass steam gasification runs were studied in fluidized bed gasifier and a secondary catalytic fixed bed reactor by Rapagna *et al.* [9]. The fluidized bed gasifier consists of an austenitic stainless steel cylindrical vessel of internal diameter 62 mm in a cylindrical Carbolite Furnace. The temperatures in reactor are measured by two thermocouples, one immersed in the bed and the other located under the distributor. The biomass was fed by feeding probe (internal diameter 8mm and cooled by flowing air through a jacket). The secondary catalytic fixed bed reactor (internal diameter 60 mm), which is filled with catalyst; either nickel catalysts or calcined dolomite, is located after the fluidized bed gasifier and a ceramic candle filter, respectively. The results show that fresh nickel catalysts are extreamly active in removing methane and tars. As a result, hydrogen product is found to be higher than 60% by volume.

Franco *et al.* [10] studied the biomass steam gasification process which was carried out in an atmospheric fluidized bed. The gasifier of 500 mm in total height and circular cross section with inside diameter of 70 mm was packed inside an electric furnace. The biomass was fed from the top by a continuous feeding system under gravity, consisted of a screw feeder and a variable speed motor. The gasifier was operated at over temperature range of 700-900 ^{O}C, varying steam/biomass ratio from 0.4 to 0.85 w/w with three types of biomass: Pinus pinaster(softwood), Eucalyptus globules and holm oak (hardwood). The results obtained at the optimized condition, at temperature 830 ^{O}C and steam biomass ratio of 0.6-0.7 w/w, were gas richer in hydrogen and decrease in hydrocarbon and tars. It was found that H_2 content increased by 10-20% and heavier hydrocarbons decreased by 3-5% while the temperature was increased.

Srinakruang *et al.* [11-12] studied the development of Ni based on dolomite catalyst (Ni/Dolomite) in terms of their performance and characters for the tar gasification. It was claimed that Ni based on dolomite catalyst is an effective catalyst for fixed bed gasification of tar. The Ni/Dolomite catalyst showed excellent activity for tar decomposition and anti-coking of toluene and naphthalene.

Sato *et al.* [13] developed Ni/MgO–CaO (based on dolomite) catalyst which was doped with WO3 as a sulfur-resistant promoter in the tar reforming. The characteristics of the newly-developed were investigated using a simulated gas containing naphthalene as tar. The result has confirmed that the developed catalyst shows a high naphthalene reforming activity and is stable even in gas containing hydrogen sulfide. The catalyst also exhibited superior resistance to coking as well as sulfur poisoning compared to several commercial steam-reforming catalysts.

Bridegwater *et al.* [18-23] reviewed that tar could be reduced by thermal cracking in a fluidized bed gasifier. Meanwhile, biomass-derived tar was very refractory and hard to crack by thermal treatment alone. In order to effectively decompose the tar, the following ways were suggested: increasing residence time, such as using a fluidized bed reactor freeboard, but this method was only partially effective; Direct contacting with an independently heated hot surface, which required a significant energy supply and decreased the overall efficiency. At the same time, the method was also partly effective and depended on good mixing; Partial oxidation by adding air or oxygen could increase CO levels at the expense of conversion efficiency decrease and operation cost enhancement.

Tomishige *et al.* [60-61] investigated the biomass gasification (cedar wood) on Rh/CeO$_2$/SiO$_2$ (60) with fluidized bed of 5cm in height and 15 mm i.d. that is located just at the middle of the quartz glass reactor with the height of 66 cm. The biomass is fed by vibrating the vessel with an electric vibrator composing of a conical glass vessel with screw valve at the bottom. Syngas was produced between temperatures of 550 and 700 K. The carbon in biomass was converted to gas product at 600 K with 98-99% C-conversion. It is showed that Rh/CeO$_2$/SiO$_2$ (60) catalyst was appropriate for the biomass gasification at low temperatures.

Zhang *et al.* [62] investigated tar catalytic destruction in a tar conversion system consisting of a guard bed and catalytic reactor. Three Ni-based catalysts (ICI46-1, Z409 and RZ409) were proven to be effective in eliminating heavy tars(>99% destruction efficiency). Hydrogen yield was also improved by 6-11 vol%(dry basis). The experimental results also demonstrated that space velocity had little effect on gas compositions, while increasing temperature boosted hydrogen yield and reduced light hydrocarbons(CH_4 and C_2H_4) formation, which suggested that tar decomposition was controlled by chemical kinetics.

Zhu *et al.* [63] studied the catalytic gasification of char from co-pyrolysis of coal and wheat straw was studied. Alkali metal salts, especially potassium salts, are considered as effective catalysts for carbon gasification by steam and CO_2, while too expensive for industry application. The herbaceous type of biomass, which has a high content of potassium, may be used as an inexpensive source of catalyst by co-processing with coal. The reactivity of chars from co-pyrolysis of coal and straw was experimentally examined. The chars were prepared in a spout-entrained reactor with different ratios of coal to straw. The gasification characteristics of chars were measured by thermogravimetric analysis (TGA). The co-pyrolysis chars revealed higher gasification reactivity than that of char from coal, especially at high level of carbon conversion. The influence of the alkali in the char and the pyrolysis temperature on the reactivity of co-pyrolysis char was investigated. The experimental results show that the co-pyrolysis char prepared at 750 °C have the highest alkali concentration and reactivity.

Zabaniotou *et al.* [64] have claimed that lignocellulosic biomass is an interesting and necessary enlargement of the biomass used for the production of renewable biofuels. It is expected that second generation biofuels are more energy efficient than the ones of first generation, as a substrate that is able to completely transformed into energy. The present study is part of a research program aiming at the integrated utilization of rapeseed suitable to Greek conditions for biodiesel production and parallel use of its solid residues for energy and second generation biofuels production. In that context, fast pyrolysis at high temperature and fixed bed air gasification of the rapeseed residues were studied. Thermogravimetric analysis and kinetic study were also carried out. The obtained results indicated that high temperature pyrolysis could produces higher yields of syngas and hydrogen production comparing to air fixed bed gasification.

CHAPTER 3

Experimental Procedures

3.1. Thermogravimetric Analysis (TGA)

The thermogravimetric analysis (TGA) evaluated the weight change in biomasses as a function of temperature. The measurement is carried out with a heating rate of 10 ^{o}C/min from 20 to 500 ^{o}C in 100 ml/min of air and nitrogen atmosphere by ULVAC SINKU-RIKU TGD 9600.

3.2. The scanning electron microscope (SEM)

The scanning electron microscope (SEM) is a type of electron microscope that images the sample surface by scanning it with a high-energy beam of electrons in a raster scan pattern. The electrons interact with the atoms that make up the sample producing signals that contain information about the sample's surface topography, composition and other properties such as electrical conductivity. The samples were analyzed by JEOL JSM-5800 LV model.

3.3.X-ray Diffractometer

An X-ray diffractometer (XRD, Rigaku, RINT 2000) was used to investigate the structures of Ni/dolomite. The crystalline average size was calculated by $L = K\lambda / \Delta(2\theta)\cos\theta_0$, where L is the crystalline size, K is a constant (K =0.9 ~ 1.1), λ is the wavelength of X-ray (CuK_α = 0.154 nm), and $\Delta(2\theta)$ is the width of the peak at half height.

3.4. Catalyst Preparation

The Ni/Dolomite was prepared by precipitation method with containing 10 % of Ni from aqueous solution of nickel nitrate hexahydrate with ammonium carbonate in hot distilled water in the presence of dispersed dolomite, which is calcined at 1200 ^{o}C for 24 hours. After that, the catalyst was filtered and washed with hot water then dried at 120 °C overnight and finally calcined in air at 500 °C for 2 hours.

The newly developed Ni-WO_3/Dolomite catalyst (12%WO_3 by weight.) was prepared by precipitating nickel and tungsten aqueous solutions with MgO-CaO (calcined Dolomite)as a precipitant and carrier in hot distilled water. After the precipitate was filtered and washed with hot water. It was dried overnight at 120 °C and then calcined in air at 800 °C overnight.

3.5. Biomass Pyrolysis followed by Gasification Experimental Set Up

The schematic diagram of the biomass pyrolysis followed by gasification which was controlled by temperature programmed method was shown in Figure 3.1. The biomass pyrolysis followed gasification experiment was carried out with a fixed bed in quartz reactor with inner diameters of 10 mm. The reactor was externally heated by two electric furnaces and their temperatures were measured with two thermocouples at the center position of the reactor. This reactor was divided into 2 parts; the upper part was the pyrolysis zone at the temperature range of 150 to 400 °C and the lower part was the gasification zone at temperature 700, 750 and 800 °C with Ni/Dolomite catalyst. The Ni/Dolomite catalyst was reduced with hydrogen at temperature 700 °C for 2 hours.

Four kinds of biomass in dry basis were studied: wood chip, coconut shell, bamboo, and corncob. Each biomass with total amounts of 0.5 g in stainless steel mesh basket, hydrogen feed75 mmol/h, argon carrier 193 mmol/h and steam flow rate 178, 222 and 244 mmol/h from evaporator were fed through the top of the reactor. Gaseous products (CO, CO_2, CH_4 and H_2) from the bottom of the reactor were analyzed by TCD activated carbon column gas chromatograph after removing water.

By the way, char which is one of the main products from pyrolysis process was subjected to the steam gasification to evaluate the reaction temperature by a temperature programmed gasification (TPG) method. The char gasification system was similar to that of the pyrolysis where no catalyst zone exist. Char (0.15 g) in the stainless mesh basket was set in the reactor, followed by feeding the mixed gas steam 222 mmol/h hydrogen 75 mmol/h, Argon 193 mmol/h with heating from 400 to 850 °C for 1 hour. Moreover, the effect of Ni/dolomite catalyst on char gasification was studied the gaseous products.

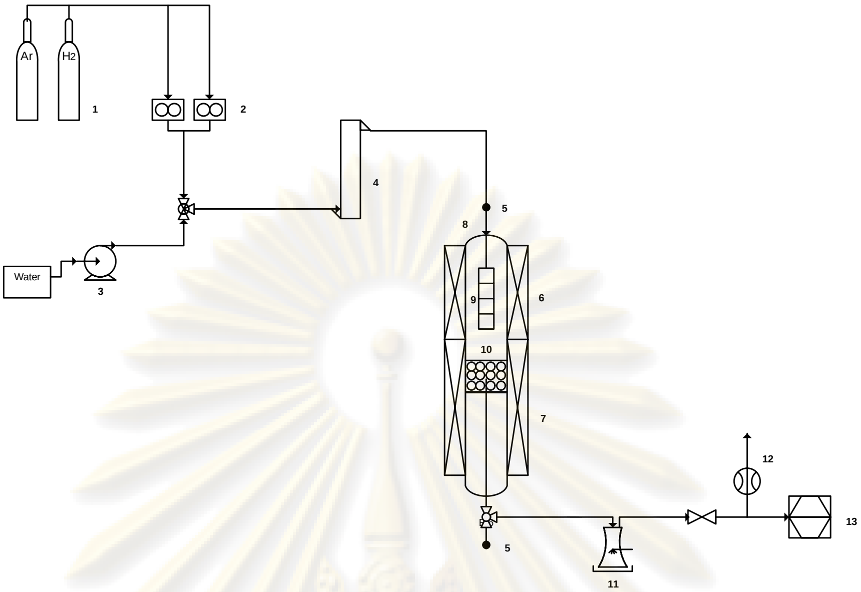

Figure3.1 Schematic diagram of the experimental set up for biomass fixed bed gasification (1: Gas tanks; 2: Mass flow controller; 3: Steam generator; 4: Evaporator; 5: Thermocouples; 6: The first furnace; 7: The second furnace; 8: Quartz reactor; 9: Biomass sieve basket; 10: Ni/Dolomite catalyst bed; 11: Liquid collector; 12: Gas flow meter; 13: Gas chromatograph).

3.6. Biomass Gasification with Fluidized Bed Experimental Set Up

Figure 3.2 shows the schematic diagram of biomasses gasification with fluidized bed. The cylindrical stainless steel tube reactor with inner diameter of 38.7 mm and 705 mm of height was located inside an electric furnace, which is heated by temperature programmed method. The flow of argon and hydrogen with gasifying medium (steam) from water pump were fed into evaporator and then flowed through a gas distributor which is placed at the bottom of the reactor and contain Ni/Dolomite catalyst. Before gasification occurred, Ni/Dolomite was reduced by hydrogen at 700 ^{o}C for 2 hours in order to be the effective and performance catalyst as a metal nickel form. The various amounts of biomasses were fed from the top under gravity by continuous feed and analyzed every 4 minutes. The gaseous products flow through the top of reactor into impinger bottles which contained isopropyl alcohol (IPA) for tar trap and were analyzed by TCD gas chromatograph. From the previous literatures [2-8], they have claimed carbon-based conversion (%C) which can be calculated by

((ΣCO+CO_2+CH_4)/Total carbon feeding in biomass)x100. The amount of tar is measured by weight from impinger bottles. The amount of char is defined as (100-(%C conversion)- Tar(%)).The conditions of this experiment were shown in Table3.1.

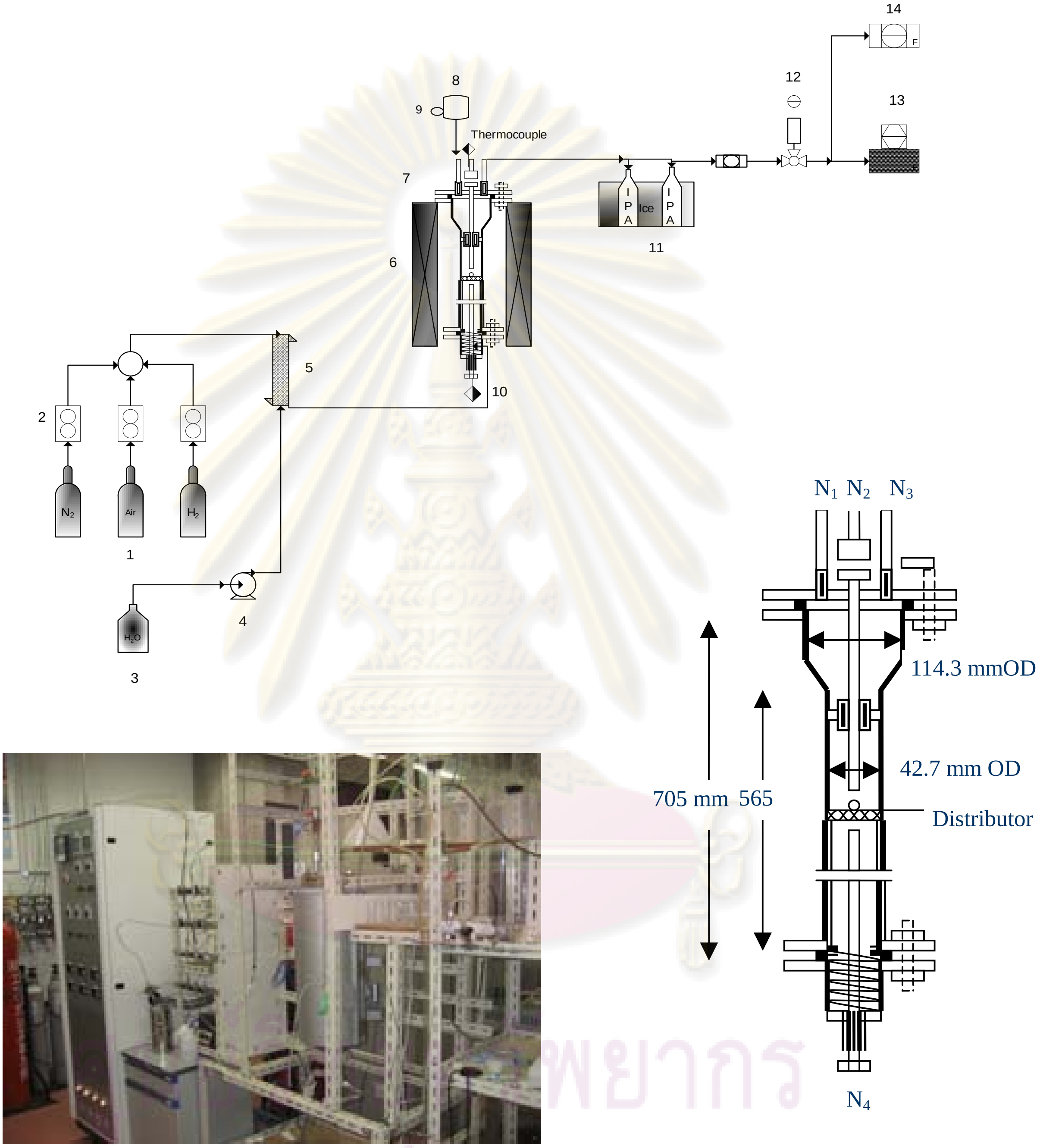

Figure3.2 Schematic diagram of the experimental set up for biomass fluidized bed gasification(1: Gas tanks; 2: Mass flow controllers; 3: Water; 4: Water pump; 5: Evaporator; 6: Electric furnace; 7: The cylindrical steel vessel reactor; 8:The biomass feeder; 9: Vibrator; 10: Thermocouples; 11: Impinger bottles; 12: Injection; 13: Gas chromatographs; 14: Gas flow meter).

Table 3.1 The parameters in biomass gasification with fluidized gasification

Parameters	
Biomass types	Wood chip, Bamboo, Coconut shell, Corn cob and Palm shell
Temperatures(^{o}C)	750, 780 and 810 ^{o}C
Steam flow rates	177, 222 and 244 mmol/h
Gas flow rates for fluidization (ml/min) Argon +$H_2$50 ml/min	350, 450 and 550 ml/min
Biomass feed rate	7.5, 15 and 30 g/h
Catalyst weights	10 and 20 g
Oxygen inputs	30, 50 and 75 ml/min

CHAPTER 4

The Characteristic and Unit Reaction of Biomass Pyrolysis and Gasification with Fixed Bed

4.1. The Properties of Biomasses

Table 4.1 shows the elemental analysis the compositions of carbon, oxygen, hydrogen, nitrogen and ash that contain in five types of biomass such as wood chip[Japan], bamboo[Japan], coconut shell[Thailand], corncob[Japan] and palm shell[Thailand] by the elemental analysis.

Table 4.1 Analysis of five types of biomass in dry basis

	Wood chip	Coconut shell	Bamboo	Corncob	Palm shell
Elemental analysis(%wt)[a]					
Carbon	47.3	46.5	46.2	41.4	45.8
Hydrogen	6.2	6.0	6.1	6.3	6.4
Nitrogen	0.29	0.35	0.34	1.1	2.6
Oxygen	46.2	46.7	47.4	45.2	45.2

[a] Determined by CHN elemental analysis.

The thermogravimetric analysis (TGA) evaluated the weight change in biomasses as a function of temperature as shown in Figures 4.1a and 4.1b. The measurement is carried out with a heating rate of 10 ^{o}C/min from 20 to 500 ^{o}C in 100 ml/min of air and nitrogen atmospheres by ULVAC SINKU-RIKU TGD 9600.

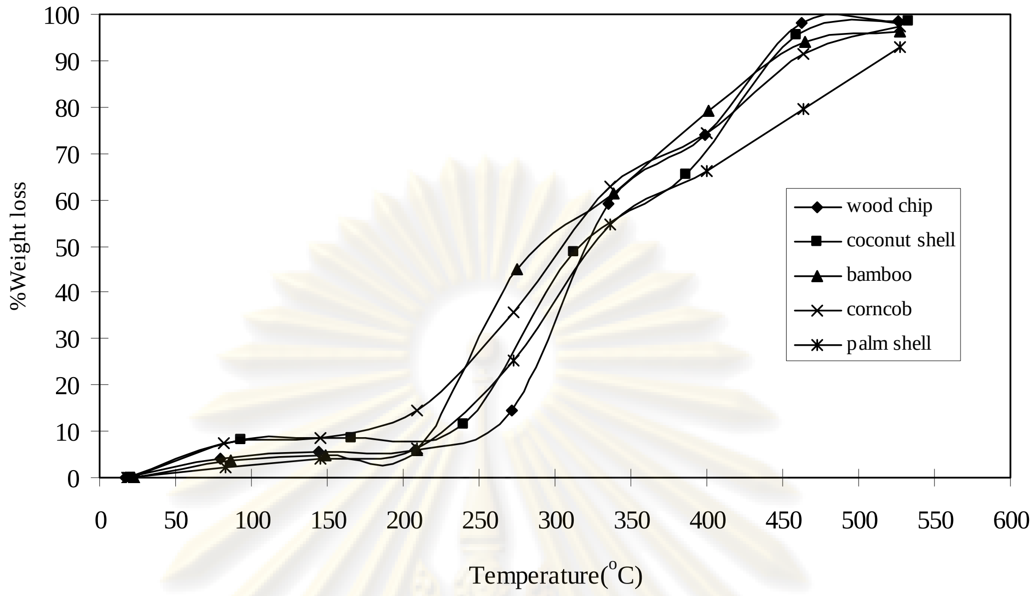

a.

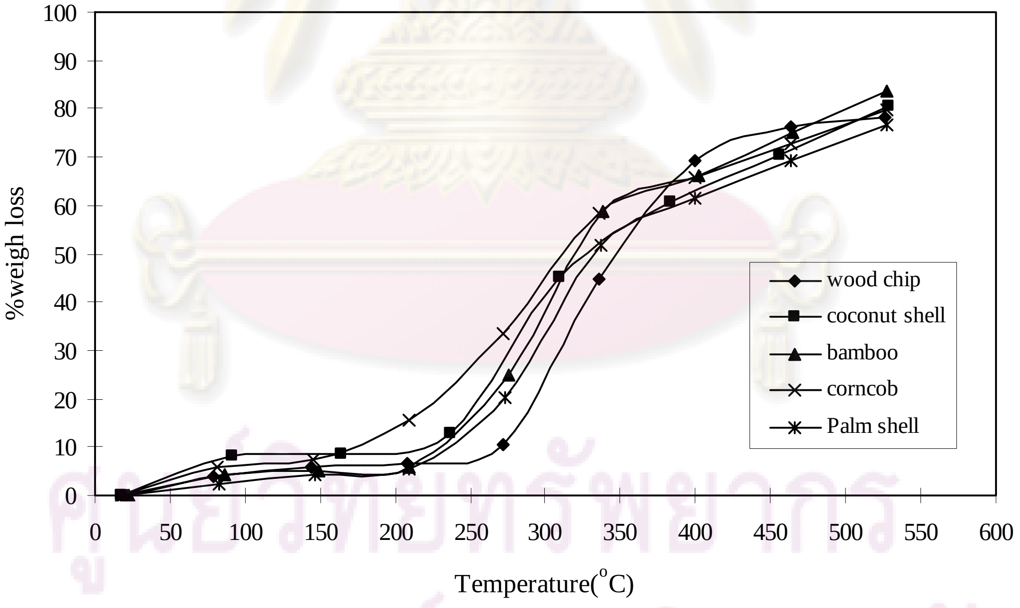

b.

Figure 4.1 The thermogravimetric analysis (TGA) of five types biomass. (a) in air atmosphere, (b) in N_2 atmosphere.

According to Figure 4.1a, three steps of weight decrease occurs in air atmosphere: first, a temperature range of 50-200 ^{o}C which is attributed to the dehydration of biomass, the weight decrease (exothermic) in a range temperature of 200-420 ^{o}C is attributed to the formation gases, tar, and char finally, the weight loss at above 420 ^{o}C is the oxidation. As shown in Figure 4.1b, the thermogravimetric analysis (TGA) shows that three steps of weight decrease occurs in N_2 atmosphere. Firstly, the weight loss over 50-200 ^{o}C which can attribute to the dehydration, the exothermic weight decrease over 200-420 ^{o}C can be attributed to the formation of gases, tar and char. Finally, the slow weight loss at above 420 ^{o}C may be attributed to the CO or CO_2 from char.

According to Figure 4.1b, the weight loss due to thermal decomposition of each biomass, which concerned with pyrolysis process in the range temperature of 180 - 400 ^{o}C, can be prioritized in terms of decomposed amount at certain temperature as following: corncob > bamboo > pine wood chip > coconut shell, respectively. This primary order data is the advantage for decomposition or pyrolysis of the various types of biomass as a function of temperature study because the decomposition or pyrolysis reaction of each biomass at the certain temperature is different.

4.2. The Clarification of Unit Reactions in Pyrolysis followed by Catalytic Tar Gasification

Thermogravimetric analysis (TGA) suggested the pyrolysis of biomass was composed of (1) dehydration, (2) pyrolysis to tar and char. Step (2) was studied with the Temperature Program Reaction (TPR) method, which is followed by the catalytic steam reforming.

Since the quick determination of tar generation or its composition is quite difficult. We adopted the quick gasification technology, when the tar and gas are generated from biomass, then were introduced to the Ni/Dolomite catalyst bed (kept at 750 ^{o}C). The carrier gas composed of H_2O (steam), H_2 and Argon. In the catalyst bed, the tar material is completely converted to gases (CO, CO_2, H_2 and CH_4), which were determined quickly by an on-line GC at every 5 minutes.

4.2.1. Pyrolysis Experiment

Figure 4.2 presents the result of Temperature Programmed Reaction (TPR) method of coconut shell in argon atmosphere without catalyst in the lower part. Biomass, which is located at the upper part of reactor, was pyrolyzed from 180-400 °C by temperature program. The gas products were analyzed by TCD gas chromatograph as a function of temperature. The result presents the gas products from biomass after pyrolysis.

It was found that the total amounts of carbon monoxide, carbon dioxide and methane from biomass corresponded to less than 10% of total biomass in carbon basis in the temperature range of 200-300 °C and the other product is composed of tar and char. Both of them were stable over 300-450 °C. It can be concluded that most gaseous products were derived from tar.

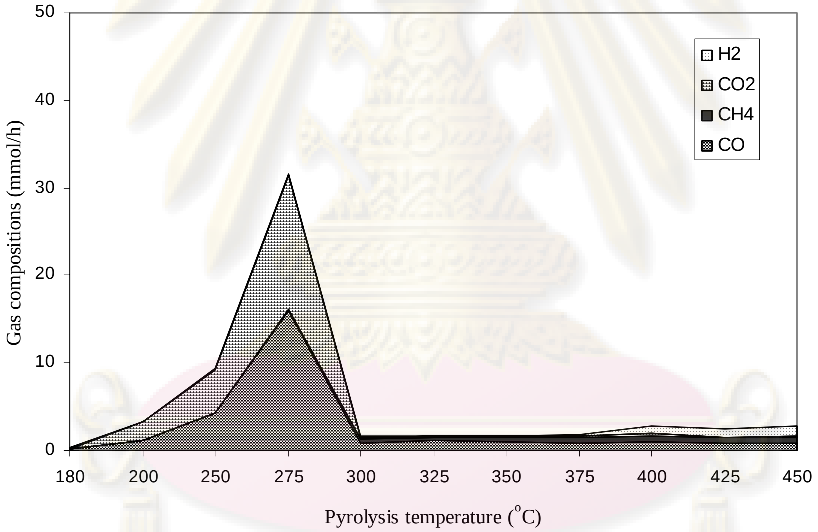

Figure 4.2 Effect of temperature on gas compositions from biomass pyrolysis in argon atmosphere by using temperature program.

4.2.2. Pyrolysis followed by Catalytic Tar Gasification

Results of TPR followed by catalytic tar reforming for each biomass (pine wood chip, coconut shell, bamboo and corncob) are shown in Figures.4.3a-4.3d. By comparing the data in Figure 4.2 with those of Figure4.3b, it is clear that the biomass pyrolysis started from 200 °C then reached the maximum level at around 300 °C and finished at around 400 °C. Also, it is clear that for 4 types of biomass, coconut shell is most easy to be pyrolyzed and pine wood chip is most difficult to be pyrolyzed. Remarkably, hydrogen was produced at pyrolysis temperature of 180 °C because volatile matter started to be released at this temperature and through the catalyst bed at 750 °C.

It can be concluded that gas productions (CO, CH_4, CO_2 and H_2) in this experiment are mostly derived from tar produced in pyrolysis step followed by their gasification on Ni/dolomite catalyst at 750 °C. Char is not decomposed at temperature lower than 400 °C. Table 4.2 and Figure 4.4 present the percentages of remaining char after the pyrolysis experiment in carbon basis. The weight ratio of remaining char was in the following order pine wood chip (25.8%) > coconut shell (24.5%) > bamboo (21.9%) > corncob (16.8%). However, the liberated tar was in the reverse order. It shows that around 61-77 % of the total biomass feeds in carbon basis is converted to tar and hydrogen. The summations of carbon monoxide, carbon dioxide and methane ($CO+CH_4+CO_2$), which are total carbon of gas and tar against total biomass are placed in the order; pine wood chip (67%) < bamboo (70%) <coconut shell (71%) < corncob (72%) in carbon basis.

Table 4.2 The percentages of the products in pyrolysis and gasification step in carbon basis

Biomasses	Gases($CO+CH_4+CO_2$) (wt%)[a]	Char(wt%)[b]	Deposited tar (wt%)[b]
Pine wood chip	61.9	25.8	2.8
Coconut shell	70.7	24.5	2.8
Bamboo	71.3	21.9	2.8
Corncob	77.3	16.8	2.8

[a] measured by TCD gas chromatograph.

[b] measured by weight.

Comparing the properties among four types of biomass in the present work as shown in Figures.4.3a-4.4d; wood chip, coconut shell, bamboo and corncob, the compositions of carbon, hydrogen and oxygen contained in each biomass were not far apart but the result of gasification and decomposition was slightly different. Among four types of biomass gasification in the fixed bed as a function of the temperature, coconut shell can be pyrolyzed and gasified at 230 °C, while pyrolysis of pine wood chip, bamboo and corncob start from 180 °C.

The results of different biomass pyrolysis are corresponded to the decomposition of biomass in N_2 atmosphere by TGA. It has claimed that coconut shell is most difficult to be pyrolyzed in the temperature range of 200-300 ^oC, whereas corncob, bamboo and pine wood chip are pyrolyzed at the temperature range of 150 – 250 ^oC. Moreover, it was found that woodchip was more difficult to be pyrolyzed and gave the lowest gaseous products. These differences should be attributed to not only the porous texture of each biomass but also the structure of carbohydrate exhibits strong effects on the gasification and decomposition of biomasses. Moreover, the content of cellulose and lignin affected their volatilization. The pyrolysis rate of the biomass with higher cellulose content became faster than the biomass with higher lignin content.

The mechanism of biomass pyrolysis followed by catalytic gasification to form gas compositions can be explained that the products from biomass pyrolysis, which is the upper part, are gases (CO and CO_2), tar and char as shown in equation (1). Tar is passed through the catalytic bed at 750 ^oC, which is located in the lower part, to form the synthesis gas. In the lower part, the influence of tar reforming, steam reforming and water gas shift is the main reactions to produce the gas products. Char can not be decomposed at the low temperature and remains in the stainless steel sieve basket after pyrolysis reaction.

$$\text{Biomass} + H_2O \longrightarrow CO + CO_2 + \text{Tar} + \text{Char} \quad (1)$$

$$\Downarrow$$

$$C_xH_y(\text{Tar}) + x\,H_2O \xleftrightarrow{Ni(750^oC)} xCO + (x+\frac{y}{2})\,H_2 \quad (2)$$

$$C_xH_y\,(\text{Tar}) + y\,H_2O \xleftrightarrow{Ni(750^oC)} x\,CO_2 + (x+y)\,H_2 \quad (3)$$

$$C_xH_y\,(\text{Tar}) + x\,CO_2 \xleftrightarrow{Ni(750^oC)} 2x\,CO + (\frac{y}{2})\,H_2 \quad (4)$$

$$C_xH_y\,(\text{Tar}) + (\frac{4x-y}{2})\,H_2 \xrightarrow{Ni(750^oC)} x\,CH_4 \quad (5)$$

$$CO + H_2O \leftrightarrow CO_2 + H_2 \quad (6)$$

$$CO + 3H_2 \leftrightarrow CH_4 + H_2O \quad (7)$$

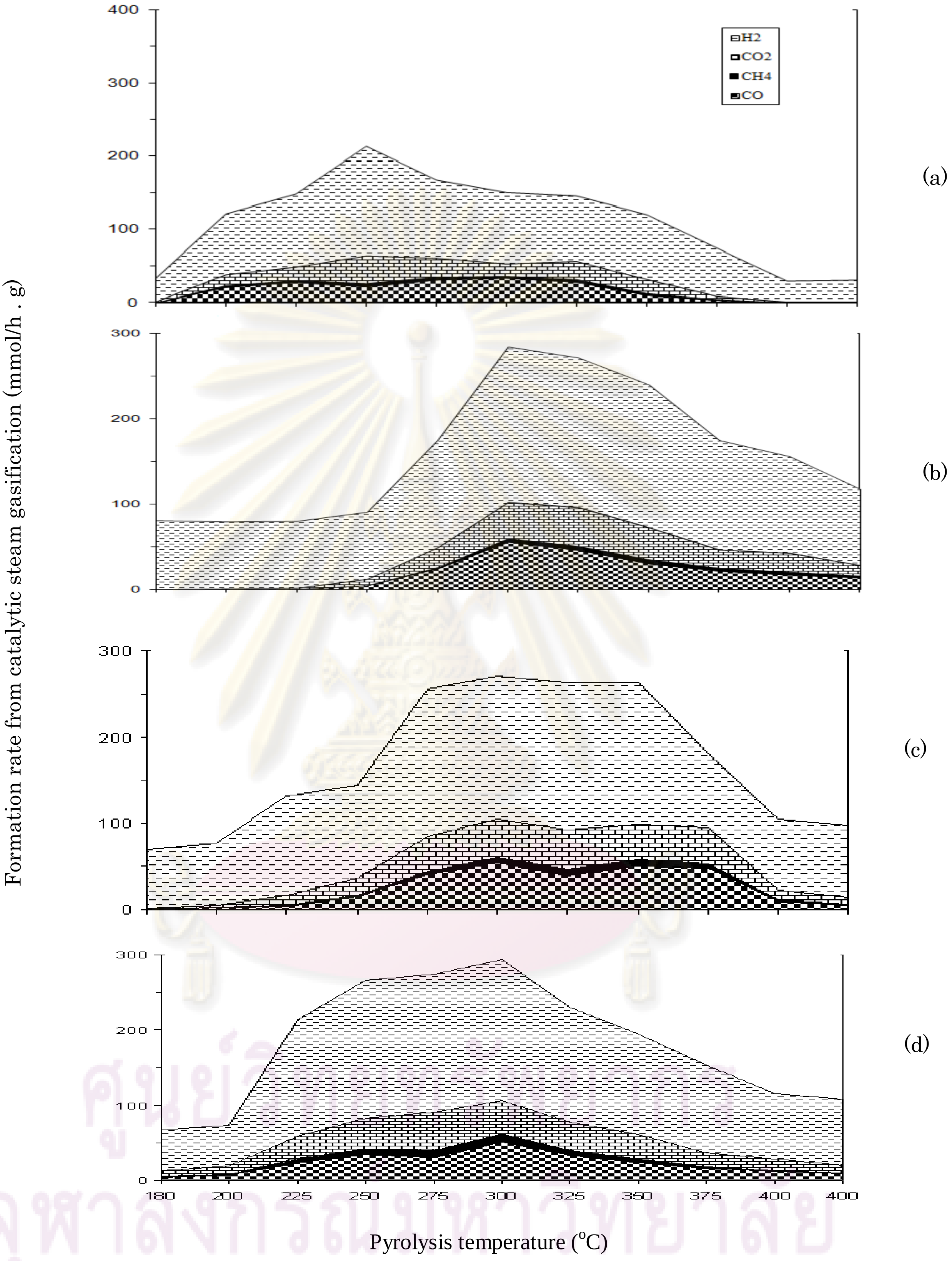

Figure 4.3 Effect of temperature on gas compositions from temperature programmed pyrolysis followed by steam gasification with Ni/Dolomite at 750 °C and steam 222 mmol/h. (a). Pine wood chip, (b). Coconut shell, (c). Bamboo, (d).Corncob.

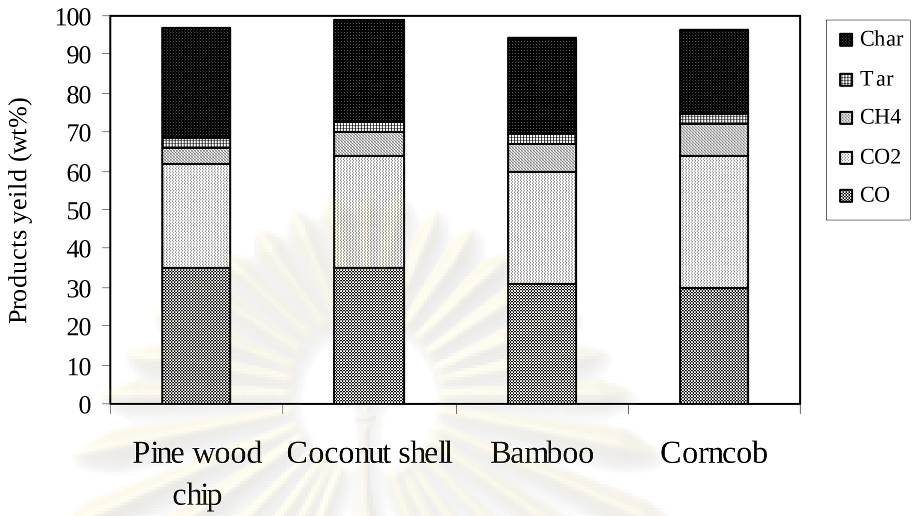

Figure 4.4 The products of biomass pyrolysis followed by catalytic gasification by temperature programmed method in carbon basis at steam flow rate 222 mmol/h, H_2 75 mmol/h, Ar 193 mmol/h and biomass 0.5 g.

Tar, which is one of the main products from pyrolysis zone, was well known that can be eliminated by the excellent catalyst in the suitable circumstances. From the above discussion, gaseous products are mostly derived from tar and the significant of eliminated tar mechanisms will be explained in this article. Wood chip was selected to find the suitable conditions of tar gasification. After pyrolysis occurred, gases and tars were reached on the Ni/Dolomite catalyst to be gasified. Since the temperature and the steam concentration are the important parameters, the gasify temperatures were set up at 700, 750, and 800 ^{o}C, respectively. Temperature at 750 ^{o}C and the best composition of reforming gas is H_2/H_2O (220/75) were shown as the best performance in catalytic tar gasification which is the same result as Srinakruang *et al.* [11-12] that claimed the property of Ni/Dolomite catalyst- *It could become the high performance at the temperature around 750-780 ^{o}C in toluene and naphthalene gasification*. The tar reforming gasification by steam (eq.(2)), water gas shift reaction(eq.(6)), and steam reforming reaction(eq.(7)) could explain the consequences of gas compositions.

Ni/Dolomite catalyst was used for tar gasification under the suitable conditions both steam (222 mmol/h) and temperature (750 ^{o}C) with Ni/Dolomite catalyst. When gasification was carried on, tar has been derived to react with reduced nickel to form nickel carbide and finally reacted with steam to be synthesis gas. After tar was gasified through Ni/Dolomite catalyst, tar can be completely eliminated into the synthesis gas.

The catalytic mechanisms are presented in the reaction (8) to (10), Ni/Dolomite catalyst is reduced with hydrogen to form reduced $Ni^{(0)}$ and then cracked with tar to form the synthesis gas when gasification occurred.

$$NiO + H_2 \longrightarrow Ni^{(0)} + H_2O \qquad (8)$$

$$Ni^{(0)} + C_x H_y \longrightarrow NiC_x + H_y \qquad (9)$$

$$NiC_x + H_y \xrightarrow{Steam} Ni + CO + H_2 \qquad (10)$$

4.2.3. *Char Gasification*

The reactions of char [65-71] steam gasification without catalyst to promote gas products are shown below:

$$2\,C\,(Char) + 3H_2O \longrightarrow CO + 3H_2 + CO_2 \qquad (11)$$

$$CO_2 + H_2 \leftrightarrow CO + H_2O \qquad (12)$$

Chars were derived from biomass pyrolysis and could not decompose at lower temperature than 400 ^{o}C. Table 4.3 illustrates the analysis of char composition that was derived from four types of biomass. The range of temperature is examined to eliminate char in gasification process.

Table 4.3 Analysis of four types of char from biomass

	Pine wood chip	Coconut shell	Bamboo	Corncob
Elemental analysis of char(%wt)^{a}				
Carbon	71.9	76.1	74.6	75.2
Hydrogen	2.4	3.8	3.7	3.4
Nitrogen	0.0	0.0	0.0	0.5
Oxygen	25.7	20.1	21.7	20.9

^{a}Determined by CHN elemental analysis.

Temperature Programmed Reaction (TPR) method was used in this experiment from 400 °C to 850 °C in 20 minutes. In Figures.4.5a-4.5d, the char gasification of four species of biomass as pine wood chip, coconut shell, bamboo and corncob is shown as a function of temperature. From the figures, it can be seen that char started to be gasified to form carbon monoxide from 680 °C and sharply increased at over 800 °C. After heating up to 850 °C, no char remained. It can be concluded that char gasification can be operated smoothly at temperature above 800 °C. Table 4 shows the composition in mol (%) for four species of biomass char in carbon basis. The composition of gaseous products depends to some extent on the source of the char, the major products are CO, the next one is CO_2 and the yield of CH_4 is low (2 ~ 5 mol (%)).

Char is the component of lignin content, which is not decomposed at low temperature. According the figures, the gas compositions of four biomass chars are different, especially bamboo char. Although the CHN elemental analysis presents the percentages of carbon, hydrogen and oxygen in four chars of biomass, which are similarly among four char biomass types. It can be explained that bamboo is most the soft wood. It can be gasified easiest with steam. Moreover, the pore and morphology have claimed the important influence to steam gasification [37, 72-73]. On the other hand, coconut shell, which is the hard wood, is hardest to be gasified with steam giving the small amounts of gas products. It can be summarized that the characteristic of the soft wood and the hard wood is the important influence in gasification.

Table 4.4 The gas productions in char gasification in carbon basis

Chars	CO(mol %)	CH_4(mol%)	CO_2 (mol%)
Pine wood chip	51.8	5.6	43.1
Coconut shell	66.0	5.2	28.8
Bamboo	68.4	2.4	29.2
Corncob	62.9	2.6	34.5

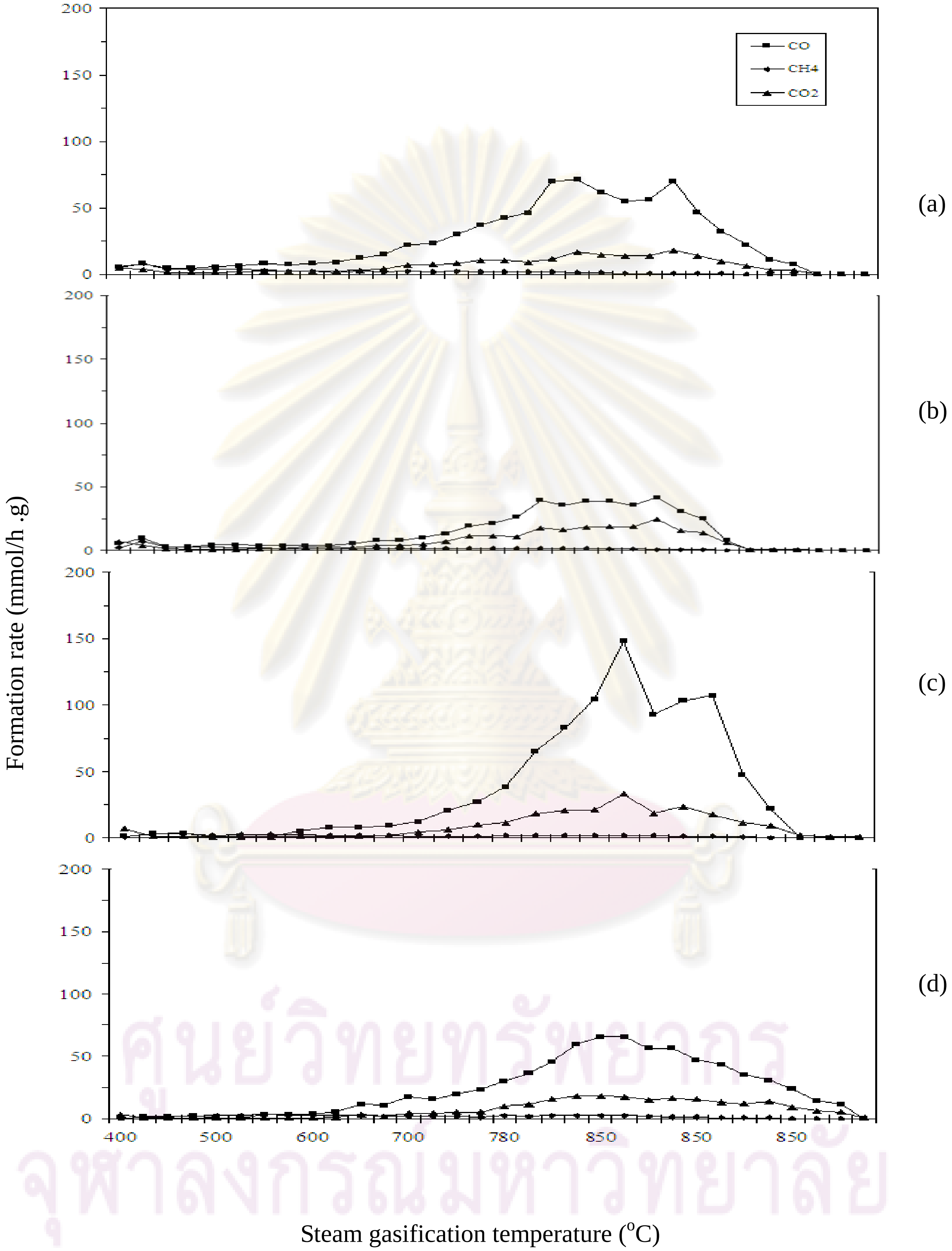

Figure 4.5 The char steam gasification without Ni/Dolomite catalyst at the high temperature by temperature program at steam 222 mmol/h, H_2 75 mmol/h, Ar 193 mmol/h and char 0.15 g. (a). Pine wood chip, (b). Coconut shell, (c). Bamboo, (d) Corncob.

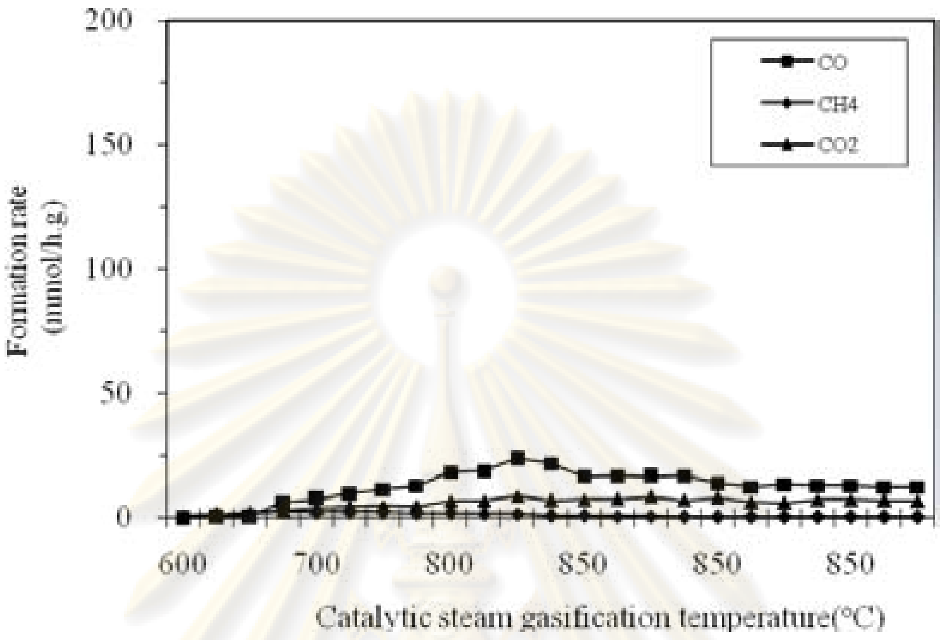

Figure 4.6 The char steam gasification of coconut shell with Ni/Dolomite catalyst at steam 222 mmol/h, H_2 75 mmol/h, Ar 193 mmol/h and char 0.15 g.

Furthermore, the effect of Ni/Dolomite on char from coconut shell gasification was also investigated for comparing with and without catalyst as shown in Figure.4.6 and Figure.4.5b. Surprisingly, the effect of this catalyst was negative for char gasification giving smaller gases. This result can be summarized that Ni/dolomite is unnecessary or even negative for the char gasification. The carbon deposition was found on Ni/Dolomite surface after experiment finished which is analyzed by TGA as shown in Figure 4.7. Although the reason is not clear, the possibility of secondary reaction of gas (CO) may take place.

$$2CO \xrightarrow{Ni} CO_2 + C \qquad (13)$$

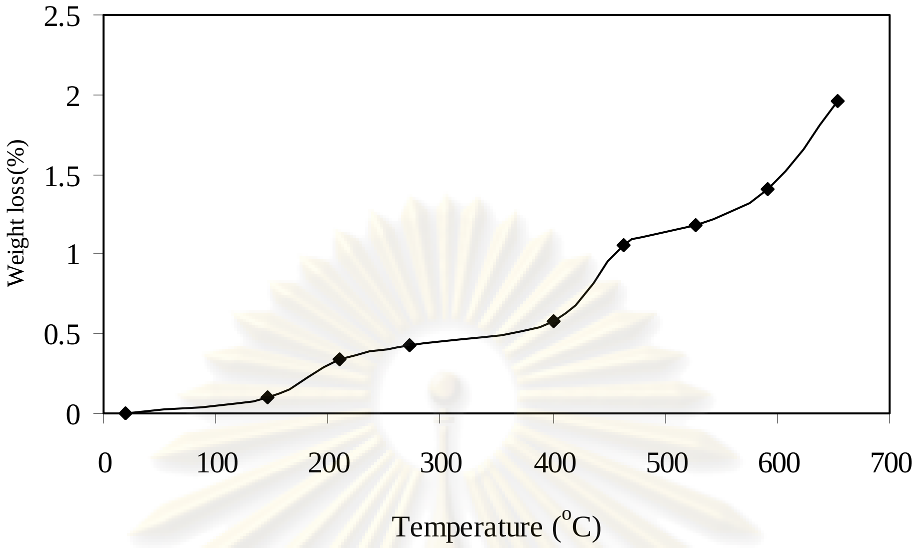

Figure 4.7 Char decomposition on Ni/dolomite catalyst surface by thermogravimetric analysis (TGA).

As the result from the above experiments, it can be summarized the characteristic of pyrolysis and steam gasification with and without catalyst on the gas compositions from low temperature (180 °C) to high temperature (850 °C) by temperature programmed reaction (TPR) method as shown in Figures 4.8a – 4.8c.

The figures present the characteristics of gas compositions in the various situations such as pyrolysis in argon, pyrolysis followed by gasification in argon and steam and pyrosis followed by gasication in argon and steam with Ni/Dolomite catalyst. Coconut shell is chosen to investigate the gas compositions at the various circumstances. The results of gas production at the variety situations in this chapter can be the primary data of biomass pyrolysis, tar catalytic gasification and char gasification lead to the application of biomass gasification.

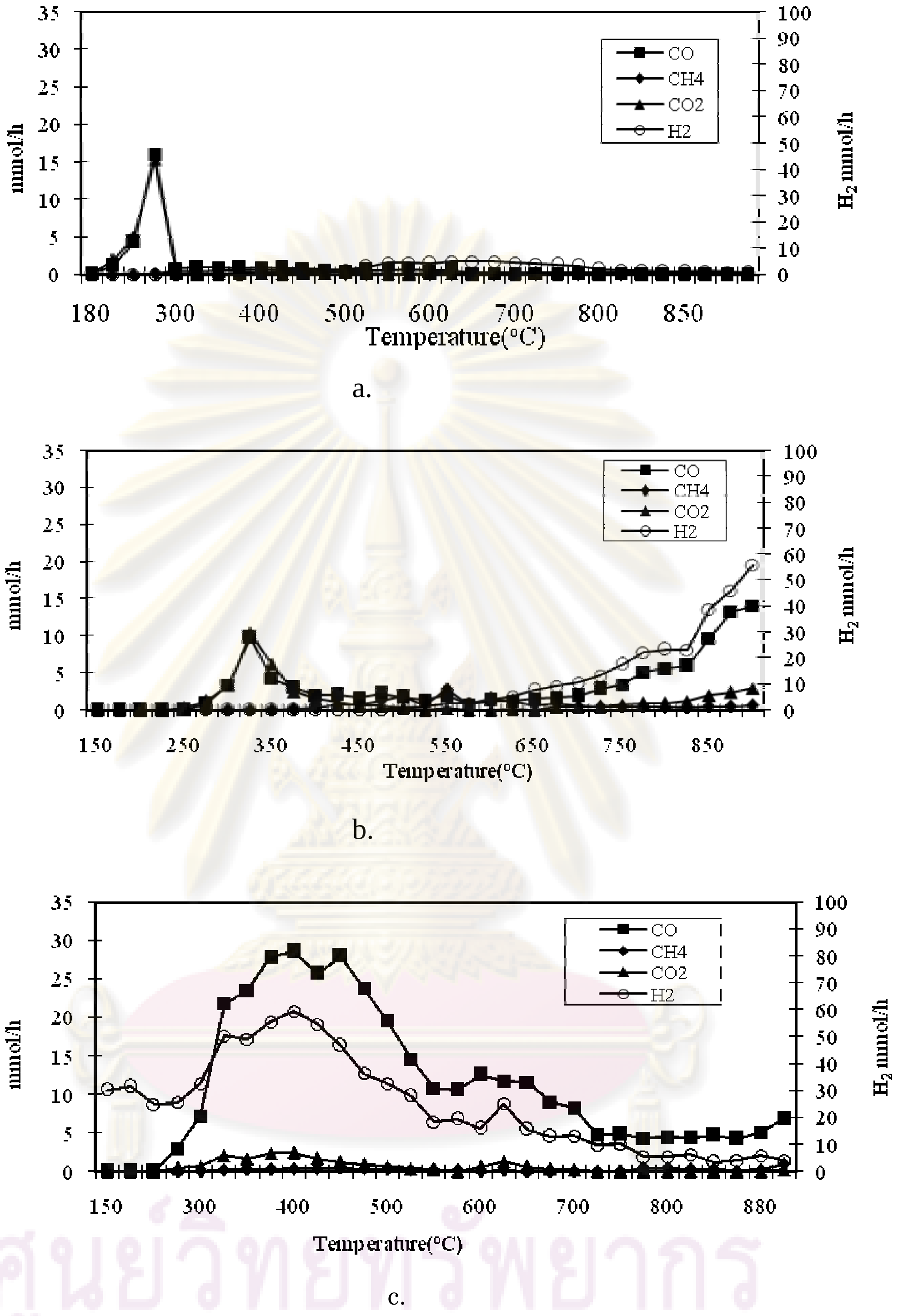

Figure 4.8 The summarization of gas compositions on temperature program at the various situations. (a) Pyrolysis coconut of shell in argon atmosphere, (b). Steam pyrolysis and gasification of coconut shell at steam 222 mmol/h, H_2 75 mmol/h, Ar 193 mmol/h and coconut shell 0.5 g, (c). Steam pyrolysis followed by catalytic gasification coconut shell at steam 222 mmol/h, H_2 75 mmol/h, Ar 193 mmol/h, Ni/Dolomite catalyst 5 g and coconut shell 0.5 g.

4.3. Conclusions

From thermogravimetric analysis (TGA) of four types of biomass showed three steps of weight loss occurred in the presence of N_2: (1) the dehydration of biomass (50-200 ^oC); (2) the formation gases, tar, and char (200-420 ^oC); and (3) char steam gasification (600-800 ^oC). The predicted in-situ pyrolysis and gasification of biomass in the Ni catalyzed system is shown in Figure 4.9.

The biomass (pine wood chip, coconut shell, bamboo and corncob) pyrolysis was characterized by the Temperature Programmed Reaction (TPR) method in fixed bed followed by the steam reforming of tar. About 30% (carbon basis) char, the TPR of char with steam showed the reaction proceeded at temperature higher than 750 ^oC without catalyst giving CO, CO_2 and H_2 as the major products. The pyrolysis reactivity was in the order; pine wood chip < bamboo < corncob < coconut shell while the char gasification activity was in the order; bamboo > corncob > coconut shell > pine wood chip.

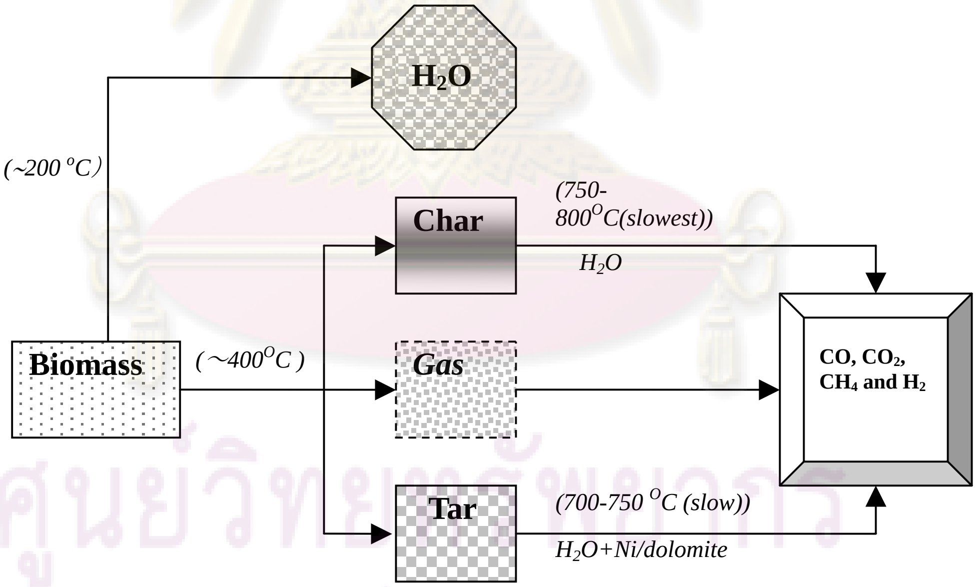

Figure 4.9 The predicted in-situ pyrolysis and gasification of biomass in the Ni catalyzed system.

CHAPTER 5

The Utilization of Biomasses in Simultaneous Gasification and Reforming Process in Fluidized Bed

5.1. The Effect of Gasification Parameters

The effect of various parameters on gas composition from gasification was studied. In this chapter, the results of gasification and reforming experiments with fluidized bed are illustrated in term of the gas composition.

5.1.1. The effect of temperature

The temperature is the main role for gasification process. In this research, it is controlled by temperature programmed method at 750, 780 and 810 ^{o}C, respectively. The steam/carbon ratio of 0.77 is presented to demonstrate the effect of temperature. Bamboo was selected to study the gasification because it could easily be gasified as mentioned in chapter 3. The gasification of bamboo with the feeding rate of 7.5 g/h was investigated the gas products as a function of temperature. Figure 5.1 presents the effect of temperature on gas compositions (CO, CH_4, CO_2 and H_2). It was found that the temperature of 780 ^{o}C was the most suitable temperature, which gave the high carbon monoxide and the low methane and carbon dioxide. Char formation was found to be reduced at this temperature from 10.5% to 6.5%. Moreover, the ratio of H_2/CO at 780 ^{o}C was obtained around 2, which was the ratio of methanol synthesis. The formation of carbon monoxide and hydrogen decreased at higher temperature. Tar was found at a small level of around 0.4%. Table 5.1 shows the products from the effect of temperature in carbon basis. The C-conversion was around 89-93%. These results seem to show that tar reforming and the steam reforming prevail at the higher temperature to derive the high carbon monoxide. The compositions of gas products due to the effect of temperature in this experiment have also concerned with Franco C *et al.* [10] who claimed that the operating temperature was a strong influence on the gas composition. The CO amount decreased slightly in the range temperature of 750 and 850 ^{o}C whereas the H_2 amount increased.

$$\text{Tar} + H_2O \xrightarrow{Ni} CO + H_2 \qquad \textit{Tar reforming reaction}$$

$$\text{Tar} + H_2O \xrightarrow{Ni} CO_2 + 2H_2$$

$$CH_4 + H_2O \Leftrightarrow CO + H_2 \qquad \textit{Steam reforming reaction}$$

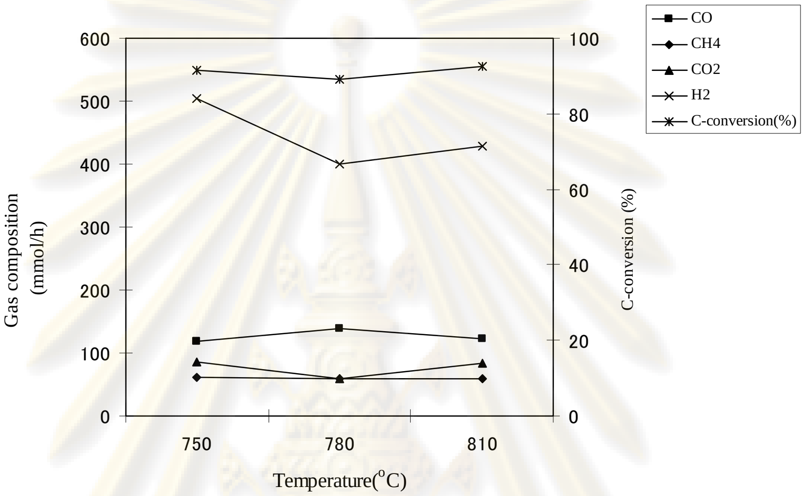

Figure 5.1 The effect of temperature on gas compositions for biomass gasification with fluidized bed at steam flow rate 222 mmol/h, fluidized velocities 450 ml/min and bamboo 7.5 g/h/10 g of Ni/Dolomite catalyst.

Table 5.1 The effect of temperature on the products of biomass gasification with fluidized bed in carbon basis

Temperature(°C)	CO	CH_4	CO_2	H_2	%C conversion	Char(%)[a]	Tar(%)[b]
		mmol/h					
750	117.7	60.9	87.4	524.6	89.1	10.5	0.4
780	137.8	59.9	69.9	612.6	93.1	6.5	0.4
810	123.4	59.8	84.4	566.1	92.5	7.1	0.4

Bamboo 7.5 g/h/10 g of Ni/Dolomite catalyst (C-total 289 mmol/h), steam 222 mmol/hr, fluidized velocities 450 ml/min.

[a] and [b] measured by average weight.

5.1.2. The effect of steam flow rate

The influence of steam/carbon ratio on the steam gasification process for bamboo biomass was also studied. The steam/carbon ratio could be varied either by changing the steam flow rate while keeping the biomass feed rate constant. In the experiments undertaken, the steam flow rates of 177, 222 and 244 mmol/h were studied at the temperature of 780 °C while keeping the biomass feed rate constant.

The steam flow rate at 222 mmol/h or the steam/carbon ratio at 0.77 was observed to be the most appropriate condition as shown in Figure 5.2. The formation of H_2 seems to be favoured for steam/biomass ratio of about 0.77-0.84 w/w. The amount of hydrogen was sharply increased while carbon monoxide decreased at the highest steam rate. The formation of carbon dioxide and methane was stable giving small amount as shown in Table 5.2. The C-conversion was around 92%. The results suggest that for steam/carbon ratio at 0.61 w/w, there was not enough steam to react with all the biomass added to gasifier. When steam/carbon ratio higher than 0.7 w/w was used, the formations of H_2 and CO_2 were released. On the other hand, CO_2 and CH_4 remained constant. The steam reforming, water-gas shift and tar reforming were dominated the main roles to produce the synthesis gas, especially hydrogen. The result was also similar with the experiment of Franco C *et al.* [10], who found that the steam/ carbon ratio of 0.6-0.7 w/w produce the higher conversion and favouring H_2 formation.

$$\text{Tar} + H_2O \xrightarrow{Ni} CO + H_2$$ *Tar reforming reaction*

$$\text{Tar} + H_2O \xrightarrow{Ni} CO_2 + 2H_2$$

$$CO + H_2O \Leftrightarrow CO_2 + H_2$$ *Water-gas shift reaction*

$$CH_4 + H_2O \Leftrightarrow CO + H_2$$ *Steam reforming reaction*

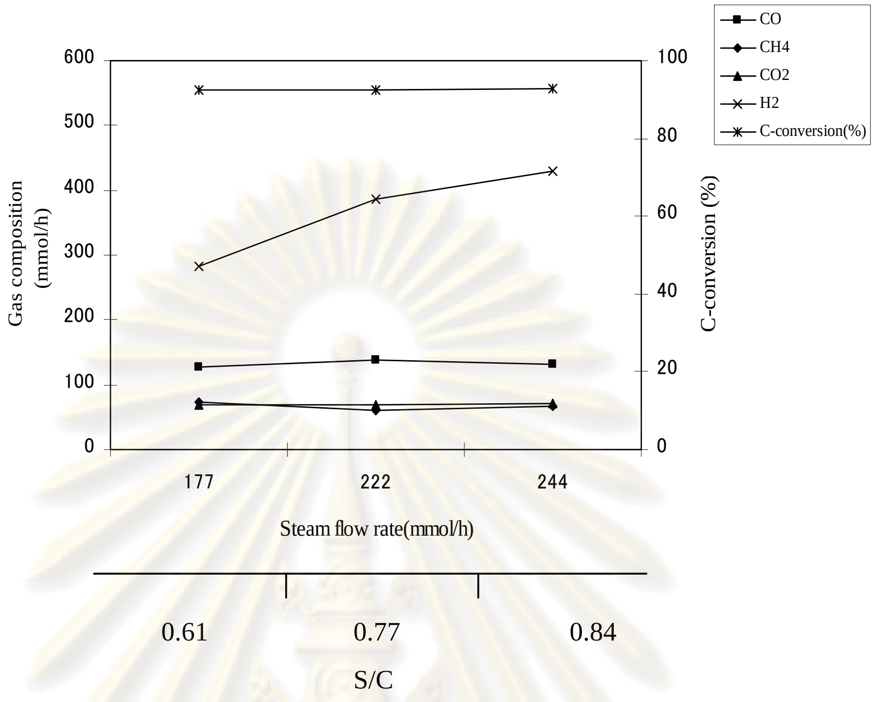

Figure5.2. The effect of steam on gas compositions for biomass gasification with fluidized bed at temperature 810 ^{o}C, gas flow rate for fluidization 450 ml/min and bamboo 7.5 g/h/10 g of Ni/Dolomite catalyst.

Table 5.2 The effect of steam on the products of biomass gasification with fluidized bed in carbon basis

Steam rate (mmol/hr)	S/C	CO	CH_4	CO_2	H_2	%C conversion	Char(%)[a]	Tar(%)[b]
			mmol/hr					
177	0.61	126.5	72.3	68.8	281.8	92.5	7.1	0.4
222	0.77	137.8	59.9	69.9	387.0	92.6	7.0	0.4
244	0.84	130.8	66.2	71.6	428.9	92.7	6.9	0.4

Bamboo 7.5 g/h/10 g of Ni/Dolomite catalyst (C-total 289 mmol/h), steam 222 mmol/h and gas flow rate for fluidization 450 ml/min.

.[a] and [b] measured by average weight.

5.1.3. The effect of gas flow rates for fluidization

The influences of gas flow rates for fluidization were investigated during the reaction. The minimum gas flow rate for fluidization in quartz tube was studied which found to be at 350 ml/min. The various Argon gases such as 300, 400 and 500 ml/min mixed with hydrogen 50 ml/min were fed into the reactor for fluidization. From the Figure 5.3, carbon monoxide was increased when fluidization increased while methane and carbon dioxide decreased, especially hydrogen. From the effect of fluidization on the higher carbon monoxide, it can be explained that the tar formation from biomass could be promoted at the high fluidization and then was activated with tar reforming reaction, which led to the high carbon monoxide. Also, the prevailing of steam reforming and water-gas shift is the main importance to produce gas products. The products are shown in Table 5.3.

$$\text{Tar} + H_2O \xrightarrow{Ni} CO + H_2 \qquad \textit{Tar reforming reaction}$$

$$CH_4 + H_2O \Leftrightarrow CO + H_2 \qquad \textit{Steam reforming reaction}$$

$$CO + H_2O \Leftrightarrow CO_2 + H_2 \qquad \textit{Water-gas shift reaction}$$

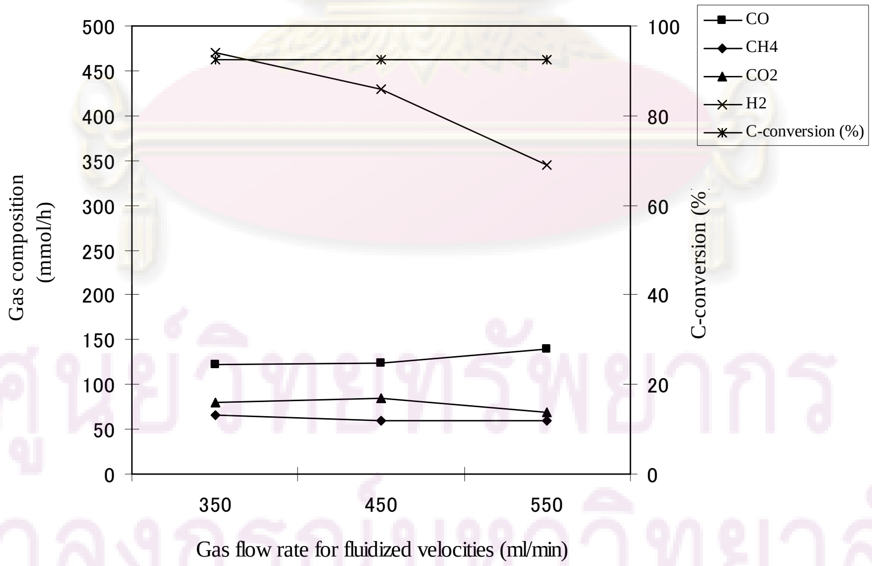

Figure5.3 The effect of fluidized velocities on gas compositions for biomass gasification with fluidized bed at temperature 780 °C, steam rate 222 mmol/h and biomass 7.5 g/h/10 g of Ni/Dolomite catalyst.

Table 5.3 The effect of fluidized velocities on the products of biomass gasification with fluidized bed in carbon basis

Gas flow rate for fluidizations (ml/min)	CO	CH_4	CO_2	H_2	%C conversion	Char(%)[a]	Tar(%)[b]
	mmol/h						
350	121.8	66.6	79.2	470.9	92.6	7.0	0.4
450	123.4	59.9	84.4	429.6	92.6	7.0	0.4
550	139.7	58.8	68.9	345.2	92.5	7.1	0.4

Bamboo 7.5 g/h/10 g of Ni/Dolomite catalyst (C-total 289 mmol/h), steam 222 mmol/h.

[a] and [b] measured by average weight.

5.1.4. The effect of biomass feeding rate

Biomass feeding rate was investigated to produce the gaseous products. The steam/carbon ratio of 0.77, 0.19 and 0.38 w/w were continuously fed on the top of the reactor under gravity at the temperature of 780 °C and steam flow rate of 222 mmol/h constants , where the amount of Ni/Dolomite catalyst in the reactor bed was fixed at 10 g. The formation of CO, CO_2 and CH_4 proportionally increased with increasing the feeding rate of biomass and hydrogen constantly. The carbon conversion to gas was around 92-93%. The gaseous products are shown in Figure 5.4 and Table 5.4. The formation of carbon monoxide was higher than hydrogen at the highest biomass feed rate. The reactions, as shown below, present the mechanisms of reforming and gasification in fluidized bed, where the biomass feeding rate is increased in carbon basis and the steam flow rate is kept constant. The carbonaceous gas products in carbon basis are sharply increased whereas hydrogen is decreased due to a constant steam flow rate.

$$\text{Biomass} \longrightarrow CO + CO_2 + \text{Tar} + \text{Char}$$

$$\text{Tar} + H_2O \xrightarrow{Ni} CO + H_2$$ *Tar reforming reaction*

$$\text{Tar} + H_2O \xrightarrow{Ni} CO_2 + 2H_2$$

$$\text{Char} + H_2O \longrightarrow CO + CO_2 + H_2$$ *Char gasification*

$$CO + H_2O \Leftrightarrow CO_2 + H_2$$ *Water-gas shift reaction*

$$CH_4 + H_2O \Leftrightarrow CO + H_2$$ *Steam reforming reaction*

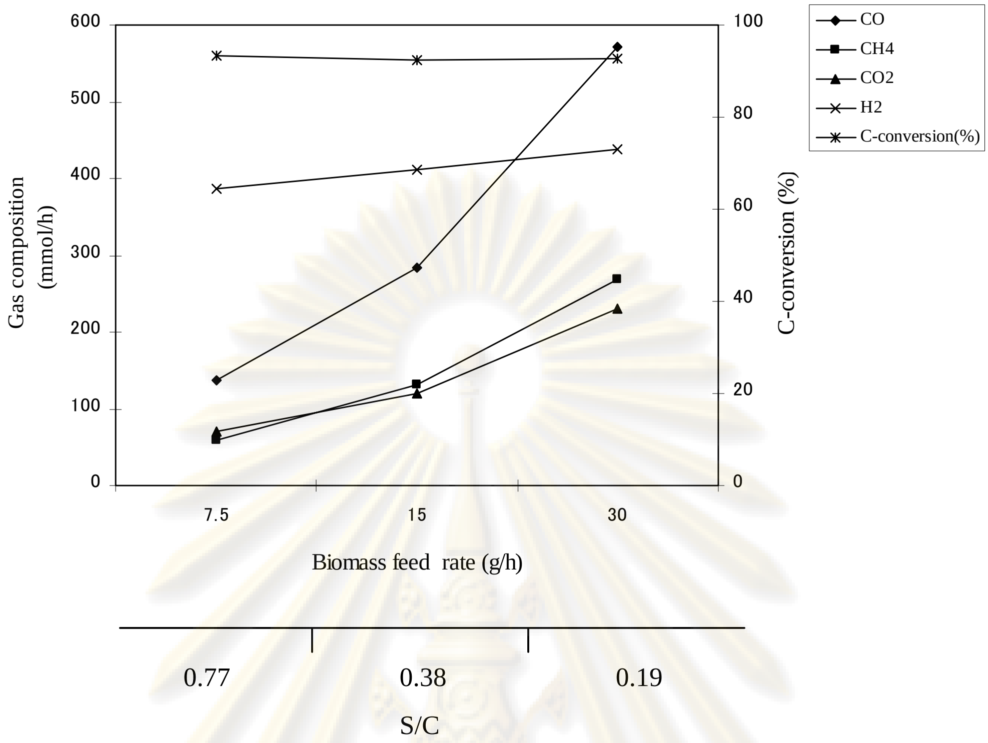

Figure 5.4 The effect of biomass feed rate on gas compositions for biomass gasification with fluidized bed at temperature 780 °C, steam flow rate 222 mmol/h, gas flow rate for fluidization 450 ml/min and Ni/Dolomite catalyst 10 g.

Table 5.4 The effect of biomass feed rate on the products of biomass gasification with fluidized bed in carbon basis

Biomass feed rate (g/h)	Steam/Carbon (w/w)	CO	CH_4	CO_2	H_2	%C conversion	Char(%)[a]	Tar(%)[b]
		mmol/h						
7.5	0.77	139.8	59.9	69.9	307.0	93.3	7.0	0.4
15	0.30	283.1	131.8	119.7	411.6	92.5	7.0	0.4
30	0.19	570.8	268.2	231.3	438.0	92.6	7.0	0.4

Bamboo 7.5 g/h(C-total 289 mmol/h), 15 g/h(C-total 578 mmol/h), 30 g/h(C-total 1156 mmol/h), Ni/Dolomite catalyst 10 g, steam 222 mmol/h and gas flow rate for fluidization 450 ml/min.

[a] and [b] measured by average weight.

In the same way, the various types of biomass were investigated as shown in Figure 5.6. Nowadays, the utilization of biomass was become popular in the industry because it is the renewable energy. The soft woods [bamboo, corncob and pine wood ship] and hard wood [coconut shell and palm shell] were selected for the gasification to characterized the gas compositions. The differences of soft wood and hard wood are the pore size and morphology, which is the main factor for gasification process [37]. It can be seen that soft wood was easier gasified than hard wood.

The main components of biomass are carbon, oxygen and hydrogen, which are carbohydrate function groups and can be developed to the useful gases lead to the methanol or DME production. According to the figure, it can be seen that the gaseous products of five types of biomass can be produced in the same rate because most of them have similar the compositions of carbon, hydrogen and oxygen from the CHN elemental analysis. Table 5.5 shows the products of five types of biomass in gasification process with fluidized bed. The gas compositions of each biomass type are not so different in carbon basis because the elemental analysis shows nearly the same amount of carbon, oxygen and hydrogen. Also, the effect of hemicellulose, cellulose, and lignin compounds in each biomass is the important influence in gasification. The discussions of this effect are claimed in chapter 4 and the literature review [37].

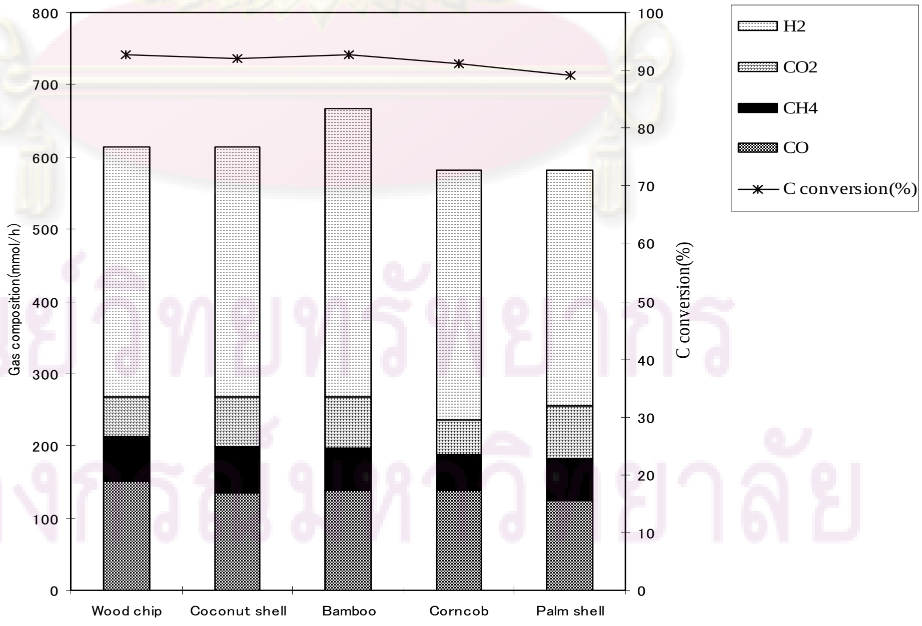

Figure 5.5. The gas compositions for five types of biomass gasification with fluidized bed at temperature 780 °C, steam rate 222 mmol/h, gas flow rate for fluidization 450 ml/min and Ni/Dolomite catalyst 10 g.

Table 5.5 The products of five types of biomass gasification with fluidized bed in carbon basis

Biomasses	CO	CH$_4$	CO$_2$	H$_2$	%C	Char(%)[a]	Tar(%)[b]
(g/h)		mmol/h			conversion		
Wood chip	150.2	62.7	54.7	345.6	90.5	9.1	0.4
Coconut shell	134.2	63.6	69.8	345.5	92.1	7.5	0.4
Bamboo	137.8	59.9	69.9	400.0	92.6	7.0	0.4
Corncob	137.7	49.9	47.8	345.6	92.3	7.3	0.4
Palm shell	124.3	58.1	72.8	326.6	89.2	10.4	0.4

Wood chip (C-Total 289 mmol/h), Coconut shell (C-total 290.6 mmol/h), Bamboo (C-total 289 mmol/h), Corncob (C-total 258.6 mmol/h) and Palm shell (C-total 286.1 mmol/h), Ni/Dolomite catalyst 10 g, steam flow rate 222 mmol/h and gas flow rate for fluidization 450 ml/min.

[a] and [b] measured by average weight.

5.1.5. The effect of catalytic weights

Also, the weight of Ni/Dolomite catalyst was investigated. It was found that the products are rather similar or not so high different as shown in Table 5.6. Thus, the catalyst weight of 10 g was selected to operate the gasification experiment.

Table 5.6 The products of biomass gasification with fluidized bed in carbon basis

Ni/Dolomite	CO	CH$_4$	CO$_2$	H$_2$	%C	Char(%)[a]	Tar(%)[b]
(g)			mmol/h		conversion		
10	301.7	121.2	111.8	411.6	92.8	7.0	0.4
20	319.7	117.9	90.9	434.1	91.4	7.0	0.4

Bamboo 15 g/h (C-total 289 mmol/h), steam flow rate 222 mmol/h, H$_2$ 133 mmol/h, Ar 1071 mmol/h.

[a] and [b] measured by average weight.

5.1.6. The effect of oxygen input

In the above experiment, the gasification was studied without oxygen situation because Ni/Dolomite catalyst has claimed that it deactivated in air to form NiO. This may result in a low effective and performance. Thus, the effect of oxygen was investigated the influence lead to the gaseous productions. The flow rate of oxygen also was the important role, which it was flowed at 30, 50, 75 and 100 ml/min. The total fluidization velocity of gas flow rate of 450 ml/min, temperature of 780 °C and steam flow rate at 222 mmol/h were selected in the reaction to study the effect of oxygen input on gas compositions.

The effect of oxygen input is shown in Figure 5.6. It was found that oxygen has significant influence to perform the amounts of carbon monoxide and carbon dioxide forms. The partial oxidation in equation (1) occurs at low oxygen input, which gives the higher carbon monoxide than carbon dioxide. Where oxygen flow rates were increased, it can be seen sharply that carbon dioxide increased and methane decreased. At the highest oxygen flow rate, it was observed that carbon dioxide was higher than carbon monoxide, which the influence of oxidation (2) is prevailing. Besides, the steam reforming (3) and the water gas shift reactions (4) also participated to produce the gas products.

$$C + \tfrac{1}{2} O_2 \longrightarrow CO \qquad (1)$$

$$C + O_2 \longrightarrow CO_2 \qquad (2)$$

$$CH_4 + H_2O \Leftrightarrow CO + 3H_2 \qquad (3)$$

$$CO + H_2O \Leftrightarrow CO_2 + H_2 \qquad (4)$$

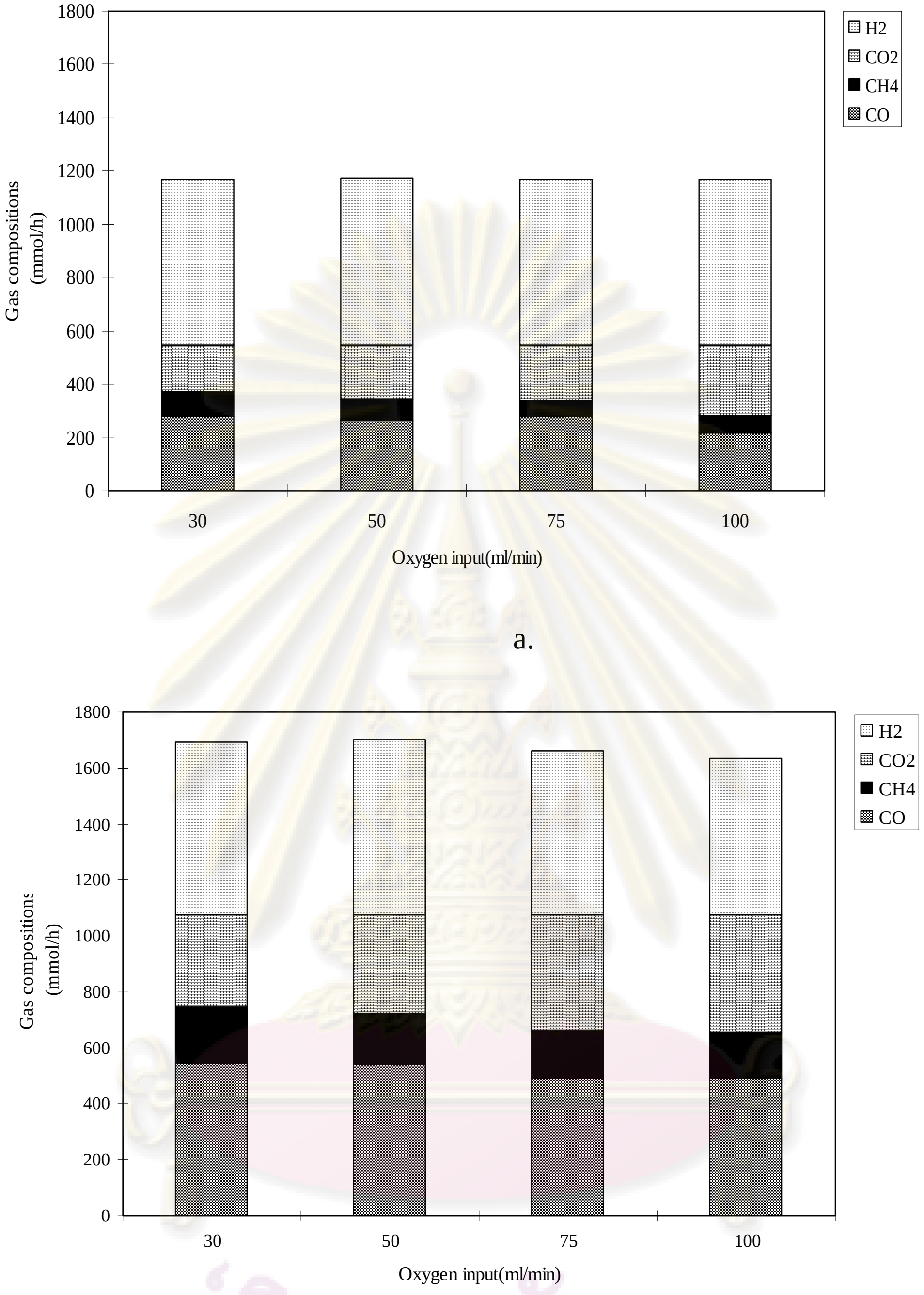

a.

b.

Figure 5.6 The effect of oxygen input on gas compositions at temperature 780 ^{o}C, steam flow rate 222 mmol/h, gas flow rate for fluidization 450 ml/min.and Ni/Dolomite catalyst 10 g. At biomass feed rate (a). 15 g/h; (b). 30 g/h.

Table 5.7 The effect of oxygen input on gas compositions in biomass gasification with fluidized bed in carbon basis

Biomass feed rate	Oxygen (ml/min)	CO	CH_4	CO_2	H_2	%C conversion	Char(%)[a]	Tar(%)[b]
		mmol/h						
15 g/h	30	277.9	94.6	175.3	621.7	94.9	5.1	0.2
	50	254.6	77.6	205.9	627.8	93.3	6.7	0.2
	75	275.7	65.5	206.8	621.6	94.8	5.0	0.2
	100	215.2	68.7	264.1	620.4	94.8	5.0	0.2
30 g/h	30	543.3	203.1	329.9	618.3	93.1	6.7	0.2
	50	542.4	181.2	352.3	624.3	93.1	6.7	0.2
	75	489.1	172.0	415.1	587.5	93.1	6.7	0.2
	100	491.1	165.9	419.1	557.2	93.0	6.8	0.2

Biomass feed rate 15 g/h (C-total 578 mmol/h) and 30 g/h (C-total 1156 mmol/h), Ni/Dolomite catalyst 10 g, steam flow rate 222 mmol/h , H_2 133 mmol/h, Ar 1071 mmol/h.

[a] and [b] measured by average weight.

Moreover, Figure 5.7 and Figure 5.8 show the product distribution and C-conversion on Ni/Dolomite catalyst as a function of time-on-steam. The gasification experiment was carried out in the conditions of temperature at 780 ^oC, steam flow rate at 222 mmol/h, gas flow rate for fluidization of 450 ml/min and Ni/Dolomite catalyst of 10 g. The biomass feed rates at 15 g/h and 30 g/h were selected, whereas oxygen inputs of 50 ml/min and 100 ml/min were fed into the reactor, respectively. The gas compositions were investigated by TCD gas chromatograph every 5 minutes, while biomass was continuously fed. The gas products were also studied endlessly after biomass was stopped feed. The amount of oxygen input also studied to illustrate the effect on gas compositions after finished biomass feed to produce gas products from biomass or char residues in the reactor.

According to the figures, the C-conversion was within 92-93% at the beginning of the reaction, where biomass was continuously fed. At the highest oxygen input (100 ml/min), hydrogen was found decreased as a function of time-on-steam. The influence of hydro-oxidation reaction (5) was prevailed at this situation.

$$H_2 + ½ O_2 \longrightarrow H_2O \qquad (5)$$

After the feeding of the biomass into the reactor was finished to feed into reactor, the gas formation rate decreased gradually with time on steam. On the other hand, gas compositions (CO, CO, H_2 and small CH_4) were also released at this zone. Because the char residues that accumulated in the reactor were gasified with steam and oxygen to produce the gas products. The influence of char gasification, partial oxidation and oxidation prevailed at this situation to promote CO, CO_2, H_2 and small CH_4.

Comparing with gas products at low oxygen input (50ml/min) and at the highest oxygen input (100 ml/min) after finished biomass feed, it can be seen that carbon monoxide, carbon dioxide and hydrogen are formed and no methane occurred at low oxygen input (50ml/min). The formation of carbon monoxide was higher than carbon dioxide due to the influence of partial oxidation. Furthermore, carbon dioxide has produced and higher than carbon monoxide at the highest oxygen (100 ml/min) after finishing biomass fed because of the influence of oxidation.

Figure 5.9 and Table 5.8 illustrate the products as a function of the various biomasses feeding rates in the term of steam/carbon ratio, where steam flow rate was kept constant rate and oxygen input also is fed into the reactor. Whereas biomass feed rates are increased, the amounts of gaseous products also increased. Comparing with the Table 5.4 and Table 5.8 in case of the presence and absence of oxygen input, it was found that CO, CH_4, tar and char decreased while CO_2 increased after oxygen input.

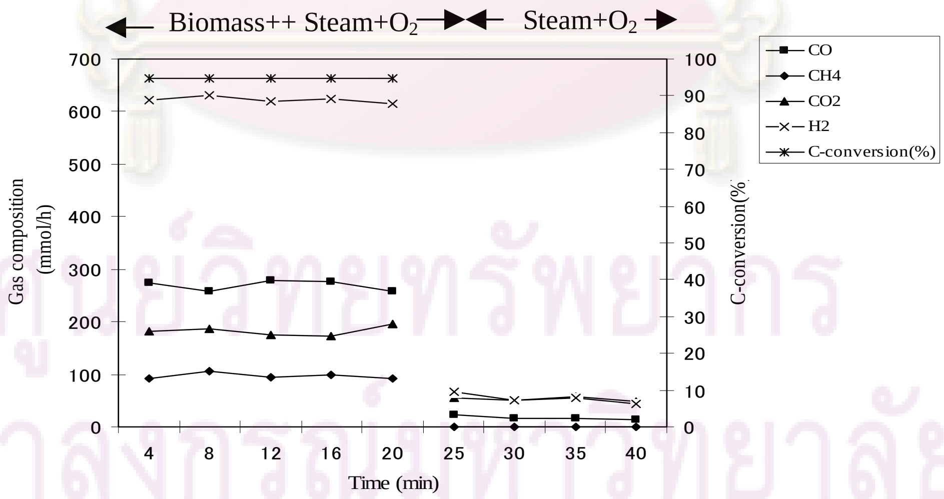

Figure 5.7 The gas compositions on time-on-steam with fluidized bed at temperature 780 ^{o}C, steam flow rate 222 mmol/h, gas flow rate for fluidization 450 ml/min, Ni/Dolomite catalyst 10 g, biomass feed rate 15 g/hr and oxygen input at 50 ml/min.

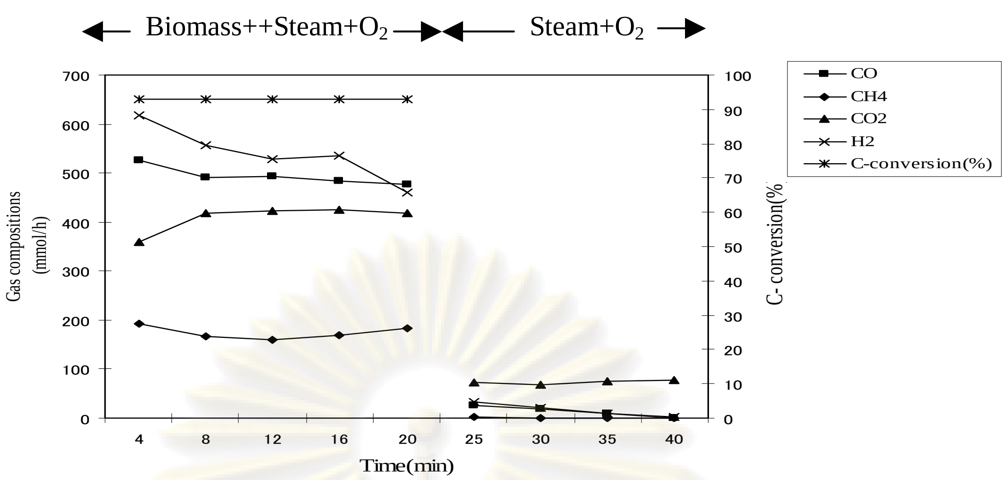

Figure 5.8 The gas compositions on time-on-steam with fluidized bed at temperature 780 °C, steam flow rate 222 mmol/h, gas flow rate for fluidization 450 ml/min and Ni/Dolomite catalyst 10 g, biomass feed rate 30 g/hr and oxygen input at 100 ml/min.

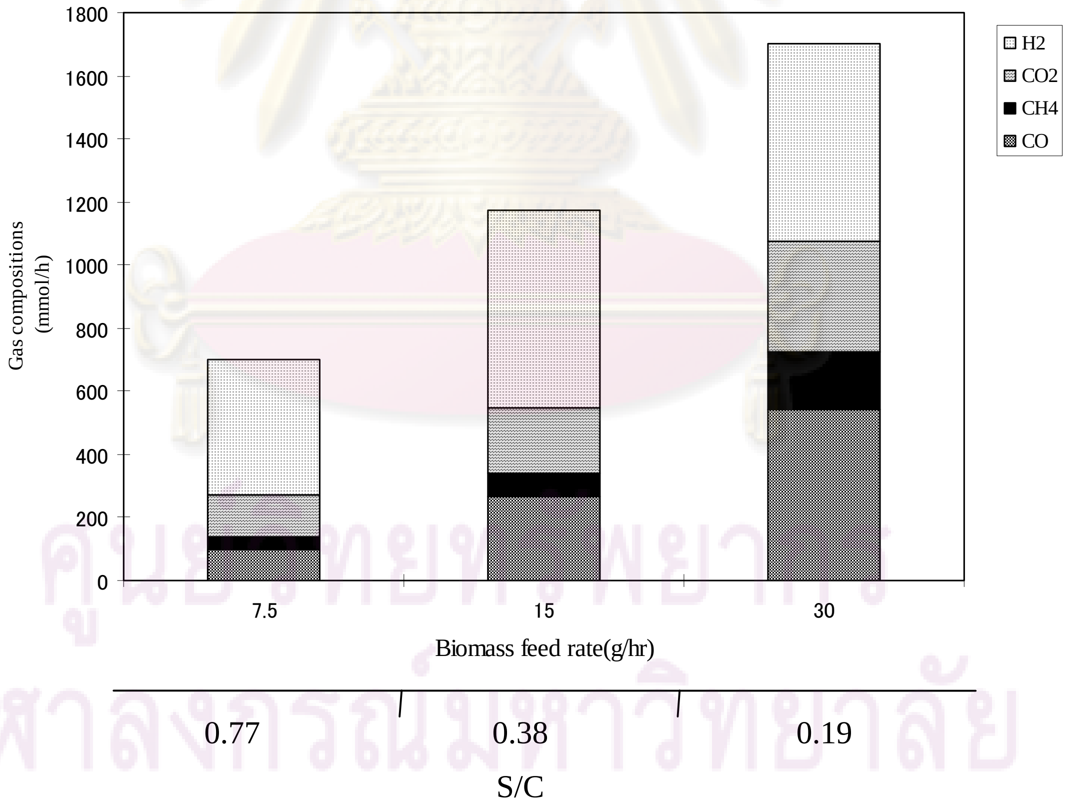

Figure 5.9 The gas compositions as a function of increasing biomass feed rate at temperature 780 °C, steam flow rate 222 mmol/h, gas flow rate for fluidization (Ar 400ml/min+O_2 50 ml/min) and Ni/Dolomite catalyst 10 g.

Table 5.8 The effect of biomass feed rate in steam/carbon ratio with oxygen input on the products of biomass gasification with fluidized bed in carbon basis

Steam/Carbon (w/w)	CO	CH_4	CO_2	H_2	%C conversion	Char(%)[a]	Tar(%)[b]
	mmol/h						
0.77	99.6	38.5	135.1	427.5	94.5	5.3	0.2
0.38	264.3	77.6	205.9	627.8	94.8	5.0	0.2
0.19	542.4	181.2	352.3	624.3	93.0	6.8	0.2

Bamboo 7.5 g/h(C-total 289 mmol/h), 15 g/h(C-total 578 mmol/h), 30 g/h(C-total 1156 mmol/h), Ni/Dolomite catalyst 10 g, steam flow rate 222 mmol/h, and gas flow rate for fluidization (Ar400ml/min+O_2 50 ml/min).

[a] and [b] measured by average weight.

5.1.7. The mechanism for biomass gasification in fluidized bed

Figure 5.10 illustrates the expected mechanism that occurs in the fluidized bed. Actually, the effectiveness of biomass gasification with fluidized bed occurred where the suitable conditions were set up. When gasification occurred, biomass was gasified with steam to produce gases, tar and char. Tar was eliminated with Ni/Dolomite catalyst, which led to the increase in synthesis gas. Char was reacted with steam to the gaseous products. Moreover, water gas shift and steam reforming, which are the reversible reactions, also played the important role to form gaseous products.

$$\text{Biomass} \longrightarrow CO+CO_2+CH_4+H_2 \qquad (1)$$

$$\text{Tar} + H_2O \xrightarrow{Ni} CO + H_2 \qquad (2)$$

$$\text{Tar} + H_2O \xrightarrow{Ni} CO_2 + 2H_2 \qquad (3)$$

$$\text{Char} + H_2O \longrightarrow CO + H_2 + CO_2 \qquad (4)$$

$$CO + H_2O \leftrightarrow CO_2+H_2 \qquad (5)$$

$$CH_4 + H_2O \leftrightarrow CO+H_2 \qquad (6)$$

$$C + 1/2\ O_2 \longrightarrow CO \qquad (7)$$

$$C + O_2 \longrightarrow CO_2 \qquad (8)$$

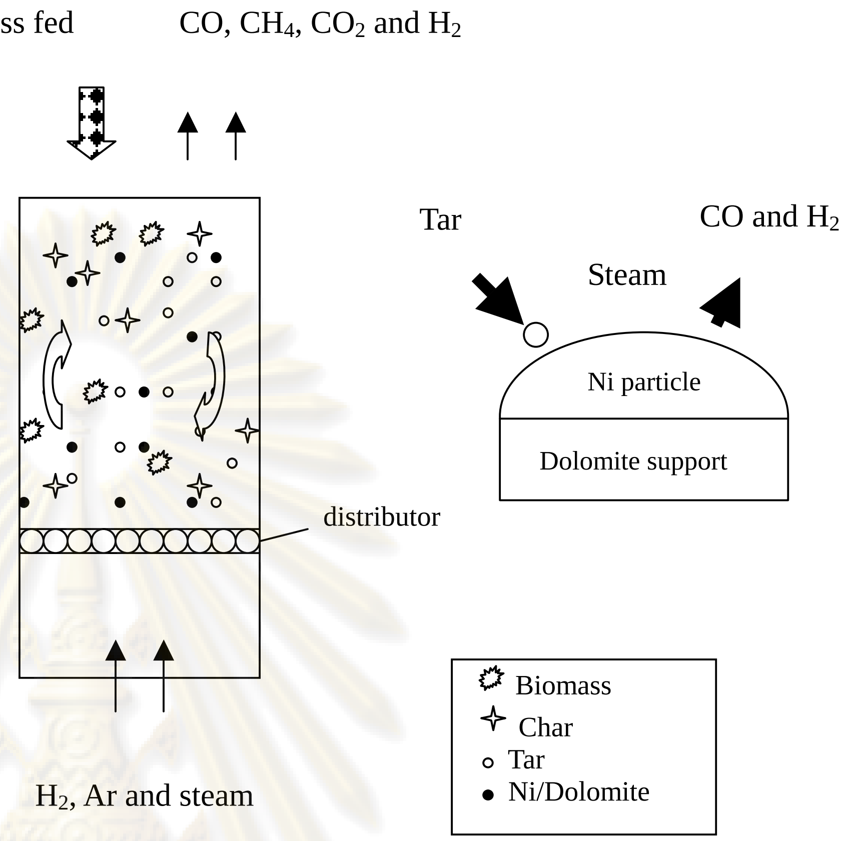

Figure 5.10 The mechanism of biomass gasification in fluidized bed with Ni/Dolomite catalyst.

5.2. The Characteristic of Ni/Dolomite Catalysts

Form the previous work, Srinakruang *et al.* [11-12] have presented the effectiveness and performance of Ni/Dolomite catalyst that can eliminate tar formation. According to XRD analysis in Figure 5.11, the structure of Ni/Dolomite catalyst was observed as $CaCO_3$ (2θ=29.48 ^{o}). It was claimed that $MgNiO_2$, NiO and MgO were detected at 37.2^o, 43.2^o and 62.8^o in the same result as Srinakruang *et al.* [11-12]. NiO was reduced with hydrogen at 700 ^oC to be reduced nickel ($Ni^{(0)}$) form in reaction (1). When gasification was carried on, tar has been derived to react with reduced nickel to form nickel carbide in reaction (2) and finally reacted with steam to be synthesis gas in reaction (3).

$$NiO + H_2 \longrightarrow Ni^{(0)} + H_2O \qquad (1)$$

$$Ni^{(0)} + C_xH_y \longrightarrow NiC_x + H_y \qquad (2)$$

$$NiC_x + H_y \xrightarrow{Steam} Ni + CO + H_2 \qquad (3)$$

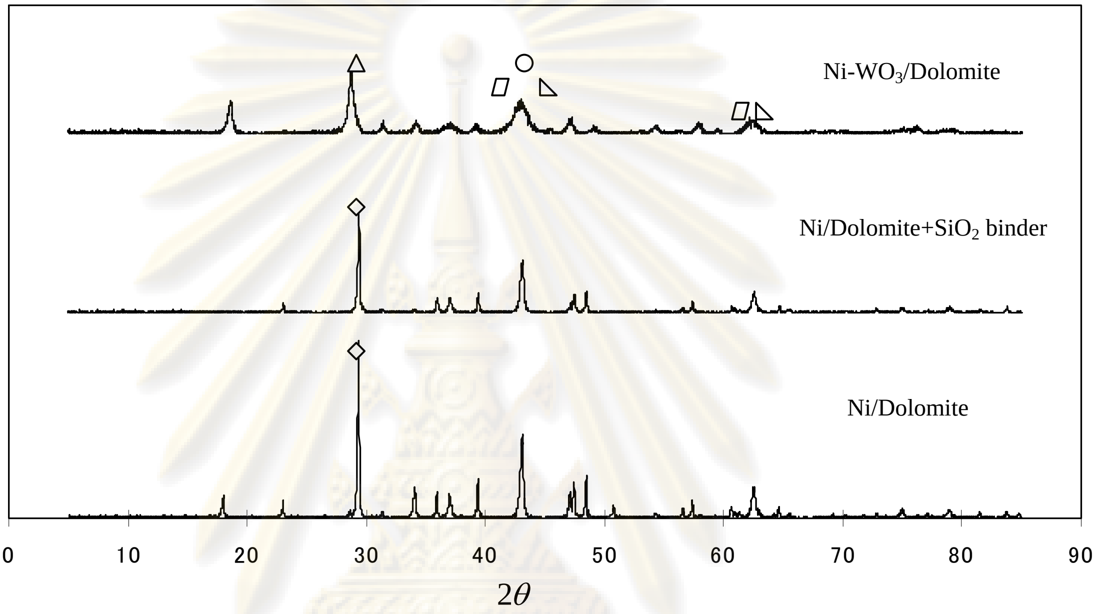

Figure 5.11. XRD analysis of three types of Ni/Dolomite catalyst. (a). Ni/Dolomite; (b). Ni/Dolomite+SiO_2 binder; (c). Ni-WO_3/Dolomite.

(◇) $CaCO_3$, (▱)$NiMgO_2$, (◺) NiO, (○) MgO, (△) $CaWO_4$

Ni/Dolomite + SiO_2 binder was developed because Ni/Dolomite structure might break during the process of crushing and sievimg. SiO_2 binder was added to support the stronger structure.

In addition, the newly developed Ni-WO_3/Dolomite catalyst has been studied to get the highest performance by Sato *et al* [13]. It was found that the new catalyst exhibited higher activity at low temperature, and better resistance to sulfur and coking. In the new catalyst, an added component that promotes dissociation of the combined sulfur elements accelerates the reactions as shown in equations (4) and (5), presumably retaining the lager part of active Ni. Ni–W catalyst is known to be highly active for hydrodesulfurization (HDS). In HDS process, WS_x on Ni catalyst promotes conversion of organic sulfur compounds to H_2S. It is also confirmed that H_2S desorbs from sulfide Ni catalyst in the presence of H_2 at high temperature. Therefore, it is possible that W promotes sulfur dissociation shown in equations (4) and (5).

In the Figure 5.11, it is shown that XRD analysis of Ni-WO_3/Dolomite catalyst which the structure of Ni/dolomite catalyst was observed as $CaWO_4$ ($2\theta = 18.58^o$ and 28.74^o). It has been claimed that $MgNiO_2$, NiO and MgO were detected at 37.2^o, 43.2^o and 62.8^o.

$$NiS_x + W \longrightarrow Ni + WS_x \qquad (4)$$

$$WS_x + xH_2 \longrightarrow W + xH_2S \qquad (5)$$

Table 5.9 presents the characteristics of three types of Ni/Dolomite catalyst that are used in this experiment. NiO was the main structure that is the keyword in the tar gasification. Also, BET and metallic surface area are shown in the below table. The SEM photography of three catalysts is presented to see the impregnated characterization of Ni based on dolomite in Figure 5.12.

Table 5.9 Properties of three types of Ni/Dolomite catalysts

Type	Catalysts	Ni form[a]	BET(m^2/g)[b]	Metallic surface area(m^2/g)[c]
1	Ni/Dolomite	NiO, $NiMgO_2$	27.0	0.5
2	Ni/Dolomite+SiO_2 binder	NiO, $NiMgO_2$	27.0	0.4
3	Ni-WO_3/Dolomite	NiO, $NiMgO_2$	30.3	1.3

[a] measured by XRD analysis.

[b] calculated from N_2 adsorption isotherm.

[c] calculated from H_2 adsorption after Ni reduction at 900 °C with 20% H_2.

Ni/Dolomite Ni/Dolomite+SiO_2 binder Ni-WO_3/Dolomite

Figure 5.12 The SEM of three types of Ni/Dolomite catalyst.

5.3. The Performance of Catalysts

Figure 5.13 shows the result of three types of catalyst on gas compositions in gasification with fluidized bed. Bamboo was used to check the products because It was so interesting in gasification process and was available in abundant in Thailand. According to the figures, the biomass feed rates at 30 g/h was fed continuously. When comparing with the three types of catalyst, it may be seen that the newly Ni-WO_3/Dolomite catalyst can produce higher the synthesis gas than Ni/Dolomite and Ni/Dolomite + SiO_2 binder. Also, carbon dioxide and methane were decreased. Hence, this experiment can be supported by the result of Srinakruang *et al.* [11-12], which used toluene and naphthalene as tar model, that the performance of Ni/Dolomite can be operated in the real biomass gasification for tar elimination to form the synthesis gas. Compare with the literature of Asadullah *et al.* [2-8] who studied the cedar wood gasification on Rh/CeO_2/SiO_2 catalyst, the advantage of Rh/CeO_2/SiO_2 catalyst could play at the low temperature and also could produce the high carbon conversion. However, the cost of this catalyst is relatively higher than conventional catalyst, since the work was done at the laboratory level. The chemicals used for catalyst preparation were high grades and expensive. Thus, Ni/Dolomite catalyst was also another choice in biomass gasification due to its cost, method of preparation and life time were completely the appropriate catalyst [11-13], which can be brought in a commercial scale laboratory.

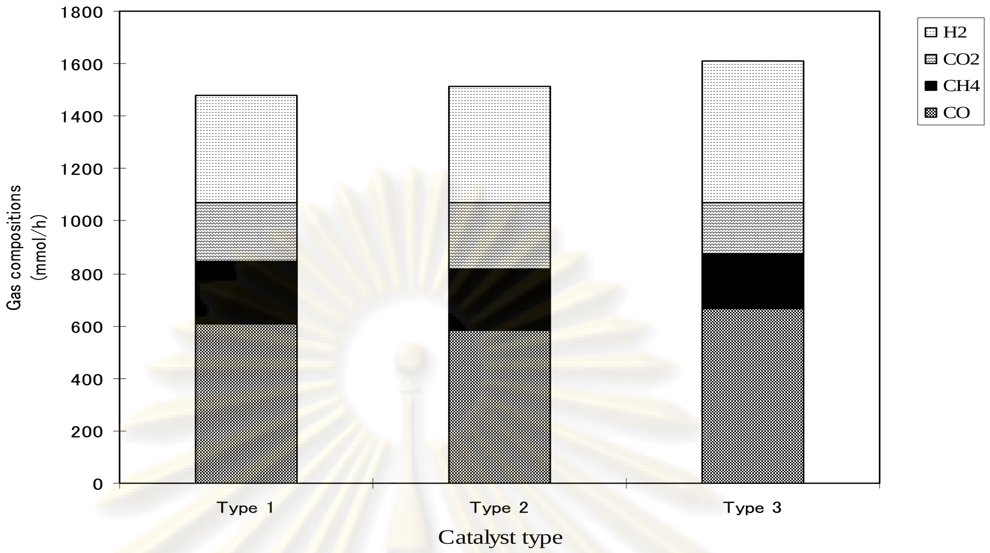

Type 1: Ni/Dolomite;

Type 2: Ni/Dolomite + SiO_2 binder;

Type 3: Ni-WO_3/Dolomite.

Figure 5.13 The gas compositions for bamboo biomass gasification with fluidized bed at temperature 780 °C, steam flow rate 222 mmol/h, gas flow rate for fluidization 450 ml/min, 30 g/h of bamboo and Ni/Dolomite catalyst 10 g.

Table 5.10 The biomass gasification with the various types of Ni/Dolomite on the gas compositions

Biomass feed rate (g/h)	CO	CH_4	CO_2	H_2	%C conversion	Char(%)[a]	Tar(%)[b]
	mmol/h						
Ni/Dolomite	610.2	234.9	225.1	407.1	92.4	7.2	0.4
Ni/Dolomite+SiO_2 binder	585.8	232.4	252.5	441.6	92.6	7.0	0.4
Ni-WO_3/Dolomite	666.7	209.9	193.6	541.2	92.6	7.0	0.4

Bamboo 30 g/h (C-total 1156 mmol/h), Ni/Dolomite catalyst 10 g, steam flow rate 222 mmol/h, and gas flow rate for fluidization 450 ml/min.

[a] and [b] measured by average weight.

The characteristics of catalysts after gasification were studied regarding the structures and carbon deposition. Figure 5.14 shows TGA analysis which was done to investigate the weight loss of carbon deposition on Ni/Dolomite in 100 ml/min of air atmosphere, which was around 0.37 mg. XRD analysis was also carried out to check the structure of catalysts after used in gasification. According to Figure 5.15, the structures of three catalysts were shown to be $CaCO_3$, CaO, $MgNiO_2$, NiO and MgO for Ni/Dolomite and Ni/Dolomite + SiO_2. The newly developed Ni-WO_3/Dolomite catalyst was $CaWO_4$, $MgNiO_2$, NiO, Carbon and MgO.

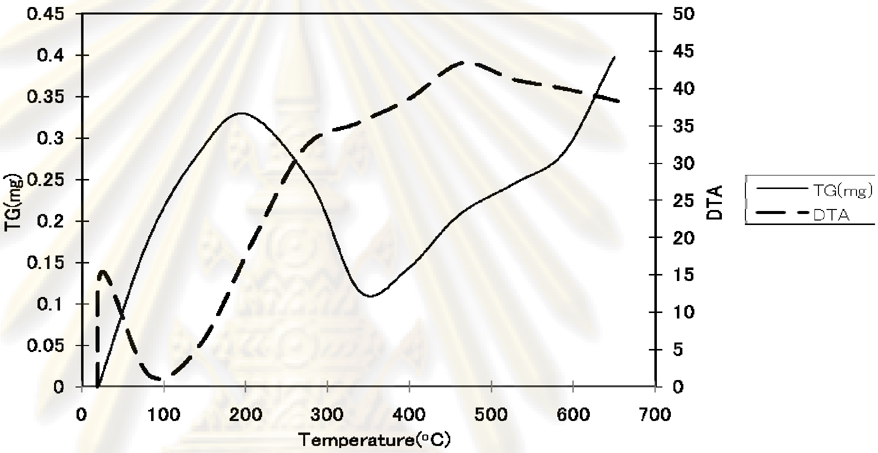

Figure 5.14 TGA analysis of carbon deposition on Ni/Dolomite catalyst after used in biomass gasification.

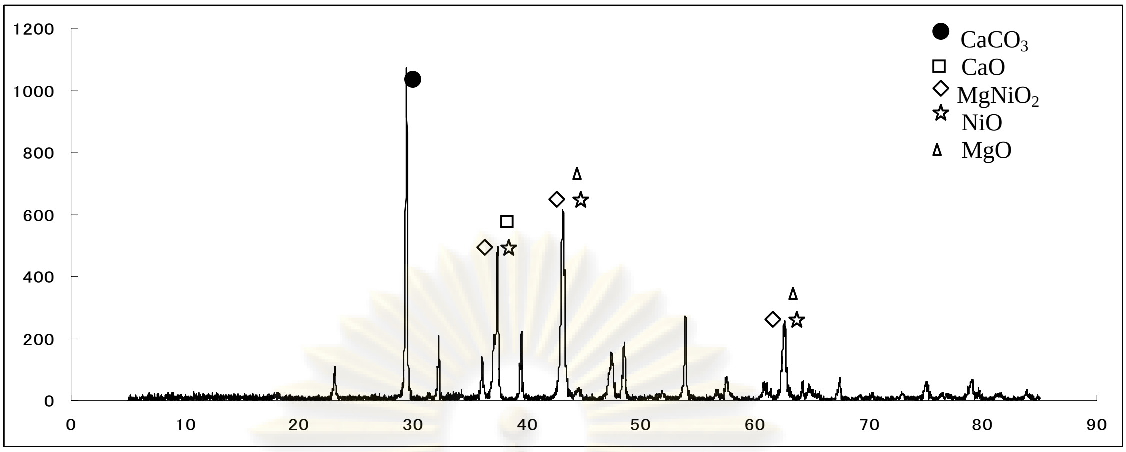

a.

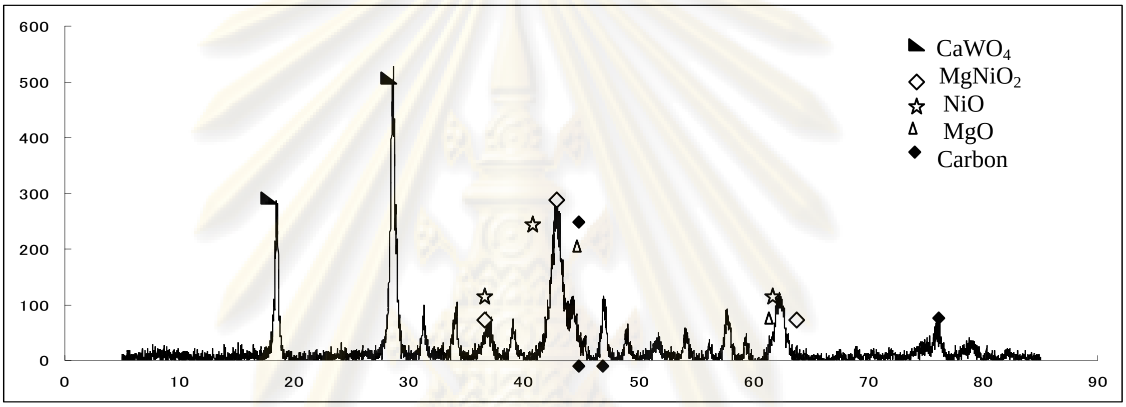

b.

Figure 5.15 XRD analysis of three types of Ni/Dolomite catalyst after used in biomass gasification. (a). Ni/Dolomite and Ni/Dolomite+SiO_2 binder; (b). Ni-WO_3/Dolomite.

5.4. Conclusions

In the present work, the biomass gasification and the catalytic tar gasification were combined in one system. The newly designed apparatus was set up and studied to analyze the performance and the effect of various conditions such as temperature, steam, etc. The effect of them was summarized as follows:

1. The effect of temperature: at 780 °C was selected as the suitable temperature, which can produce high carbon monoxide.
2. The effect of steam: at 222 mmol/h is suitable and hydrogen is increased at higher steam flow rate.

3. The effect of gas flow rate for fluidization velocities: when gas flow rate is increased, CO is increased and H_2 is decreased and reactions of gasification are so fast due to the high fluidization which was the influence of tar formation that lead to the activation of tar reforming.
4. Carbon conversions of biomasses were around 90-93%. Tar was found to be so small around 0.4% and char was around 7%.
5. Five types of biomass: most of them can produce similarly the gaseous products because the compositions of carbon, hydrogen and oxygen of each biomass are similar.
6. Biomass feed rates: when biomass feed rates were increased, CO increased and higher than hydrogen.
7. The effect of oxygen: where oxygen input was increased, carbon dioxide increased and higher than carbon monoxide at the highest oxygen flow rate. Moreover, methane was found to be decreased where input oxygen. The influences of partial oxidation, oxidation and steam reforming are dominant to produce gas products. Char and tar also were found that decreased.
8. It is claimed that Ni/Dolomite catalyst is the effective and give best performance for tar cracking. The newly developed Ni-WO_3/Dolomite catalyst is investigated to resist sulfur and coking. Three types of catalyst were used in the biomass gasification, which are Ni/Dolomite, Ni/Dolomite + Silica binder and Ni-WO_3/Dolomite. From the XRD analysis, the structures of Type 1(Ni/dolomite) and Type 2 (Ni/Dolomite+Silica binder) were similar which were in $CaCO_3$, $MgNiO_2$, NiO and MgO forms. Type 3 (Ni-WO_3/Dolomite) was $CaWO_4$, $MgNiO_2$, NiO and MgO forms. When the catalytic gasification was operated, the newly Ni-WO_3/Dolomite catalyst was the best catalyst for bamboo and palm shell biomasses which could produce the high carbon monoxide and hydrogen but low methane and carbon dioxide were found. Furthermore, the characteristic of used catalyst also studied in term the structure and carbon deposition. The used Ni-WO_3/Dolomite catalyst was found $CaWO_4$, $MgNiO_2$, NiO, Carbon and MgO. Carbon deposition on catalyst was around 0.37 mg according to the TG analysis.

CHAPTER 6

General Conclusions

TG analysis for five types of biomass shows three steps of weight loss occurs in air atmosphere: the dehydration of biomass is the temperature range of 50-200 ^{o}C, at the temperature range of 200-420 ^{o}C is attributed to the gases, tar, and char formation and finally, at above 420 ^{o}C is the oxidation. In nitrogen atmosphere, the dehydration and the pyrolysis occur at 50-200 ^{o}C and 250-400 ^{o}C, respectively.

From the experiment, it can be suggested that gas products such as the carbon monoxide and carbon dioxide from biomass pyrolysis corresponded to less than 10 % of total carbon basis in biomass.

Moreover, pyrolysis followed by catalytic gasification reaction by temperature programmed method presented that almost all the gas products were derived from tar formation.

Gas products started to be pyrolized at temperature of 200 ^{o}C and at the maximum level of300 ^{o}C, which can be designed as the first zone.

In the second zone tar from the first zone is gasified with the Ni/Dolomite catalyst, which was kept at 750 ^{o}C. The gaseous products almost are derived from tar in pyrolysis step and reacted with catalyst.

The final step is the char gasification with steam. Since char began to be gasified at 700 ^{o}C and could smoothly be gasified at above 800 ^{o}C, no char remained after reaction. The steam rate of 222 mmol/h was found to be a suitable condition in biomass catalyst gasification and char gasification. Tar could becompletely gasified with the Ni/Dolomite catalyst. Moreover, the effect of Ni/Dolomite catalyst was negative for char gasification giving smaller gas products.

The biomass (pine wood chip, coconut shell, bamboo and corncob) pyrolysis is characterized by the Temperature Programmed Reaction (TPR) method in fixed bed followed by the steam reforming of tar. About 30% char in carbon basis, the TPR of char with steam showed that the reaction proceeded at temperature higher than 750 ^{o}C without catalyst while giving CO, CO_2 and H_2 as the major products. The pyrolysis reactivity was in the following order; pine wood chip < bamboo < corncob < coconut shell while the char gasification activity was in the following order; bamboo > corncob > coconut shell > pine wood chip.

The development of biomass gasification has been studied continuously for the highest efficiency and safety. The newly apparatus has set up to study the effect of various conditions such as temperature and steam to produce gas products. The temperature at 780 ^{o}C selected as the suitable temperature, which can produce the high carbon monoxide. Steam flow rate 222 mmol/h was suitable and hydrogen was increased at high steam rate. Fluidization velocities (V_f) was increased, CO was increased whereas H_2 was decreased and reactions of gasification were so fast. Carbon conversions of biomasses were around 90-93%. Tar was found to be so small around 0.4% and char was around 7%. For types of biomass, most of them can produce the gaseous products because the compositions of carbon, hydrogen and oxygen of each biomass were similar. When biomass feed rates was increased, the product of CO was increased and was higher than hydrogen. Where oxygen input was increased, it is found that carbon dioxide increased higher than carbon monoxide at the highest oxygen flow rate. Moreover, methane, tar and char were found to be decreased after oxygen input.

At the temperature of 780 ^{o}C , steam flow rate at 222 mmol/h, biomass feed rate of 15 g/h (the steam/carbon ratio was around 0.77) and fluidization at 450 ml/min could produce the ratio of synthesis gas of around 2. The carbon conversion was around 92.6%, char 7.0% and tar 0.4%.

The newly developed Ni-WO_3/Dolomite catalyst is the best catalyst for biomass gasification to produce the high carbon monoxide and hydrogen whereas small amount of methane and carbon dioxide still be expected.

Acknowledgement For The Experiments

The author would like to thank The New Energy and Industrial Technology Development Organization (NEDO), Prof. Li and Prof. Asami at The University of Kitakyushu, Japan for their kindness and supports in the biomass gasification experiment. The authors are also grateful to Dr. Kazuhiro Sato, Takuma Co, Ltd., for the Ni/Dolomite catalysts and their data. Moreover, our gratitude is extended to thankful National Center of Excellence for Petroleum, Petrochemicals, and Advanced Materials (NCE-PPAM) and Department of Chemical Technology Chulalongkorn University.

References

[1] Chaudhari, S.T., Bej, S.K., Bakhshi, N.N., and Dalai, A.K. Steam Gasification of Biomass- Derived Char for the Production of Carbon Monoxide-Rich Synthesis Gas. Energy & Fuels 2001;15:736-42.

[2] Asadullah, M., Tomishige, K., Fujimoto, K. A novel catalytic process for cellulose gasification to synthesis gas. Catalysis Communication 2001; 2:63-8.

[3] Asadullah, M., Miyazawa, T., Ito, S., Kunimori, K., and Tomishige, K. Demonstration of real biomass gasification drastically promoted by effective catalyst. Applied Catalysis A: General 2003; 246:103-16.

[4] Asadullah, M., Miyazawa, T., Ito, S., Kunimori, K., Tomishige, K. Role of catalyst and its fluidization in the catalytic gasification of biomass to syngasat low temperature. Ind. Eng. Chem. Res 2002; 41: 4567-75.

[5] Asadullah, M., Miyazawa, T., Ito, S., Kunimori, K., Tomishige, K. Catalyst performance of $Rh/CeO_2/SiO_2$ in the pyrogasification of biomass. Energy & Fuels 2003; 17: 842-49.

[6] Asadullah, M., Miyazawa, T., Ito, S., Kunimori, K., Tomishige, K. Catalyst development for the gasification of biomass in the dual-bed gasifier. Applied Catalysis A: General 2003; 255: 169-80.

[7] Asadullah, M., Miyazawa, T., Ito, S., Kunimori, K., Tomishige, K. gasification of different biomasses in dual-bed gasifier system: General combined with novel catalysts with high energy efficiency. Applied Catalalysis A 2004; 267: 95-102.

[8] Asadullah, M., Miyazawa, T., Ito, S., Kunimori, K., Tomishige, K. Resistance to sulfur poisoning of hot as cleaning catalysts for the removal of tar from the pyrolysis of cedar wood. Applied Catalysis B: Environmental 2005: 299-307.

[9] Rapagna, S., Jand, N., Foscolo, P.U. Catalytic gasification of biomass to produce hydrogen rich gas. Hydrogen Energy 1998; 23: pp.551-57.

[10] Franco, C., Pinto, F., Gulyurtlu, I., Cabrita, I. The study of reactions influencing the biomass steam gasification process. Fuel 2003; 82:835-42.

[11] Srinakruang, J., Sato, K., Vitidsant, T., Fujimoto, K. A highly efficient catalyst for tar gasification with steam. Catalysis Communication 2005; 6:437-40.

[12] Srinakruang, J., Sato, K., Vitidsant, T., Fujimoto, K. Highly efficient sulfur and coking resistance catalysts for tar gasification with steam. Fuel 2006; 85: 2419-26.

[13] Sato, K., Fujimoto, K. Development of new nickel based catalyst for tar reforming with superior resistance to sulfur poisoning and coking in biomass gasification. Catalysis Communications 2007; 8: 1697–1701.

[14] Bayarsaikhan, B., Sonoyama, N., Hosokai, S., Shimada, T., Hayashi, J., Li, C.Z., Chiba, T. Inhibition of steam gasification of char by volatiles in a fluidized bed under continuous feeding of a brown coal. Fuel 2006; 85:340-49.

[15] Peacocke, G.V.C .,Bridgwater,A.V. Ablative plate pyrolysis of biomass for liquids. Biomass and Bioenergy 1994; 7(16): 147-154.

[16] Peacocke,G.V.C.,1994.Ph.D.thesis,AstonUniversity.

[17] Toft, A.J. Ph.D. thesis, Aston University, Birmingham, UK 1996.

[18] Bridgwater, A.V., Meier, D., Radlein, D. An over view of fast pyrolysis of biomass. Organic Geochemistry 1999; 30: 1479-93.

[19] Bridgwater, A.V. The opportunities for fast pyrolysis of biomass. In: Proceedings10th EC Bioenergy Conference, Wurtzburg, June1998, CARMEN, Germany.

[20] Bridgwater, A.V. Principles and practice of biomass fast pyrolysis processes for liquids. J.Analytical and Applied Pyrolysis1999; 51: 3-22.

[21] Bridgwater, A.V.,Evans, G.D. An assessment of thermochemical conversion systems for processing biomass and refuse. Reportto UKDTI 1993; 254pp (ETSUB/ T1/ 00207/ REP).

[22] Bridgwater, A.V., Peacocke, G.V.C. Fast pyrolysis processes for biomass. In: Sustainable and Renewable Energy Reviews,Elsevier 1999: pp.172.

[23] Bridgwater, A.V. Biomass pyrolysis technologies, biomass for energy and industry. London: Elsevier Applied Science; 1990.

[24] McKendry, P. Energy production from biomass (part 1): overview of biomass. Bioresource Technology 2002; 83: 37-46.

[25] McKendry, P. Energy production from biomass (part 2): conversion technologies. Bioresource Technology 2002; 83: 47-54.

[26] McKendry, P. Energy production from biomass (part 3): gasification technologies. Bioresource Technology, 2002; 83: 55-63.

[27] Diebold, J.P. A review of the toxicity of biomass pyrolysis liquids formed at low temperature, In:Bridgwater, A.V.etal.(Eds.), Fast Pyrolysis: Handbook. (CPL1999, ISBN1872691072) 1999: pp.135-163.

[28] Boukis, I., Maniatis, K., Bridgwater, A.V., Kyritsis, S., Flitris, Y., Vassilatos, V. Flash pyrolysis of biomass in an air blown circulating fluidized bed reactor. In: Bridgwater AV(Ed.), Advances in Thermochemical Biomass Conversion. Blackie 1993. pp.451-1164.

[29] Boroson, M.L., Howard, J.B., Longwell, J.P., Peters, W.A. Product yields and kinetics from the vapour phase cracking of wood pyrolysis tars. AIChE Journal 1989; 35: 120-128.

[30] Raveendran, K., Ganesh, A., Khilar, K.C. Influence of mineral matter on biomass pyrolysis characteristics. Fuel 1995; 74(12): 1812-22.

[31] Maa, P.S., Bailie, R.C. Influence of particle sizes and environmental conditions on high temperature pyrolysis of cellulose material. Combust Sci Technol 1973; 7: 257-69.

[32] GrΦnli, M.G., Varhegyi, G., DiBlasi, C. Thermogravimetric analysis and devolatilization kinetics of wood. Ind Eng Chem Res 2002;41:4201-8.

[33] Williams, P.T, Besler, S. The pyrolysis of rice husks in a thermogravimetric analyzer and static batch reactor. Fuel 1993; 72: 1519.

[34] Williams, P.T., Besler, S. Influence of temperature and heating rate on the slow pyrolysis of biomass. Renew Energy 1996;7: 233-50.

[35] Safi, M.J., Mishra, I.M., Prasad, B. Global degradation kinetics of pine needles in air. Thermo chem. Acta 2004; 412: 155-62.

[36] Energy kid's page, http://www.eia.doe.gov/kids/energyfacts/sources/renewable/biomass.html, accessed on June 20th, 2008.

[37] Gani, A., Naruse, I. Effect of cellulose and lignin content on pyrolysis and combustion characteristics for several types of biomass. Renewable Energy 2007; 32: 649-61.

[38] Li, C., Suzuki, K. Tar property, analysis, reforming mechanism and model for biomass gasification—An overview. Renewable and Sustainable Energy Reviews 2008.

[39] Milne, T.A., Evans, R.J., Abatzoglou, N. Biomass gasifier ‘tars’: their nature, formation, destruction, and tolerance limits in energy conversion devices.In: Overend RP, Chornet E, editors. Proceedings of the 3rd biomass conference of the Americas, vol. 1. 1997. p. 729–38.

[40] Milne, T.A., Abatzoglou, N., Evance, R.J., Biomass Gasifire “Tars”: Their Nature, Formation and Conversion, NREL/TP-570-25357: 1998; 1-68.

[41] Simell, P., Sta°hlberg, P., Kurkela, E., Albrecht, J., Deutsch, S., Sjo¨stro¨m, K. Provisional protocol for the sampling and analysis of tar and particulates in the gas from large-scale biomass gasifiers. Biomass Bioenerg 2000; 18(1): 19–38 (Version 1998).

[42] Elliott, D.C. Relation of reaction time and temperature to chemical composition of pyrolysis oils. In: Soltes EJ, Milne TA, editors. Proceedings of the ACS symposium series 376, pyrolysis oils from biomass, 1988.

[43] Baker, E.G., Brown, M.D., Elliott, D.C., Mudge, L.K. Characterization and treatment of tars from biomass gasifiers, Denver CO: AIChE 1988 Summer National Meeting, 1–11.

[44] Maniatis, K., Beenackers, A.A.C.M. Tar Protocols. IEA Bioenergy Gasification Task Biomass Bioenergy 2000; 18(1): 1–4.

[45] Anna, P., Sylwester, K., Wlodzimierz, B. Effect of operating conditions on tar and gas composition in high temperature air/steam gasification (HTAG) of plastic containing waste. Fuel Processing Technology 2006;87:223–33.

[46] Sousa, L.C.R. Gasification of wood, urban wastewood (Altholz) and other wastes in a fluidised bed reactor. Technische Wissenschaften ETH Zurich; 2001.

[47] Aygun, F.,Demirci, A.,Ozcimder, M. Liquid chromatographic method for the determination of benzo[*a*] pyrene in filtertar of Turkish cigarettes. J Agric Food Chem 1996; 44: 1488-90.

[48] Alben,K.Gas chromatographic-mass spectrometric analysis of chlorination effects on commercial coal-tar leachate. Anal Chem1980; 52: 1825-8.

[49] Eisermann, W., Johnson, P., Conger, W.L. Estimating thermodynamic properties of coal, char, tar and ash. Fuel Process Technol 1980; 3:39-53.

[50] Hyman, D., Kay, W.B. Heat capacity and content of tars and pitches. Ind Eng Chem 1949; 41: 1764-8.

[51] Thunman, H., Niklasson, F., Johnsson, F., Leckner, B. Composition of volatiles gases and thermochemical properties of wood for modelling of fixed or fluidized beds. Energy Fuels 2001; 15: 1488–97.

[52] Mason, D.M.,Gandhi, K.N. Formulas for calculating the calorific value of coal and coal chars: development, tests, and uses. Fuel Process Technol 1983; 7: 11-22.

[53] Hosoya, T., Kawamoto, H., Saka, S. Pyrolysis behaviors of wood and its constituent polymers at gasification temperature. J.Anal.Appl.Pyrolysis 2006.

[54] Jess, A. Mechanisms and kinetics of thermal reactions of aromatic hydrocarbons from pyrolysis of solid fuels. Fuel 1996; 75(12):144-1448.

[55] Nair, S.A., Yan, K., Pemen, A.J.M., Van, Heesch, E.J.M., Ptasinski, K.J., Drinkenburg, A.A.H. Tar removal from biomass-derived fuel gas by pulsed corona discharges. A chemical kinetic study. Ind Eng Chem Res 2004; 43: 1649-58.

[56] Devi, L., Ptasinski, K.J., Janssen, F.J.J.G. Pretreated olivine as tar removal catalyst for biomass gasifiers: investigation using naphthalene as model biomass tar. Fuel Process Technol 2005; 86: 707-30.

[57] Swierczynski, D., Courson, C., Kiennemann, A. Study of steam reforming of toluene used as model compound of tar produced by biomass gasification. Chem Eng Process 2008; 47(3): 508-13.

[58] Swierczynski, D., Libs, S., Courson, C., Kiennemann, A. Steam reforming of tar from a biomass gasification process over Ni/olivine catalyst using toluene as a model compound. Appl Catal B: Environ 2007; 74: 211-22.

[59] Taralas, G., Kontominas, M.G., Katatsios, X. Modeling the thermal destruction of toluene (C_7H_8) as tar-related species for fuel gas clean up. Energy Fuels 2003; 17:329-37.

[60] Tomishige, K., Asadullah, M., Kunimori, K. Syngas production by biomass gasification using $Rh/CeO_2/SiO_2$ catalysts and fluidized bed reactor. Catalysis Today 2004; 89: 389- 403.

[61] Tomishige, K., Miyazawa, T., Takeo, K., Kimio, K. Novel catalyst with high resistance to sulfur for hot gas cleaning at low temperature by partial oxidation of tar derived from biomass. Catalysis Communication 2005:37-40.

[62] Zhang, C., Zhang, X., Yang, J., Liu, Z. Analysis of polynuclear aromatic hydrocarbons in heavy products derived from coal and petroleum by high performance liquid chromatography. J Chromatogr A 2007; 1167: 171-7.

[63] Zhu, W., Song ,W., Lin, W. Catalytic gasification of char from co-pyrolysis of coal and biomass. Fuel Processing Technology 2008; 89: 890-96.

[64] Zabaniotou, A., Ioannidou, O., Skoulou, V. Rapeseed residues utilization for energy and 2nd generation biofuels. Fuel 2008; 87: 1492–1502.

[65] Haykiri, H.A., Yaman, S., Kucukbayrak, S.Gasification of biomass chars in steam–nitrogen mixture. Energy Conversion and Management 2006; 47:1004-13.

[66] Klose, W., Wolki, M. On the intrinsic reaction rate of biomass char gasification with carbon dioxide and steam. Fuel 2005; 84: 885-92.

[67] Kirubakaran, V., Sivaramakrishnan, V., Nalini, R., Sekar, T., Premalatha, M., Subramanian, P. A review on gasication of biomass. Renewable and Sustainable Energy Reviews 2007; 1979-90.

[68] Liu, H., Luo, C., Kato, S., Umeiya, S., Kaneko, M., Kojima, T. Kinetics of CO_2/Char gasification at elevated temperatures: Part I: Experimental results. Fuel Processing Technology 2006; 87: 775-81.

[69] Lowry, H.H. Chemistry of coal utilization. NewYork:Wiley; 1963. Pinto, F., Franco, C., Lopes, H., Andre, R., Gulyurtlu, I., Cabrit, I. Effect of used edible oils in coal fluidized bed gasification. Fuel 2005; 84: 2236-47.

[70] Werther, J., Saenger, M., Hartage, E.U., Ogada, T., Siagi, Z. Combustion of agricultural residues. Prog Energy Combust Sci 2000; 26:1.

[71] Abbas, T., Costem, P.G., Lockwood, F.C. Solid fuel utilization: from coal to biomass. In: 26th symposium(international) on combustion. The Combustion Institute, Pittsburgh, PA; 1996. p3041-58.

[72] Abatzoglou, N., Barker, N.,Hasler, P.,Knoef, H. The development of a draft protocol for the sampling and analysis of particulate and organic contaminants in the gas from small biomass gasifiers. Biomass Bioenergy 2000; 18(1):5-17.

[73] Azner, M.P., Caballero, M.A., Gil, J., Martin, J.A. Commercial steam reforming catalysts to improve biomass gasification with steam-oxygen mixtures.2. Catalytic tar removal. Ind Eng Chem Res 1998; 37: 2668-80.

[74] Byun, I.S., ChoiO,L., ChoiJ,G., LeeS,H. In situ photo acoustic study of water gas shift reaction over magnetite/chromium oxide and copper/zinc oxide catalysts. Bull Korean Chem Soc 2002; 23(11): 151-37.

[75] Berndes, G., Hoogwijk, M., Broek, R.V. The contribution of biomass in the future global energy supply: a review of 17 studies. Biomass Bioenergy 2003; 25: 1–28.

[76] Bergman, P.C.A., Paasen, V.B., Boerrigter, H. The novel ‘‘OLGA’’ technology for complete tar removal from biomass producer gas, Pyrolysis and Gasification of Biomass and Waste, Expert Meeting, September 30, 2002, Strasbourg, France.

[77] Bain, R.L., Dayton, D.C., Carpenter, D.L., Czernik, S.R., Feik, C.J., French, R.J., et al. Evaluation of catalyst deactivation during catalytic steam reforming of biomass-derived syngas. Ind Eng Chem Res 2005; 44: 7945-56.

[78] Shazadeh, F. Pyrolysis and combustion of cellulosic material. Adv Carbohydr Chem 1968; 23: 419-74.

[79] Senneca, O. Kinetics of pyrolysis, combustion and gasification of three biomass fuels. Fuel Processing Technology 2006; 88: 87-97.

[80] CEN technical specification " biomass gasification-tar and particle in producer gases-sampling and analysis".Prepared by CEN task force BT/TF143WICSC03002.4TC, 2005.

[81] Corella, J., Toledo, J.M., Aznar, M. Improving the modeling of the kinetics of the catalytic tar elimination in biomass gasification. Ind Eng Chem Res 2002; 41: 351-6.

[82] Corella, J., Caballero, M.A., Aznar, M., Brage, C. Two advanced models for the kinetics of the variation of the tar composition in its catalytic elimination in biomass gasification. Ind Eng Chem Res 2003;42:3001-11.

[83] Dou, B., Gao, J., Sha, X., Baek, S.W. Catalytic cracking of tar component from high temperature fuel gas. Appl Therm Eng 2003; 23:2229-39.

[84] Delgado, J., Aznar, M.P., Corella, J. Biomass gasification with steam in fluidized bed: effectiveness of CaO, MgO, and CaO-MgO for hot raw gas cleaning. Ind Eng Chem Res 1997; 36: 1535-43.

[85] Grassi, G., Gosse, G., Dos-Santos, G. Biomass for energy and industry. London: Elsevier Applied Science; 1990.

[86] Knoef, H., Koele, H.J. Survey of tar measurement protocols. Biomass Bioenergy 2000;18:55-9.

[87] Karellas, S., Karl, J. Analysis of the product gas from biomass gasification by means of laser spectroscopy. Optics Lasers Eng 2007; 45:935-46.

[88] Kirubakaran, V., Sivaramakrishnan, V., Nalini, R., Sekar, T., Premalatha, M.Subramanian, P. A review on gasification of biomass. Renewable and Sustainable Energy Reviews 2007.

[89] Lv, P., Yuan, Z., Wu, C., Ma, L., Chen, Y., Tsubaki, N. Bio-syngas production from biomass catalytic gasification. Energy Conv Manage 2007; 48: 1132-9.

[90] Narvaez, I., Orio, A., Aznar, M.P., Corella, J. Biomass gasification with air in an atmospheric bubbling fluidized bed. Effect of six operational variables on the quality of the produced raw gas. Ind Eng Chem Res 1996; 35(7): 2110-20.

[91] Ross, D.P., Yan, H., Zhang, D. Modelling of a laboratory-scale bubbling fluidised-bed gasifier with feeds of both char and propane. Fuel 2004; 83:

[92] Reid, R.C., Prausnitz, J.M., Polling, B.E. The properties of gases & liquids, 4th ed., McGraw-Hill; 1988.

[93] Remackers, Heynis, Weide,V.D. In: Proceedings of the engines and adaptation of engines for producer gas, the second international producer gas course and conference; 1985.

[94] Sutton, D., Kelleher, B. ,Ross, J.R.H. Review of literature on catalysts for biomass gasification. Fuel Processing Technology 2001; 31: 55-173.

[95] Sricharoenchaikul, V., Frederick, W.J., Agrawal, P. Black liquor gasification characteristics 2. Measurement of condensable organic matter (tar) at rapid heating conditions. Ind Eng Chem Res 2002; 41:5650-8.

[96] Simell, P.A., Hirvensalo, E.K., Smolander, V.T., Krause, A.O.I. Steam reforming of gasification gas tar over dolomite with benzene as a model compound. Ind Eng Chem Res 1999;38:1250-7.

[97] Ultra-sensitive coal tar distillate analysis by GC-PID, by Kevin Attra Courtesy of Buck Scientific Inc.,Originally published 2006, http://www.environmental-expert.com.

.

Appendices

Appendix A

Steam flow rate from peristaltic pump

No.	Set by digital(ml/min)	Water out from pump in 15 ml			Average (sec)	ml/min in liquid phase	ml/min in gas phase	mmol/h in gas phase
		Time1 (sec)	Time2 (sec)	Time3 (sec)				
1	0.02	0.4	0.4	0.4	0.4	0.027	33.185	88.888
2	0.03	0.6	0.6	0.6	0.6	0.040	49.778	133.333
3	0.04	0.8	0.8	0.8	0.8	0.053	66.370	177.777
4	0.05	1	1	1	1	0.067	82.963	222.222
5	0.06	1.1	1.1	1.1	1.1	0.073	91.259	244.444
6	0.07	1.2	1.2	1.2	1.2	0.080	99.556	266.666
7	0.08	1.3	1.3	1.3	1.3	0.087	107.852	288.888
8	0.09	1.6	1.6	1.6	1.6	0.107	132.741	355.555
9	0.10	1.7	1.7	1.7	1.7	0.113	141.037	377.777

Calculations;

Water 0.027 ml/min in liquid phase $= \dfrac{(0.027 ml/\min \times 22.4 l/mol \times 1000}{18 g/mol}$

$= 33.185$ ml/min in gas phase

$= \dfrac{33.185 ml/\min \times 60 \min}{22.4 l/mol \times 1 hr}$

$= 88.888$ mmol/h

Appendix B

Gas standard from gas chromatograph

Gas standards	% mixture	Area from gas chromatograph Time 1	Area from gas chromatograph Time 2	Area from gas chromatograph Time 3	Average
H_2	40.28	6942718	7135462	7007581	7028587
CO	19.89	381725	399273	382770	387922
CO_2	19.83	822203	852246	829758	834735
CH_4	14.97	307257	316872	312267	312132

Calculations of gas products from experiment;

1. Calculated the percentage of gas products

$$\%\ \mathbf{CO} = \frac{19.89(\%) \times [\text{CO gas chromatograph area from experiment}]}{[\text{CO gas chromatograph area from experiment}]}$$

$$\%\ \mathbf{CO_2} = \frac{19.83(\%) \times [\text{CO}_2 \text{ gas chromatograph area from experiment}]}{[\text{CO}_2 \text{ gas chromatograph area from experiment}]}$$

$$\%\ \mathbf{CH_4} = \frac{14.97(\%) \times [\text{CH}_4 \text{ gas chromatograph area from experiment}]}{[\text{CH}_4 \text{ gas chromatograph area from experiment}]}$$

$$\%\ \mathbf{H_2} = \frac{40.28(\%) \times [\text{H}_2 \text{ gas chromatograph area from experiment}]}{[\text{H}_2 \text{ gas chromatograph area from experiment}]}$$

2. Gas product flow calculations

$$\text{Flow of CO} = \text{Gas out (ml/min)} \times [\%\ \text{CO}] \times \frac{273\ \text{K} \times 1\ \text{mol} \times 60\ \text{min}}{298\ \text{K} \times 22.4\ \text{l} \times 1\ \text{hr}}$$

$$\text{Flow of CO}_2 = \text{Gas out (ml/min)} \times [\%\ \text{CO}_2] \times \frac{273\ \text{K} \times 1\ \text{mol} \times 60\ \text{min}}{298\ \text{K} \times 22.4\ \text{l} \times 1\ \text{hr}}$$

$$\text{Flow of CH}_4 = \text{Gas out (ml/min)} \times [\%\ \text{CH}_4] \times \frac{273\ \text{K} \times 1\ \text{mol} \times 60\ \text{min}}{298\ \text{K} \times 22.4\ \text{l} \times 1\ \text{hr}}$$

$$\text{Flow of H}_2 = \text{Gas out (ml/min)} \times [\%\ \text{H}_2] \times \frac{273\ \text{K} \times 1\ \text{mol} \times 60\ \text{min}}{298\ \text{K} \times 22.4\ \text{l} \times 1\ \text{hr}}$$

3. Carbon in biomass calculation for material balance

$$\text{Carbon in biomass} = \frac{\text{Carbon from elemental analysis(\%)} \times \text{Biomass weight(g)}}{12}$$

$$\text{Carbon in bamboo} = \frac{46.24(\%) \times 0.5\ \text{g}}{12}$$

$$= 19.26\ \text{mmol}$$

$$\text{Carbon in char of biomass} = \frac{\text{Carbon from elemental analysis(\%) x char weight(g)}}{12}$$

$$\text{Carbon in char of bamboo} = \frac{76.09(\%) \text{ x } 0.5 \text{ g}}{12}$$

$$= 317.04 \text{ mmol}$$

4. Carbon conversion(%)

$$\text{Carbon conversion (\%)} = \frac{CO + CO_2 + CH_4 + \text{tar} + \text{char}}{\text{Carbon total in biomass}} \text{ x } 100$$

Appendix C

Biomass pyrolysis followed by catalytic gasification at 750 ^{o}C experiments

1. Pine wood chip 0.5 g, Steam flow rate 177.78 mmol/h, Ar 72 ml/min and H_2 input 28 mlmin (75 mmol/h)

Temperature (^{o}C)	Time (sec) in 25 ml	Gas flow out (ml/min)	CO area	CH_4 area	CO_2 area	H_2 area	CO (%)	CH_4 (%)	CO_2 (%)	H_2 (%)	CO mmol/h	CH_4 mmol/h	CO_2 mmol/h	H_2 mmol/h	H_2 real mmol/h
180	14.20	105.69	0	2458	4598	3528000	0.00	0.09	0.60	41.21	0.00	0.23	1.55	106.86	31.86
190	12.49	120.18	15967	5701	12422	3700025	1.58	0.21	1.62	43.21	4.67	0.62	4.77	127.44	52.44
200	12.44	120.94	66791	21275	40178	4569902	7.01	0.78	5.23	53.37	20.82	2.32	15.53	158.40	83.40
225	10.82	138.64	77045	21243	42587	4394326	8.09	0.78	5.55	51.32	27.53	2.65	18.87	174.61	99.61
250	9.98	150.38	55499	33338	79944	5204696	5.83	1.22	10.41	60.79	21.51	4.52	38.43	224.31	149.31
275	8.39	178.72	66941	24153	46675	3543396	7.03	0.89	6.08	41.38	30.83	3.89	26.66	181.50	106.50
300	8.41	178.43	72256	16221	30913	3365200	7.59	0.60	4.03	39.30	33.23	2.61	17.63	172.09	97.09
325	8.92	168.17	64199	24056	47273	3405458	6.74	0.88	6.16	39.77	27.82	3.64	25.41	164.14	89.14
340	10.26	148.24	38166	37151	91344	4444487	4.01	1.36	11.90	51.91	14.58	4.96	43.28	188.82	113.82
356	11.17	134.45	28556	21896	45478	4243922	3.00	0.80	5.92	49.57	9.89	2.65	19.54	163.53	88.53
370	11.34	132.36	11021	7536	10406	3710988	1.16	0.28	1.36	43.34	3.76	0.90	4.40	140.77	65.77
380	11.41	131.50	7384	4334	4905	3153523	0.78	0.16	0.64	36.83	2.50	0.51	2.06	118.85	43.85
400	11.82	126.92	0	2606	3008	2842165	0.00	0.10	0.39	33.19	0.00	0.30	1.22	103.38	28.38
400	12.27	122.39	0	2184	3273	2980357	0.00	0.08	0.43	34.81	0.00	0.24	1.28	104.54	29.54

2. Coconut 0.5 g, Steam flow rate 177.78 mmol/h, Ar 72 ml/min and H_2 input 28 mlmin (75 mmol/h)

Temperature (°C)	Time (sec) in 25 ml	Gas flow out (ml/min)	CO area	CH_4 area	CO_2 area	H_2 area	CO (%)	CH_4 (%)	CO_2 (%)	H_2 (%)	CO mmol/h	CH_4 mmol/h	CO_2 mmol/h	H_2 mmol/h	H_2 real mmol/h
180	10.94	137.86	0	0	0	3943202	0.00	0.00	0.00	46.05	0.00	0.00	0.00	155.80	80.80
200	10.79	140.31	0	0	0	3822388	0.00	0.00	0.19	44.64	0.00	0.00	0.65	153.71	78.71
230	10.86	138.38	0	0	3567	3867423	0.00	0.00	0.46	45.17	0.00	0.00	1.58	153.38	78.38
250	10.25	146.76	12076	0	24116	3624603	2.25	0.16	3.14	42.33	8.73	0.61	12.16	163.91	88.91
275	8.50	177.67	53460	8399	41011	3946600	5.61	0.31	5.34	46.09	24.48	1.34	23.29	200.96	125.96
300	7.58	198.01	109376	23415	66830	4531566	11.49	0.86	8.71	52.93	55.81	4.18	42.30	257.16	182.16
325	7.91	189.96	94093	27851	75080	4594364	9.88	1.02	9.78	53.66	46.06	4.77	45.59	250.13	175.13
350	8.53	175.98	66580	30798	66837	4802799	6.99	1.13	8.71	56.09	30.20	4.88	37.60	242.23	167.23
375	9.27	161.94	51799	23332	41481	4378840	5.44	0.86	5.40	51.14	21.62	3.40	21.47	203.23	128.23
400	8.82	170.45	43485	11416	24265	4365932	4.57	0.42	3.16	50.99	19.10	1.75	13.22	213.28	138.28
400	10.11	149.40	44047	25150	46670	4394591	4.63	0.92	6.08	51.33	16.96	3.38	22.29	188.16	113.16
400	11.20	135.90	39087	18718	28171	4219394	4.10	0.69	3.67	49.28	13.69	2.29	12.24	164.34	89.34

3. Bamboo 0.5 g, Steam flow rate 177.78 mmol/h, Ar 72 ml/min and H_2 input 28 mlmin (75 mmol/h)

Temperature (°C)	Time (sec) in 25 ml	Gas flow out (ml/min)	CO area	CH_4 area	CO_2 area	H_2 area	CO (%)	CH_4 (%)	CO_2 (%)	H_2 (%)	CO mmol/h	CH_4 mmol/h	CO_2 mmol/h	H_2 mmol/h	H_2 real mmol/h
180	10.13	148.13	2350	1863	3906	3881020	0.25	0.07	0.51	45.33	0.90	0.25	1.85	164.76	89.76
200	9.49	158.45	15967	5777	12690	4015860	1.68	0.21	1.65	46.90	6.52	0.82	6.43	182.36	107.36
225	9.18	163.86	31654	11667	24154	4251446	3.32	0.77	3.15	49.65	13.37	1.72	12.65	199.65	124.65
250	8.42	178.47	75373	31713	55621	4671460	7.92	1.16	7.25	54.56	21.57	3.24	23.01	220.12	145.12
275	8.25	182.10	108196	46945	74134	4974712	11.36	1.72	1.72	58.10	34.67	5.10	31.73	238.94	163.94
300	7.97	188.7	146144	60520	92145	5211034	15.35	2.22	12.00	60.86	71.08	10.29	55.58	281.84	206.84
325	7.08	211.97	70163	36709	80494	4779726	13.02	1.35	10.48	55.82	38.33	7.01	54.54	290.37	215.37
350	7.83	191.62	30906	14823	31018	4290230	7.46	0.54	4.04	50.11	42.70	2.56	19.00	235.61	160.61
375	9.09	165.22	15249	5997	13435	3727635	1.60	0.22	1.75	43.54	15.26	0.89	7.09	176.51	101.51
400	10.00	150.14	15615	7689	14434	3976471	1.64	0.28	1.88	46.44	6.04	1.04	6.93	171.11	96.11
400	10.01	149.91	9950	4615	9269	3774404	1.04	0.17	1.21	44.08	3.84	0.62	4.44	162.16	87.16
400	10.36	144.82	1171	3097	6480	3780996	0.12	0.11	0.84	44.16	0.44	0.40	3.00	156.93	81.93

4. Corncob 0.5 g, Steam flow rate 177.78 mmol/h, Ar 72 ml/min and H_2 input 28 mlmin (75 mmol/h)

Temperature (^{o}C)	Time (sec) in 25 ml	Gas flow out (ml/min)	CO area	CH_4 area	CO_2 area	H_2 area	CO (%)	CH_4 (%)	CO_2 (%)	H_2 (%)	CO mmol/h	CH_4 mmol/h	CO_2 mmol/h	H_2 mmol/h	H_2 real mmol/h
180	9.51	157.73	11328	8361	16584	2841418	1.19	0.31	2.16	33.19	4.60	1.19	8.36	128.45	53.45
200	9.21	162.94	16907	11013	21206	2745026	1.78	0.40	2.76	32.06	7.10	1.62	11.04	128.19	53.19
225	8.55	175.57	53368	32524	53972	4539020	7.56	1.60	8.82	55.83	34.94	7.38	40.77	258.11	183.11
250	7.98	188.42	71954	43508	67703	4779887	6.92	2.00	11.65	58.04	30.73	8.90	51.75	257.86	182.86
275	8.30	181.05	65870	54610	89430	4969617	10.94	2.15	9.44	55.40	51.87	10.18	44.76	262.71	187.71
300	7.81	193.24	104168	58516	72468	4743573	7.75	1.59	8.63	55.54	33.34	6.84	37.14	238.96	163.96
325	8.56	175.35	73788	43339	66272	4755095	5.66	1.36	7.98	51.31	23.02	5.52	32.48	208.78	133.78
350	9.05	165.81	53862	36991	61276	4393344	4.05	0.76	4.55	47.97	16.14	3.01	18.14	191.19	116.19
375	9.24	155.82	35039	18239	32931	4063922	3.68	0.67	4.29	47.46	14.07	2.56	16.40	181.49	106.49
400	10.94	137.79	33405	17276	32740	4109104	3.51	0.63	4.26	47.99	11.86	2.14	14.42	162.26	87.26
400	10.61	141.71	25013	12195	22517	4002826	2.63	0.45	2.93	46.75	9.13	1.56	10.20	162.57	87.57
400	10.34	145.93	13578	6979	14927	3874272	1.43	0.26	1.94	45.25	5.11	0.92	6.96	162.03	87.03

Char steam gasification experiments

1. Char of pine wood chip 0.2 g, Steam flow rate 177.78 mmol/h and Ar 72 ml/min.

Temperature (°C)	Time (sec) in 25 ml	Gas flow out (ml/min)	CO area	CH_4 area	CO_2 area	H_2 area	CO (%)	CH_4 (%)	CO_2 (%)	H_2 (%)	CO mmol/h	CH_4 mmol/h	CO_2 mmol/h	H_2 mmol/h
400	17.30	86.71	23475	29121	43436	5883224	2.47	1.07	5.66	68.71	5.25	2.27	12.04	71.19
420	17.30	86.71	43883	88383	22142	5861349	4.61	3.24	2.88	68.46	9.81	6.90	6.14	70.65
460	17.05	87.98	11810	31362	6993	5984400	1.24	1.15	0.91	69.89	2.68	2.49	1.97	75.89
480	17.16	87.49	10974	32200	4433	6129474	1.15	1.18	0.58	71.59	2.47	2.54	1.24	78.70
500	17.19	87.26	19638	32051	3446	6204115	2.06	1.18	0.45	72.46	4.42	2.52	0.96	80.16
520	17.52	85.62	20264	30124	4176	5985380	2.13	1.11	0.54	69.91	4.47	2.32	1.14	71.87
560	16.73	89.66	16324	25884	6856	5891486	1.71	0.95	0.89	68.81	3.77	2.09	1.96	76.39
580	16.83	89.26	15988	19984	9542	5886854	1.68	0.73	1.24	68.76	3.68	1.61	2.72	75.60
600	16.18	92.71	15985	21161	14724	6083353	1.68	0.78	1.92	71.05	3.82	1.77	4.36	86.63
620	16.50	90.91	16576	21554	14815	5746301	1.74	0.79	1.93	67.11	3.88	1.76	4.30	74.72
660	15.70	95.54	22178	20234	13460	5925080	2.33	0.74	1.75	69.20	5.46	1.74	4.11	87.24
680	16.12	93.05	33658	21028	22078	6200770	3.53	0.77	2.88	72.42	8.07	1.76	6.57	90.36
700	16.31	91.96	33569	21186	21612	6342556	3.53	0.78	2.82	74.08	7.96	1.75	6.35	92.16
720	15.80	95.17	41258	20425	27108	6346807	4.33	0.75	3.53	74.13	10.12	1.75	8.25	98.11
760	15.63	96.24	53414	17773	40674	5620026	5.61	0.65	5.30	65.64	13.25	1.54	12.51	80.01
780	15.20	98.68	74941	20254	61044	6291458	7.87	0.74	7.95	73.48	19.06	1.80	19.25	102.94
800	15.46	97.04	84935	18932	62922	6750781	8.92	0.69	8.20	78.85	21.24	1.65	19.52	112.75
820	14.09	106.51	95232	16539	55383	6505200	10.00	0.61	7.21	75.98	26.14	1.59	18.85	123.57
850	14.24	105.38	145342	18794	92041	7401025	15.26	0.69	11.99	86.44	39.47	1.78	31.00	148.52
850	13.35	112.68	122941	14568	76893	6880209	12.91	0.53	10.02	80.36	35.70	1.48	27.69	147.18
850	11.90	126.24	118228	12303	77515	7003126	12.41	0.45	10.10	81.79	38.46	1.40	31.28	178.38

2. Char of coconut shell 0.2 g, Steam flow rate 177.78 mmol/h and Ar 72 ml/min

Temperature (°C)	Time (sec) in 25 ml	Gas flow out (ml/min)	CO area	CH_4 area	CO_2 area	H_2 area	CO (%)	CH_4 (%)	CO_2 (%)	H_2 (%)	CO mmol/h	CH_4 mmol/h	CO_2 mmol/h	H_2 mmol/h
400	10.47	143.30	15818	39577	18317	3765672	1.66	1.45	2.39	43.98	5.84	5.11	8.39	79.66
420	10.22	146.83	21180	59040	13394	3669588	2.22	2.17	1.74	42.86	8.01	7.81	6.29	79.42
460	10.39	144.41	12960	29909	4833	3852415	1.36	1.10	0.63	44.99	4.82	3.89	2.23	84.44
480	10.51	142.77	12132	27226	3467	3977178	1.27	1.00	0.45	46.45	4.46	3.50	1.58	87.74
500	10.37	144.80	15065	26375	4231	3826548	1.58	0.97	0.55	44.69	5.62	3.44	1.96	83.80
520	10.39	144.48	17357	26455	6935	4092845	1.82	0.97	0.90	47.80	6.46	3.44	3.20	94.47
560	10.01	149.84	20945	21072	8698	3993958	2.20	0.77	1.13	46.65	8.09	2.84	4.17	96.51
580	10.09	148.72	18901	18619	7936	4151830	1.99	0.68	1.03	48.49	7.24	2.49	3.77	101.96
600	10.34	145.11	21472	18125	8041	4130858	2.26	0.67	1.05	48.25	8.03	2.37	3.73	96.79
620	10.53	142.58	25010	7281	8988	4127007	2.63	0.27	1.17	48.20	9.19	0.94	4.10	93.65
660	10.25	146.65	31499	16358	10308	4060850	3.31	0.60	1.34	47.43	11.90	2.16	4.83	95.68
680	10.31	145.60	39510	14918	16154	4345642	4.15	0.55	2.10	50.75	14.83	1.96	7.52	106.34
700	9.86	152.13	55691	16452	24084	4550962	5.85	0.60	3.14	53.15	21.83	2.25	11.71	123.42
720	9.71	154.55	58603	13293	26807	4454741	6.15	0.49	3.49	52.03	23.34	1.85	13.24	122.32
760	9.62	155.93	75264	15477	27494	4321759	7.90	0.57	3.58	50.48	30.24	2.17	13.70	118.14
780	9.56	156.98	90747	13328	35413	4531888	9.53	0.49	4.61	52.93	36.71	1.88	17.77	128.89
800	9.43	159.18	103546	12812	35578	4379914	10.87	0.47	4.63	51.15	42.48	1.84	18.10	124.82
820	9.15	163.88	110125	12568	30205	4983427	11.56	0.46	3.93	58.20	46.51	1.86	15.82	159.06
850	8.84	169.79	160236	10260	36899	4611445	16.83	0.38	4.81	53.86	70.11	1.57	20.02	149.39
850	8.23	182.40	151026	7843	50514	4992176	15.86	0.29	6.58	58.31	70.99	1.29	29.45	185.97
850	8.17	183.73	130265	6243	43531	4709226	13.68	0.23	5.67	55.00	61.68	1.03	25.56	172.97
850	7.86	190.95	111810	4477	39943	4475226	11.74	0.16	5.20	52.27	55.02	0.77	24.38	169.91
850	7.94	192.20	112771	4304	39757	4883014	11.84	0.16	5.18	57.03	55.86	0.7	24.42	193.98

3. Char of bamboo 0.2 g, Steam flow rate 177.78 mmol/h and Ar 72 ml/min

Temperature (^oC)	Time (sec) in 25 ml	Gas flow out (ml/min)	CO area	CH_4 area	CO_2 area	H_2 area	CO (%)	CH_4 (%)	CO_2 (%)	H_2 (%)	CO mmol/h	CH_4 mmol/h	CO_2 mmol/h	H_2 mmol/h
420	10.07	149.03	3270	3895	23937	3539262	0.34	0.14	3.12	41.34	1.26	0.52	11.40	76.17
450	10.07	148.95	8525	20562	3950	3692662	0.90	0.75	0.51	43.13	3.27	2.76	1.88	82.63
475	9.90	151.55	8525	20562	3950	3692662	0.90	0.75	0.51	43.13	3.33	2.81	1.91	85.39
500	10.31	145.58	1541	13250	1522	3548163	0.16	0.49	0.20	41.44	0.58	1.74	0.71	73.04
520	10.44	143.69	2561	18720	2251	3514677	0.27	0.69	0.29	41.05	0.95	2.42	1.03	69.74
550	9.76	153.67	2561	18720	2251	3514677	0.27	0.69	0.29	41.05	1.01	2.59	1.11	79.79
580	9.76	153.67	12424	17093	3541	3932740	1.30	0.63	0.46	45.93	4.92	2.37	1.74	98.20
600	9.69	154.93	19385	12803	4942	4049026	2.04	0.47	0.64	47.29	7.74	1.79	2.45	104.79
620	9.53	157.47	19385	12803	4942	4049026	2.04	0.47	0.64	47.29	7.87	1.82	2.49	107.74
650	9.21	162.87	21990	10253	6760	3873440	2.31	0.38	0.88	45.24	9.23	1.50	3.52	105.80
675	9.06	165.58	27441	9033	13454	4114606	2.88	0.33	1.75	48.06	11.71	1.35	7.12	120.26
700	8.85	169.87	46880	8155	19597	4310950	4.92	0.30	2.55	50.35	20.52	1.25	10.64	134.88
720	8.12	184.79	56056	8147	28549	4570416	5.89	0.30	3.72	53.38	26.69	1.36	16.86	167.04
750	7.50	200.32	74696	8740	31131	4225743	7.84	0.32	4.06	49.35	38.56	1.58	19.93	167.60
780	7.29	205.68	123375	9713	47564	4747326	12.96	0.36	6.20	55.45	65.39	1.80	31.27	204.84
800	7.22	207.66	154560	9702	53655	4859366	16.23	0.36	6.99	56.75	82.71	1.81	35.61	214.21
820	6.15	244.02	165913	8694	47227	4209185	17.42	0.32	6.15	49.16	104.34	1.91	36.84	219.37
800	6.55	229.01	250568	9936	79224	5927314	26.32	0.36	10.32	69.23	147.88	2.05	57.99	314.04
820	6.94	216.54	165913	8694	47227	4209185	17.42	0.32	6.15	49.16	92.59	1.70	32.69	186.22
850	9.45	159.61	250568	9936	79224	5927314	26.32	0.36	10.32	69.23	103.07	1.43	40.42	196.14
850	8.69	172.75	240899	7621	54455	5934601	25.30	0.28	7.09	69.31	107.25	1.19	30.07	218.82
850	9.48	158.20	116540	2937	39424	5239051	12.24	0.11	5.14	61.19	47.51	0.42	19.94	162.54
850	10.43	143.82	57408	1264	34375	5037323	6.03	0.05	4.48	58.83	21.28	0.16	15.80	132.63

4. Char of corncob 0.2 g, Steam flow rate 177.78 mmol/h and Ar 72 ml/min

Temperature (°C)	Time (sec) in 25 ml	Gas flow out (ml/min)	CO area	CH_4 area	CO_2 area	H_2 area	CO (%)	CH_4 (%)	CO_2 (%)	H_2 (%)	CO mmol/h	CH_4 mmol/h	CO_2 mmol/h	H_2 mmol/h
400	10.23	146.58	1972	1659	11765	3790102	0.21	0.06	1.53	44.27	0.74	0.22	5.51	84.22
420	10.12	148.21	3141	16120	2470	3912412	0.33	0.59	0.32	45.69	1.20	2.15	1.17	91.18
440	10.05	149.34	3141	16120	2470	3912412	0.33	0.59	0.32	45.69	1.21	2.17	1.18	92.46
480	10.10	148.59	7291	15488	1642	3924177	0.77	0.57	0.21	45.83	2.79	2.07	0.78	92.11
500	10.24	146.55	1991	20899	1518	3984196	0.21	0.77	0.20	46.53	0.75	2.76	0.71	92.33
520	10.09	148.66	1991	20899	1518	3984196	0.21	0.77	0.20	46.53	0.76	2.80	0.72	94.75
560	10.02	149.75	7918	22605	1693	3792073	0.83	0.83	0.22	44.29	3.06	3.05	0.81	87.75
580	10.10	148.95	8971	18089	2771	4091521	0.94	0.66	0.36	47.79	3.44	2.43	1.32	99.67
600	9.64	155.68	8971	18089	2771	4091521	0.94	0.66	0.36	47.79	3.60	2.54	1.38	107.55
620	9.57	156.92	14140	15942	3468	3865654	1.49	0.59	0.45	45.15	5.72	2.25	1.74	98.85
660	9.48	158.46	27218	17063	11752	4505892	2.86	0.63	1.53	52.63	11.11	2.44	5.95	129.63
680	9.20	163.11	25312	11582	6722	3794877	2.66	0.43	0.88	44.32	10.64	1.70	3.50	102.40
700	9.27	161.85	42378	11550	15442	4030804	4.45	0.42	2.01	47.08	17.68	1.68	7.99	111.97
720	9.00	166.97	37137	11534	15052	4250201	3.90	0.42	1.96	49.64	15.98	1.73	8.03	128.39
740	8.38	179.21	41644	11737	15512	3754984	4.37	0.43	2.02	43.86	19.23	1.89	8.89	117.86
760	7.87	190.71	47322	7577	14004	3894705	4.97	0.28	1.82	45.49	23.26	1.30	8.54	137.88
780	7.44	201.74	57424	12354	27239	4368336	6.03	0.45	3.55	51.02	29.85	2.24	17.56	177.57
800	7.51	199.84	70814	11937	30780	4261156	7.44	0.44	4.01	49.77	36.47	2.15	19.66	169.06
820	7.51	199.73	89290	13745	42197	4858260	9.38	0.50	5.50	56.74	45.96	2.47	26.94	203.10
840	7.59	197.70	116712	14757	51057	5079073	12.26	0.54	6.65	59.32	59.46	2.63	32.26	212.79
850	7.75	193.70	131853	15353	50884	5111791	13.85	0.56	6.63	59.70	65.82	2.68	31.50	208.78
850	8.42	178.22	143649	14284	52998	4972412	15.09	0.52	6.90	58.07	65.98	2.29	30.19	178.97
850	8.21	182.73	119338	10570	45039	4162199	12.53	0.39	5.87	48.61	56.20	1.74	26.31	142.98

5. Char of coconut shell 0.2 g, Steam flow rate 177.78 mmol/h, Ar 72 ml/min and Ni/dolomite catalyst 5 g

Temperature (^{o}C)	Time (sec) in 25 ml	Gas flow out (ml/min)	CO area	CH_4 area	CO_2 area	H_2 area	CO (%)	CH_4 (%)	CO_2 (%)	H_2 (%)	CO mmol/h	CH_4 mmol/h	CO_2 mmol/h	H_2 mmol/h
620	10.15	147.90	0	5296	2332	3977124	0.00	0.19	0.30	46.45	0.00	0.71	1.10	93.58
660	10.37	144.70	1466	9994	4258	3995538	0.15	0.37	0.55	46.67	0.55	1.30	1.97	90.70
680	10.40	144.32	1945	13399	7468	3647747	0.20	0.49	0.97	42.60	0.72	1.74	3.44	75.88
700	10.14	148.27	16177	17855	9924	4091386	1.70	0.66	1.29	47.79	6.18	2.38	4.70	98.85
720	9.71	154.74	18874	15860	12812	4087563	1.98	0.58	1.67	47.74	7.53	2.21	6.34	106.27
740	9.58	156.61	24509	14969	15462	4103905	2.57	0.55	2.01	47.93	9.89	2.11	7.74	109.20
760	9.69	154.94	28483	15832	16349	4188302	2.99	0.58	2.13	48.92	11.37	2.21	8.10	110.99
800	9.91	151.33	32728	13763	15683	4172843	3.44	0.51	2.04	48.74	12.76	1.88	7.59	105.97
820	9.80	153.17	46852	14009	23961	4268826	4.92	0.51	3.12	49.86	18.49	1.93	11.73	112.40
840	9.85	152.53	48010	11104	23799	4172688	5.04	0.41	3.10	48.73	18.87	1.53	11.60	107.41
850	9.54	157.23	59412	11359	30792	4028570	6.24	0.42	4.01	47.05	24.07	1.61	15.48	106.54
850	9.65	155.72	54911	6329	24224	4025120	5.77	0.23	3.16	47.01	22.04	0.89	12.06	104.63
850	9.28	161.76	40254	6164	24314	4025367	4.23	0.23	3.17	47.01	16.78	0.90	12.57	111.62
850	9.05	166.01	39593	4494	24944	4143225	4.16	0.16	3.25	48.39	16.94	0.67	13.24	122.13
850	8.53	176.04	36895	3726	26717	4023756	3.87	0.14	3.48	47.00	16.74	0.59	15.03	128.00
850	8.65	173.76	37575	2594	22277	3902507	3.95	0.10	2.90	45.58	16.83	0.41	12.37	119.34
850	9.06	165.68	32323	2668	26068	3988793	3.39	0.10	3.40	46.59	13.80	0.40	13.80	114.40
850	9.23	162.47	29488	2044	21380	3683500	3.10	0.08	2.78	43.02	12.35	0.30	11.10	96.52
850	9.71	154.58	33695	2145	21133	3788420	3.53	0.08	2.75	44.25	13.42	0.30	10.44	92.84
850	9.22	162.91	30538	2140	24043	4045212	3.20	0.08	3.13	47.25	12.82	0.31	12.52	113.87

Appendix D

Simultaneous biomass gasification and reforming with fluidized bed

1. The effect of temperature

Temperature (^oC)	Time (sec) in 25 ml	Gas flow out (ml/min)	CO area	CH_4 area	CO_2 area	H_2 area	CO (%)	CH_4 (%)	CO_2 (%)	H_2 (%)	CO mmol/h	CH_4 mmol/h	CO_2 mmol/h	H_2 mmol/h
750	4.43	685.02	106016	143292	37127	1458508	11.13	5.26	4.84	17.03	187.16	88.41	81.29	153.01
750	4.87	616.51	26788	49207	14788	1269977	2.81	1.81	1.93	14.83	42.56	27.32	29.14	91.06
750	4.75	632.21	2209	4682	25922	1011827	0.23	0.17	3.38	11.82	3.60	2.67	52.38	50.00
750	4.58	655.65	0	1761	1948	1058179	0.00	0.06	0.25	12.36	0.00	1.04	4.08	65.51
750	4.59	653.76	0	0	1188	1015437	0.00	0.00	0.15	11.86	0.00	0.00	2.48	56.93
750	4.37	688.37	0	0	1094	1120430	0.00	0.00	0.14	13.09	0.00	0.00	2.41	87.71
780	4.59	653.18	135524	183508	48480	1441871	14.23	6.74	6.31	16.84	228.13	107.96	101.22	136.59
780	4.88	615.23	31940	48429	16898	1209068	3.35	1.78	2.20	14.12	50.64	26.84	33.23	79.86
780	4.75	632.31	1847	4209	8494	1005371	0.19	0.15	1.11	11.74	3.01	2.40	17.17	48.86
780	4.69	640.34	0	0	1638	903213	0.00	0.00	0.21	10.55	0.00	0.00	3.35	32.43
780	4.80	625.63	0	0	1261	986893	0.00	0.00	0.16	11.53	0.00	0.00	2.52	43.62
780	4.72	635.75	0	0	1202	982363	0.00	0.00	0.16	11.47	0.00	0.00	2.44	45.66
810	5.19	578.03	128434	178212	47994	1664834	13.49	6.54	6.25	19.44	191.32	92.78	88.67	142.47
810	4.61	651.51	35320	52385	18361	1288432	3.71	1.92	2.39	15.05	59.30	30.74	38.24	107.25
810	4.81	624.10	4502	4483	19237	1036589	0.47	0.16	2.51	12.11	7.24	2.52	38.37	52.08
810	4.78	627.68	0	1094	2402	1006183	0.00	0.04	0.31	11.75	0.00	0.62	4.82	47.67
810	4.88	615.80	0	0	2342	977532	0.00	0.00	0.31	11.42	0.00	0.00	4.61	39.19
810	4.87	616.48	1948	0	1938	986042	0.20	0.00	0.25	11.52	3.09	0.00	3.82	40.89

Appendix E

1. Thermogravimetric analysis (TGA)
   Conditions;
   Model: ULVAC SINKU-RIKU TGD 9600; Biomass Type: Coconut shell; N_2 flow rate 100 ml/min; Heating rate 10 ^{o}C/min.

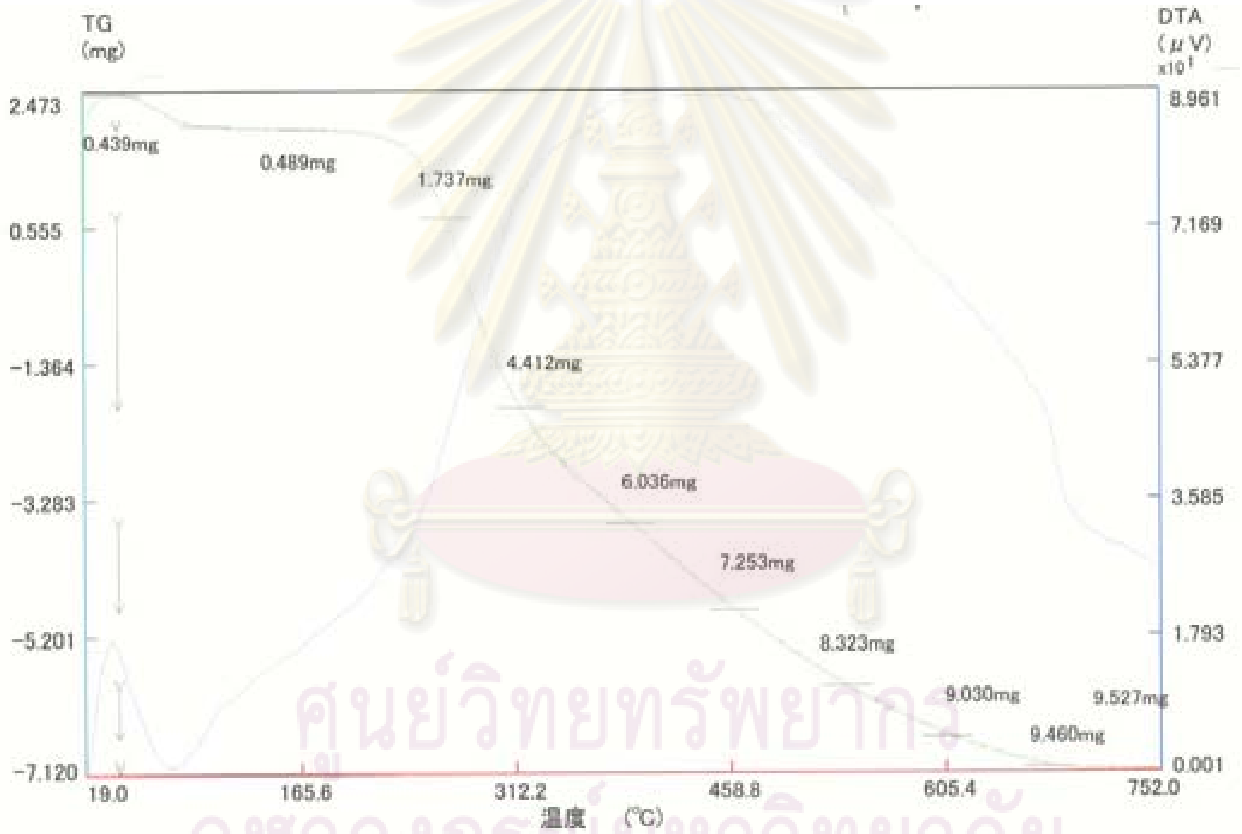

2. Thermogravimetric analysis (TGA)
   Conditions;
   Model: ULVAC SINKU-RIKU TGD 9600; Biomass Type: Coconut shell; Air flow rate 100 ml/min; Heating rate 10 °C/min.

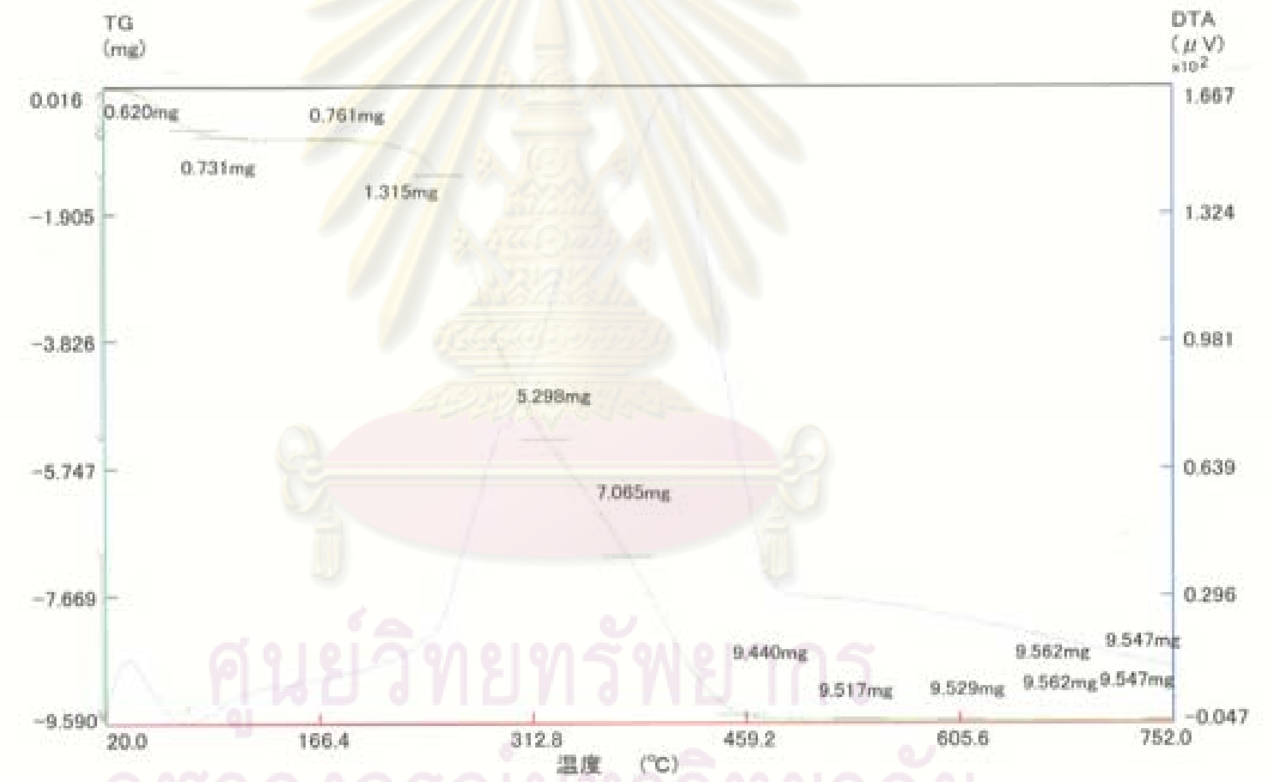

Appendix F

XRD analysis of Type1: Ni/Dolomite catalyst

XRD analysis of Type2: Ni/Dolomite + Silica binder catalyst

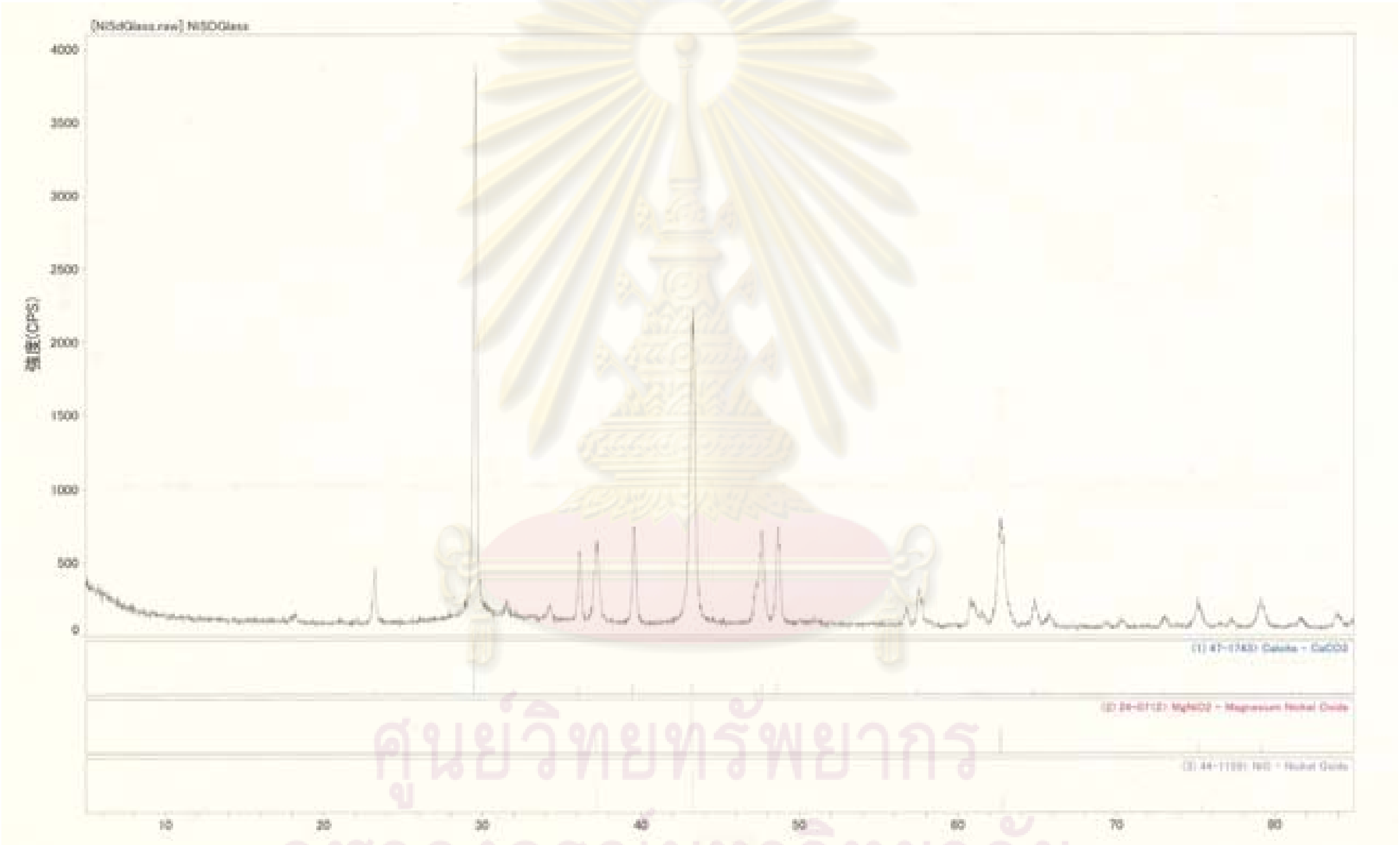

XRD analysis of Type3: Ni/Dolomite which is doped with WO_3

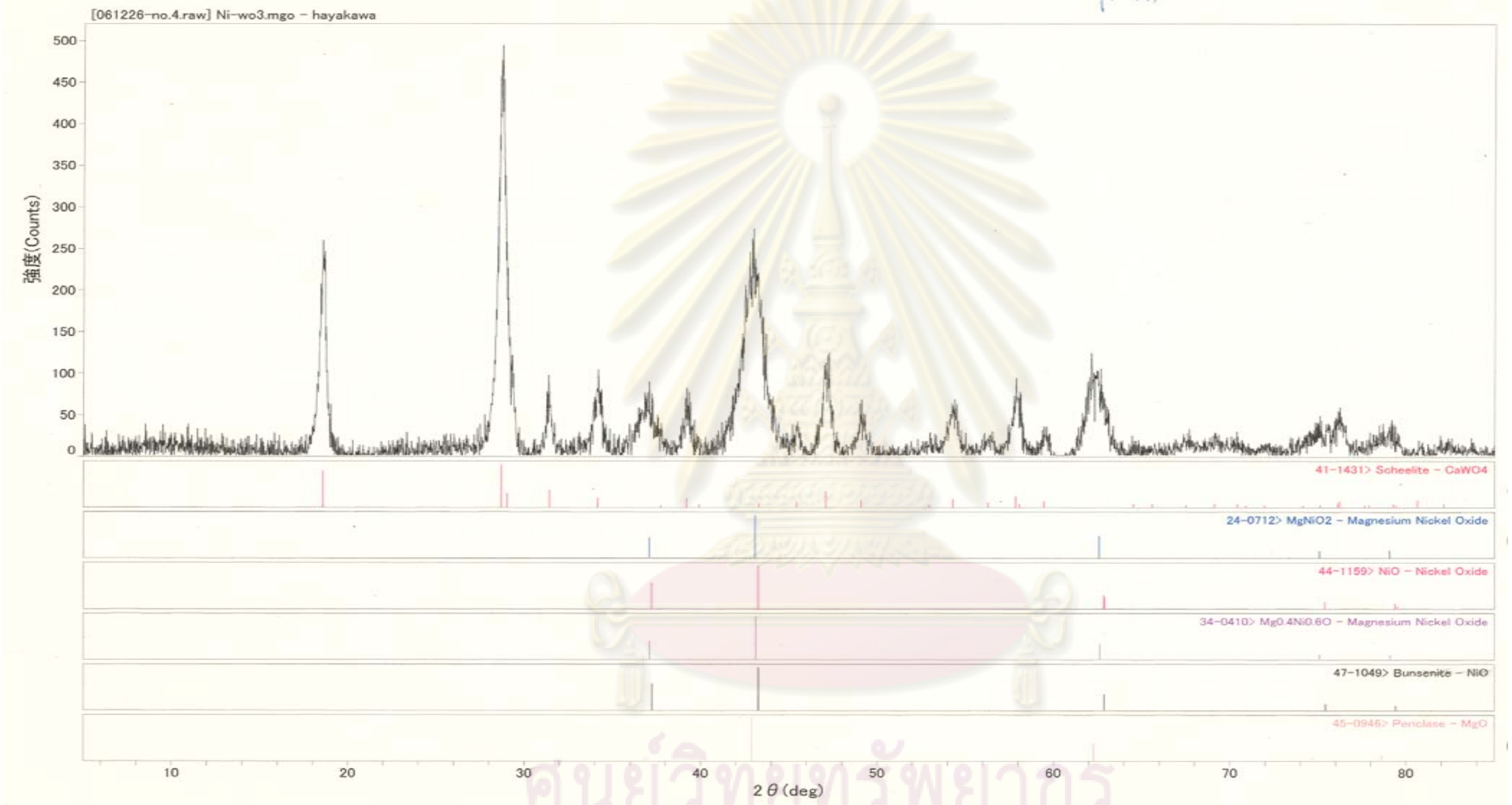

VITA

Name: Mr. Anawat Ketcong

Address: 151/6 Moo 3 Summakorn Village Ramkhamheange Rd. Saphansoong Bangkok
10240, Thailand

E-mail address: anawat_pp@hotmail.com

EDUCATION

Faculty of Science, Chulalongkorn University, *Bangkok, Thailand* 2008

- The Doctor of Philosophy in Chemical Technology supported by New Energy and Industrial Technology Development Organization (NEDO).
- Coursework: Transport Phenomena; Advanced heat and mass Transfer, Fundamental of catalyst, and Noise pollution.

Faculty of Science, Chulalongkorn University, *Bangkok, Thailand* May2002- March 2004

- Master of Science in Chemical Engineering
- Coursework: Chemical Engineering Thermodynamics; Separation Operation Applied Mathematics in Chemical Engineering; Advanced Thermodynamic; Fundamental of Momentum, Heat and Mass Transfer; Chemical Reactor Design; Catalyst Technology.

Faculty of Science, Srinakharinwirot University, *Bangkok, Thailand* June 1998 – March 2002

- Bachelor of Science in Physic
- Coursework: Machanics; Thermodynamics; Electricity & Magnetism; Modern Physics; Nuclear Physics, X-rays Crystallography, Electronic, Materials Physics, Vacuum Physics and Technology; Quantum Mechanics;Optics and Applications; Intro to Solid State Physics.